COMMUNITY-SCALE GENERATION USING A CENTRALIZED PHOTOVOLTAIC ARRAY AND BATTERY STORAGE: A FEASIBILITY STUDY OF RESIDENTIAL ENERGY INDEPENDENCE FOR DC-ONLY SYSTEMS

by

GORDON STEAD

(Under the Direction of John R Schramski)

ABSTRACT

Residential solar energy is typically a direct-current (DC) to alternating-current photovoltaic system, connected to a utility grid for backup. In contrast, an off-grid DC-only community-scaled photovoltaic array and battery bank is proposed to ameliorate environmental concerns and to reduce utility infrastructure costs through decentralized energy production. Electric demand and supply models were used to design a community-scale-generation concept and test its feasibility. Results show that a community of up to 83 family homes could exist independently from the utility grid when powered by a 1-acre single-axis solar tracking array combined, albeit with a high battery requirement of over 8600 kWh, likely necessitating supplementary power generation. The non-linear relationship between community- and required battery-size was examined and several avenues for model development were explored, including applying the model to wide geographic contexts and improving resilience by incorporating supplementary generation as a combined heating and power plant.

INDEX WORDS: Distributed, renewable, energy, microgrid, solar, photovoltaic, tracking, community, independent, sustainability, direct current, efficiency, electrical generation.

COMMUNITY-SCALE GENERATION USING A CENTRALIZED PHOTOVOLTAIC ARRAY AND BATTERY STORAGE: A FEASIBILITY STUDY OF RESIDENTIAL ENERGY INDEPENDENCE FOR DC-ONLY SYSTEMS

by

GORDON STEAD

B.A. (Hons.), Oxford University, United Kingdom, 2006

A Thesis Submitted to the Graduate Faculty of The University of Georgia in Partial Fulfillment of the Requirements for the Degree

MASTER OF SCIENCE

ATHENS, GEORGIA

2021

COMMUNITY-SCALE GENERATION USING A CENTRALIZED PHOTOVOLTAIC ARRAY AND BATTERY STORAGE: A FEASIBILITY STUDY OF RESIDENTIAL ENERGY INDEPENDENCE FOR DC-ONLY SYSTEMS

by

GORDON STEAD

Major Professor:	John R. Schramski
Committee:	KC Das
	David Gattie
	Tom Lawrence

Electronic Version Approved:

Ron Walcott
Vice Provost for Graduate Education and Dean of the Graduate School
The University of Georgia
August 2021

DEDICATION

To my wife, Mary Elizabeth, for allowing and enabling this opportunity to learn again and supporting me through the challenges.

To my parents, Graham and Myola, and late grandfather, Ken, who worked so hard to provide me the education I have enjoyed.

And to all my family, friends (especially the Fellowship), mentors, teachers, and colleagues who have encouraged me in every way to this day.

Soli Deo Gloria.

ACKNOWLEDGEMENTS

Dr John Schramski, College of Engineering, University of Georgia: for accepting me as his student and providing guidance, advice, and encouragement as my Major professor, especially in this research project.

Dr KC Das, College of Engineering, University of Georgia: for agreeing to be on my committee, for his generous funding for my research, and encouragement and guidance in it.

Drs Tom Lawrence and David Gattie: for agreeing to be on my committee and supporting my research. Dr Lawrence's instruction in his Sustainable Building Design class was invaluable in informing much of my demand-side modeling process, as was Dr Gattie's instruction in his Energy Security class for my overall appreciation of energy matters.

TABLE OF CONTENTS

Page

SECTION 1

Introduction

The direct-current-only (DC-only) community-scale-generation (CSG) concept herein is like other microgrid concepts: several loads (in this case, detached family houses) supplied by a local (distributed) energy source, with the ability to act in a self-contained manner. However, notable differences of the CSG include being deliberately electrically isolated from the utility grid, DC-only electrical architecture used throughout, and utilizing a ground-based PV array which, while common among utility-scale solar farms, is unusual in residential PV production [1], [2] where PV modules are typically rooftop-mounted. A fundamental aspect of the DC-only CSG is to exploit the conceptual design space between the existing paradigm of utility-scale on one hand and (individual) residential scale on the other. By considering the benefits of both utility and residential scales of generation, the DC-only CSG model quantifies a potentially energy-sustainable residential lifestyle, independent from the utility grid, without compromising on locally accepted living standards.

The aim of this work is, therefore, to explore if the CSG-concept can feasibly exist in an energy-independent manner, i.e., isolated from the utility grid, and at what size (i.e., how many houses)? Almost any size of community would be possible with an infinitely large PV array and battery storage, so some limits are necessary, in this case it shall be the size of the array, limited to 1.0-acres. Energy storage will be necessary for independence, to power the community in times of energy deficit such as nighttime and winter, and as it is likely that increased battery storage will increase the possible size of the community, the research question should examine the relationship between those two quantities. Thus, the research question which this work attempts to answer is:

What are 1) the maximum number of houses and 2) the community-sized battery storage requirements of an off-grid DC-only microgrid residential community powered by a 1-acre, ground-mounted, solar-tracking PV array?

Utility-scale energy generation may be characterized by a large energy-generating facility and necessary infrastructure to deliver electricity over long distances to the consumer [3]. Utility-scale generation sources include, for example, fossil fuels, biofuels, nuclear, hydro, wind, and solar, of which fossil fuels are projected to continue to generate a consistent 85% [4]. Generated at this scale, electricity is transmitted as alternating current (AC) to increase efficiencies of transfer [5]. Utility scale generation and transmission is reliable in developed countries but can have practical limitations in less developed circumstances, or simply be economically unviable for remote villages [6], [7]. Utility-scale AC transmission losses include heating of the transmission cables, reactive power from AC self-inductance, and transformer losses [6]. In contrast, distributed power, such as the CSG concept, can avoid large-scale transmission losses, with resulting infrastructure savings through a more parsimonious design.

Decentralized or distributed energy production, particularly photo-voltaic (PV) generation systems, have historically only occurred at the individual residential (at the household) scale [8]. Residential PV generation can suffer from reliability problems and require expensive maintenance but can also save transmission losses [9] and insufficient PV modules or battery storage requires a utility-scale generation supplement for electricity when the sun is not shining. Also, although the cost of PV panels and batteries has improved, residential-PV costs, which include for example site-specific structural and wiring, components, and instrumentation, remain expensive. These design and cost concerns are inevitably focused on a single customer, making it unaffordable or unattractive to many households.

The idea of the community-scale is therefore to aim for the benefits of both the utility-scale and the residential scale. The prime advantage of the former is the economies of scale available by sharing the cost of both installation and maintenance among more households. As

well as driving down the per-capita costs, the increased purchasing power should enable the community to invest in high-performance equipment, e.g., the solar-tracking units and high-efficiency solar modules, as well as sufficient battery banks to provide the energy storage with safety margins to enable energy-independence from the grid. Additionally, the combined finances of the community can be used to commission experienced and qualified engineers to maintain the PV system (more accessible as it is ground-based and centralized than PV modules mounted on individual house rooftops) and ensure high-output, reliable performance. It is suggested that the capital investment be spread over the expected 25-year lifetime of the module and bundled into a homeowners' association (HOA) fee along with the maintenance costs.

In the CSG concept, the residential development is designed to be self-sufficient in terms of energy and is therefore isolated, or "islanded", from the broader utility grid, appealing to homeowners who value energy independence whilst simultaneously limiting their residential energy consumption to the renewably generated electricity from the central community PV array. This provides the possibility of 100% renewable energy dependence, which is difficult when relying on the mixed-source utility grid [3] for any fraction of energy supply. By consolidating the PV generation in a ground-based central array, rather than on the rooftop on each house, improved performance and reliability should be achieved [10, 11]. Ground based arrays are mounted on solar trackers which boost energy production overall, whilst also widening the energy curve over the day, i.e., producing more power in the morning and evening as the trackers turn the PV modules towards the sun more during those times. This is of great benefit for those who depend heavily, or in the case of the CSG, entirely on solar power, as tracking enhances the coincidence of supply and demand. While significant battery storage will be required for any isolated community (as there is zero PV production overnight), the amount of such storage can be limited by maximizing coincidence [12]. Improved PV reliability may be realized through the enhanced maintenance the PV array will receive when it is centrally maintained (particularly the cleaning of solar panels, which is difficult and dangerous for individual householders when

mounted on their rooftops) and operated by specialized engineers contracted by the community-at-large (e.g., a homeowner's association, HOA). The proposed size of the array comes from the Reynold's Landing development [13], an Alabama Power "Smart Neighborhood" outside of Hoover, Alabama, that has inspired elements of the CSG concept. Although that community is not isolated from the grid, its 62 houses are powered by a central PV array of approximately 1.0 acres in size (Appendix A), which will be the default area of the CSG array.

Although "DC" is not in the title, the CSG development is also based on the concept of direct-current (DC) only electrical architecture. The opportunity for this arises from the CSG's isolation from the utility grid and thus no interaction with AC electricity is required. The benefits of DC-only electricity are realized through much improved electrical performance of household appliances (and thus lower residential electrical loads), improved CSG system synergy (as PV production, any required battery energy storage, community transmission, and all electrical appliances will only run on DC electricity), and reduced infrastructure costs with no inverter, point of common connection (PCC), power conditioning, or rectifier equipment required. [14-16]. The DC-only nature of the CSG concept is, in this work, mainly focused on the lack of PV inverter and the enhanced performance of domestic appliances, with the detail of the work focused on the latter aspect. Section 5, demand-side modeling (DSM), is concerned with computing an hourly profile of energy demand for the CSG development, based on the assumption that all the houses are built, wired, and equipped with DC-only appliances; indeed, the householders would need to be aware that no AC appliances would function within the community. In Section 6, supply-side modeling (SSM), the DC-only nature of the development is manifest in that no inverter or associated losses are included in the modeling process.

The model is constructed, in this first test-case, for Athens, GA, USA. The U.S. has large per-capita energy demand and carbon emissions [17, 18], including at residential level, and therefore provides an opportunity for the largest volume reduction of energy demand, resource depletion, and carbon emissions. High GDP and industrial maturity and reliability make the

adoption of a new technological concept highly feasible, and the relatively low population density, outside of cities, along with very large undeveloped areas of land in the South of the country, provides reasonable space for deploying a PV array. In this context, the residential community would be designed and built to be "culturally comfortable", that is, offering a standard of living attractive within its socio-economic context. This would encourage the required investment by homeowners to build and operate the central PV array – few people would be willing to pay more for a PV array just to live at a lower standard than they would do if connected to the utility grid.

A "house" or "residential building" may have a broad definition; for the sake of this study, a house in a CSG development will be a detached, 2,500 square foot family dwelling designed for a four-member household, and newly, purpose-built for DC-only electrical supply and internal distribution.

While the primary context is one of a developed nation and low space constraints, the CSG concept has broader horizons, and is built to be applicable to other parts of the world with different economic and space resources. Thus, the methodological stages of DSM and SSM are conducted "bottom-up" and can be tailored for any given location and socio-economic factors. Such wider application, along with possible backup generator and other concept expansion options are considered in the discussion on further work (Section 9).

SECTION 2

Literature Review

The review of literature covered research on three main aspects of the proposed CSG design, summarized below in the following order: microgrids (a form of self-contained or semi-self-contained distributed generation), direct-current-only electrical design, and the energy generation advantages of mounting solar photovoltaic modules onto solar tracking units.

2.1 Microgrids

Throughout the industrialized world, most electrical generation and transmission is through a centralized utility grid, usually dominated by large fossil fuel or nuclear power stations that, despite their technical maturity and reliability, require acceptance of large transmission losses to accommodate large distribution networks [19]. While large-scale, alternating-current (AC) generation and transmission has enjoyed predominance over smaller-scale direct-current (DC) alternatives since the 19th Century, aging infrastructure costs, natural resource consumption rates (including fossil fuels) and carbon emissions [20], the need for electricity in lesser developed nations, and energy security are some of the reasons that designers of electricity systems are seeking to "decentralize, decarbonize, and democratize" [21] with microgrid (MG) development. The three Ds provide a metaphor toward conceptualizing and modeling the drawbacks and benefits of distributed generation (DG) in renewable energy (RE) MGs. DG refers to a wide range of electrical generation at smaller-than-utility scale and MGs are generally defined [7, 20, 22, 23] as:

"... a group of interconnected loads and distributed energy resources within clearly defined electrical boundaries that acts as a single controllable entity with respect to the grid. A microgrid can connect and disconnect from the grid to enable it to operate in both grid-connected or island-

mode. A remote microgrid is a variation of a microgrid that operates in islanded conditions." U.S. Department of Energy, [24].

Similarly, Hirsch et al. [20] define a macro-grid as being installed within a region well connected to the utility grid and a microgrid as serving remote communities not connected to a greater utility grid [25]. Over a billion people live in isolated, rural regions [7], and providing those communities with electricity through a remote microgrid (RMG) is a specific goal for several studies. John-Justo et al. state that 70% of the Sub-Saharan African population live in rural locations of which less than 10% have access to reliable electricity [15]. The International Energy Agency (IEA) records indicate that 84% of people without electricity, worldwide, live in remote areas [26]. Raman et al. [6] report that 450 million people in India have no access to electricity and that the tide of urban migration may be stemmed if rural areas (which account for up to 70% of the Indian population) can be safely and reliably supplied with electricity [6]. Gandini and Almeida estimate that 1.3 billion people (18% of global population in 2017) live without access to electricity, of which those in Sub-Saharan Africa (620 million) constitute nearly half the total [27]; nearly 80% of those lacking electricity access live in poor rural areas [26]. Providing cheap, reliable electrical energy to such groups is a valuable part in improving living standards [25] including human development, reduced infant mortality and improved education, literacy, medical care, the ability for children to study at night, and opportunities for entrepreneurs [20, 28]. With increased electric lighting, up to 4.3 million premature deaths (around 600,000 of which are in Africa) could be avoided through avoiding kerosene burning indoors, which consumes between 20 to 25% of household incomes [27].

For these, and other, contexts, adopting a renewable microgrid (RMG) model of electrical service, rather than connecting to the centralized utility grid, allows developing economies to technologically leapfrog the "industrial legacy and sunk capital of industrialized nations" (i.e., building up a centralized power station and then all the required infrastructure to transmit that

energy to remote locations) and adopt a more appropriate energy source [29], which effectively exploits and integrates the freely-available local renewable resources [7, 19, 22], particularly when such a system is designed and optimized to the resources in a given location [15]. Although a wide range of RE sources are available world-wide, photovoltaic (PV) solar energy is broadly accepted as the most versatile and widely available energy source [30]. As the remote / rural context is based on independence from the utility grid, the RMG source must be designed for resilience to the intermittence and unpredictability of renewable resource [22, 25], either through being coupled with an energy storage (ES) system or by integrating the PV supply with a complementary power source, such as wind energy or dispatchable energy such as fuel-based generator [7, 15, 25, 31]. The same is true for urban MG systems when the minimization of utility grid energy is also a priority [32].

Although there are technological, environmental, and sociological reasons in favor of establishing an RMG in a remote, rural, or underdeveloped location, there are still benefits of doing so within a highly developed or urban context [20] where, thus far, MG installation has been mostly in limited contexts such as campuses and military bases [23]. By shifting the bulk of a residential community's energy consumption from the central utility grid to a distributed, renewable source, energy sources are shifted from being dominated by fossil-fuel depletion and carbon-emitting [20] to lower, almost net-zero carbon emitting, renewable sources [22].

While the U.S. Department of Energy (DOE) definition [24] of a MG uses the term "remote microgrid" (RMG) to describe those that are not connected to the external (utility) grid, there are particular advantages in even non-remote MGs (e.g., urban or suburban residential communities in highly developed countries) similarly eschewing utility grid connection [32] in what is variously termed "off-grid", "islanded", "standalone", or, "energy independent" mode. The work by Abu-Sharkh et al. and Hirsch et al. both refer to the avoided integration difficulties, between utility grid and MG, when the latter are islanded [19, 20]; Planas et al. and Rajanna and Saini describe these difficulties further as arising from the aforementioned intermittency,

randomness, and uncertainty of renewable-energy produced electricity, due to changing weather conditions [22, 25]. Additionally, for every community that is powered by an RMG, the potential increased demand to the power network is removed, potentially even meeting the current need to replace aging nuclear and coal-powered power plants [19].

Isolating a new MG community from the utility grid further avoids the need for government or utilities from having to invest heavily in intensive infrastructures [27] such as the building and maintenance of transmission wires (which may potentially be hundreds or thousands of kilometers long), and all their associated equipment (e.g., transformers, pylons, and right-of-way clearing). Through an islanded approach, the MG itself would also avoid various hardware, including any Point of Common Connection (PCC), inverter or power conditioning equipment – cumulatively these may represent a very significant economic, material, and thus environmental, cost.

2.2 DC-only electrical design

By eschewing grid connection, designers of an MG system have the opportunity to base it entirely on DC-systems. For good economic, technological, and sociological reasons, the global energy industry has been based on AC distribution given its ability for AC electricity to be transformed between low and high voltages and thus be transmitted over long distances as efficiently as technology of the time allowed [15]. However, even with long-distance transmission, recent technological developments have made DC distribution possible and even preferable, with high voltage direct current (HVDC) transmission lines being built thousands of kilometers long (2375km in Rio Madeira, Brazil), and with very high power ratings (7.2GW to 7.6GW at 7.8 MV in the Jinping-Sunan installation, China) [22], making efficient short distance DC transmission for an RMG (between the micro-PV array and individual houses) possible. DC also has energy management advantages at any scale of installation as it has none of the frequency, phase angle, or reactive power elements of AC to control [22]. Under these conditions, power losses in DC

systems are considerably lower than their AC counterparts and are predicted to be inevitable and important parts of future distribution systems [33].

Beyond transmission benefits, DC-only design has benefits in residential appliance efficiency. Personal electronic devices are an increasing proportion of domestic electric consumption [34], and are intrinsically DC technology. AC supplied and wired houses means that each TV, laptop, tablet, mobile phone and smartwatch that is charged in a traditionally wired house loses approximately 11% of energy through the rectification of AC to DC electricity [16]. The benefit of operating DC devices by feeding them directly with DC electricity (rather than requiring a transformer or rectifier to adapt the AC input to DC) is referred to as direct-DC in the work by Vossos et al. [16], which uses the term "DC-internal" to refer to the energy and performance advantage of DC appliances over their AC counterparts. DC-only may therefore refer to the cumulative efficiency and performance benefits of DC electricity in generation (lack of inverter required for the PV array), transmission (including no transformer losses and reactive power losses), and consumption (through DC-internal and direct-DC benefits).

The Vossos et al. work expands upon significant research undertaken by Garbesi at the Lawrence Berkley National Laboratory (LBNL) [14] in which the efficiency and performance benefits of various domestic DC appliances are measured. Examples include fluorescent or LED lights replacing incandescent lightbulbs with around 70% and 18% advantages in DC-internal and direct-DC respectively, heat pumps using brushless DC permanent magnet (BDCPM) motor-driven variable speed drives (VSDs) for heating, with 50% and 12% energy savings over electrical resistance heating (47% and 12% when used for cooling systems), and between 45% and 53% of DC-internal savings for refrigerators, freezers and clothes dryers (with around 11% or 12% direct-DC savings). As personal electronic devices are already all DC-internal devices, their savings are limited to direct-DC savings, which range from 20% to 31%. While the work by Letschert et al. covers various technologies (not just DC-only), it estimates that conversion from current to best available technologies worldwide between 2015 to 2030 would have saved 1500

megatons of CO2 emissions, or about 15% of global totals [35], further underlining the benefits of efficiency-based technological enhancements.

2.3 Solar tracking units

PV energy, already established as a prime option for generating power for an MG, is further described as being "simple, reliable, available everywhere, in-exhaustive, almost maintenance-free, clean, and suitable for off-grid applications" [36]. A range of researchers on solar-tracking technology (where PV modules are based on mechanisms that rotate the module, by varying degrees, to track the relative motion of the sun across the sky and thereby improve the intensity of solar radiation on the PV module) have identified significant benefits over fixed-angle PV installations, depending on its exact type and the PV location in terms of latitude and climate [10, 11, 37-49]. Basic terms are included in Table 2.1.

Table 2.1 – Summary of abbreviations and terms regarding solar tracking

Abbreviation	Meaning	Notes
SAST	Single-axis solar tracker	Broadly split into vertical-, and horizontal- axis trackers
V-axis	Vertical axis	The module's rotating axis is vertical, allowing continual variation of the module's azimuthal axis through daylight hours. This is best for small arrays or single modules.
NS-axis	North-south horizontal axis	Rotating axis is horizontal to the ground pointing from north to south; the rotation of the modules therefore tracks the daily apparent motion of the sun from east to west.
EW-axis	East-west horizontal axis	Rotating axis is horizontal to the ground pointing from east to west; the rotation varies the tilt angle which improves solar intensity for both daily and seasonal variation.
DAST	Dual-axis solar tracker	These track the sun's apparent motion with two degrees of freedom, i.e., continuously varying azimuthal and tilt angle during daylight hours.

Across the literature, it is found that:

- Dual-axis trackers offer the greatest energy advantage over fixed-angle PV modules, although this generally does not consider the effects of self-shading (a single module will perform

better on a DAST mechanism than if it is static, but the degree of that energy advantage may not hold for a large array if each module is tightly packed, creating significant shade on other modules).

- East-West oriented SASTs, in which tilt angle varies to account for changing angle of the sun from the horizon according to daily and seasonal variations, provides the next best energy advantage in most locations.
- North-South oriented SASTs also offer energy advantage over static modules, though generally less than DAST and East-West oriented SASTs.
- The degree of energy advantage generally increases with latitude, although this is moderated by a decreased proportion of energy advantage when cloudy conditions are considered.

SECTION 3

Literature applications to the CSG model

The Trends and conclusions from the literature review inform three main aspects of the CSG: first, it confirms "off-grid" or energy-independent design has sufficient environmental, technological, and economic advantages and should be pursued; second, that DC-only design also has many benefits both to the CSG development and also upstream infrastructure through reduced impact on the grid; and third, that single-axis tracking may be preferable to dual-axis tracking.

On the first of these design aspects, the off-grid approach is chosen as it should result in less burden on the centralized utility grid both in terms of generation capacity and transmission infrastructure. An islanded approach also prevents unnecessary excess energy consumption by residents who might otherwise over-consume cheap grid electricity (especially at night when PV generation is zero) rather than remaining within the limits of what the PV-battery system can provide.

On the second aspect a DC-only design is selected for three further subsidiary reasons. First, in terms of generation, transmission, and storage, less equipment is required, which reduces the financial and material cost, and reduces the need for complex energy management in terms of frequency, phase angle, mutual inductance, and reactive power management, and removes the need for inverters especially, which in turn simplifies PV design. Second, DC-only design also allows for greater synergy between PV array and battery banks, which both run off DC electricity, and removes any efficiency losses in inverters, which are no longer required. This, in turn, this allows for DC-only design in appliances, the third subsidiary reason, as DC-only appliances allow for great efficiency and performance advantages in appliances in terms of their internal operation (DC-internal) and the lack of AC rectification (direct-DC).

Lastly, for the PV array, while the literature confirms that solar tracking is broadly advantageous, which exact mode is best for the location could be a complex issue to solve. Given the test-case's latitude (too low for a v-axis array to be optimal) it is likely that an east-west oriented SAST (in which tilt-angle is continuously varied during daylight hours) is likely to be the best option, as DAST will require low GCR (and thus large PV footprint) for the second degree of freedom in tracking to overcome self-shading limitations. However, as explained in Section 6, the choice of North-South oriented SAST (with modules tracking East to West over the day) is forced by the functionality of the modeling software. These literature-informed applications to the CSG concept are summarized in Table 3.1.

Table 3.1 – Summary of CSG design choices informed or confirmed by the literature review.

Design area	CSG design choice	Operational advantages
Microgrid connection	Standalone / islanded	• Allows maximal DC-only electrical architecture. • Removes any upstream impact on generation and transmission. • Maximizes the reduction of fossil-fuel depletion and carbon emissions.
DC-only or mixed AC-DC architecture	DC-only electric architecture	• Removes the need for inverters at the PV array or in houses. • Removes the need for sophisticated electrical management in community-scale transmission. • Provides increased synergy with PV-Battery-Appliance system and removes inversion and rectification losses. • Allows for greatly improved electrical performance within houses, greatly reducing residential loads.
PV tracking	N-S SAST	• SAST provides a distinct energy advantage over fixed arrays. • SAST is cheaper and tends to be more reliable than DAST, and with limited area and large arrays, tends to have better performance than DAST. • North-South orientation is required for self-shading calculations on NREL SAM (Section 6).

SECTION 4

Model resolution

In assessing the feasibility of the CSG model to operate in an off-grid manner, the differences between the electrical demand of the entire community the supply from the PV array will be compared at an hourly resolution for the average solar day (Table 4.1) for each of the calendar months. Calculations and comparisons in terms of the average solar day for each month, rather than each day of the year, is a standard method within the solar industry [50] and allows for computational efficiency with fewer calculations required and minimal loss of accuracy. This resolution is referred to as "hourly-monthly" results within this study. With 24 hours in a day and 12 months a year, this gives a regular set of 288 results, which are referred to as "288" tables or results.

Ultimately, while this is a suitable simplification to allow for efficient computational methods, the average solar day method limits the resolution of the modeling methods, resulting in a likely underestimation of capability and overestimation of battery demands. This strengthens any off-grid feasibility determination. However, the likely over-estimation of battery requirements is undesirable, and so options for developing the modeling methods and improving resolution are discussed in Section 9.2.

Table 4.1 – Average solar day in each month

Month	Day in the month
1-January	17
2-February	16
3-March	16
4-April	15
5-May	15
6-June	11
7-July	17
8-August	16
9-September	15
10-October	15
11-November	14
12-December	10

SECTION 5

Demand-side modeling

5.1 Introduction to demand-side modeling (DSM)

Using original mechanistic modeling and EPA data, an average DC-electric power demand per home is determined for 288 monthly-hourly intervals with the entire microgrid residential system predicated on DC-only devices and electrical transmission systems (Tables 5.1 and 5.2). These are compared to the equivalent PV supply (Section 6) at the same monthly-hourly resolution to determine quantity of energy surplus or deficit at each interval (Section 7).

5.2 DSM design process

While software such as eQuest [51] can provide sophisticated building energy modeling (and from which basic energy use profiles have been utilized in this study), none were identified as being able to model the specific demands of DC-only appliances. Therefore, to model residential energy demand appropriate for the CSG model, an original model was developed in which hourly values of electrical demand were computed separately for each of the main end-use categories for the average solar day of each month, $H_{m,h}^{C}$, where m and h are the specific month and hour of the 288 monthly- hourly values for average solar days of the month (Section 4), and the C superscript is replaced with one of the end-use indices (Table 5.1).

Once the monthly-hourly demands were determined for each of the end-use categories, the total demand for each CSG house in that hour, $H_{m,h}^{T}$, was then calculated:

$$H_{m,h}^{T} = \sum_{C}^{All\ C} H_{m,h}^{C} \tag{5.1}$$

Table 5.1 - Nomenclature symbols and definitions in DSM model

Symbol	Description
	General process terminology
A	As a subscript to other parameters, to denote those as alternating current (AC)
AC	Alternating current, not air-conditioning, which is referred to as space cooling, SC
C	(End-use) category. As a superscript, to indicate an individual end-use category in general; where this is replaced with one of the end-use category symbols (below) this indicates the load for that specific category.
D	As a subscript to other parameters, to denote those as direct current (DC)
DC	Direct current
H	Hourly load for a single CSG house, with subscripts m and h indicating which hour of the 288 results, and C or T superscripts indicating a specific category or the total load respectively.
kWh	Kilowatt-hour, standard unit of electrical energy consumption, load, or demand. Equivalent to the electrical energy dissipated by one kW of electric power for one hour of time.
L	Electric load. Superscripts indicate whether it refers to a single end-use category (options below), or for the total load (T) for a house; subscripts indicate whether it is the estimated AC equivalent load (A) or the derived DC-only load (D)
MBtu	Mega British thermal unit, 1 x 10^6 Btu
T	Total load. As a superscript, used to indicate the total load for a given house, as the sum of the individual categories.
	End-use categories
CD	Clothes drying
LI	Lighting
M	Miscellaneous
RF	Refrigeration
SC	Space cooling (air-conditioning)
SH	Space heating
WH	Water heating

Residential electric loading and consumption was divided into seven categories (Table 5.1): space heating and cooling, water heating, food refrigeration (including both refrigerator and freezer units), electric lighting, clothes-drying, and miscellaneous consumption The categories are based upon the largest categories reported by the U.S. Energy Information Administration (EIA) and the Environmental Protection Agency (EPA) (Table 5.2) and are separately modeled in Appendix B4, producing 288 $H_{m,h}^{C}$ values for each category.

Table 5.2 – Dominant residential electrical end-uses in the U.S. for existing AC technology

Source		EIA[52]	EPA[53]	LBNL [14]
SH[1]		14.8%	26%	-
SC		16.9%		16%
WH		13.7%	10%	-
LI		10.3%	12%	15%
M[2]	TVs and related	6.9%	29%	-
	Other electronics	13.0%		-
	"Other uses"	12.9%	23%	-
RF		7.0%		9%
CD		4.5%		-

Notes

1. Space heating is electricity consumption only and underrepresents total energy demand in this category as many houses use natural gas.
2. Miscellaneous (M) in CSG work includes end-uses such as clothes washing, cooking, dishwashers, ceiling fans, personal electronic devices (TVs, modems and wireless routers, phones, tablets, computers, smart speakers, DVD players, and other entertainment appliances). External lighting, security systems, and pool equipment are examples of specific end-use categories not included.

In general, the computation for each category, C, were conducted according to the following basic methodology stages:

5.2.1 Stage I: Estimating the annual AC electric demand, L_A^C,

This estimation is conducted to estimate the demand in an equivalent house similar in characteristics to a home in the CSG but with legacy technology (AC appliances and wiring) and connected to the grid.

The data for this estimation is taken from the U.S. Energy Information Administration's (EIA) five-yearly Residential Energy Consumption Survey (RECS) [54]. At the time of this research the most recent available data is the 2015 survey [55] and is referred to as RECS-15. The RECS data are both broad and detailed allowing for reliable estimation of end-use loads. The data is divided into Housing Characteristics (organized into various "HC" tables [56]) and Consumption & Expenditures (in various "CE" tables [57]). Of many CE tables, table CE3.4 covers the relevant geographic region in the U.S. (the South) and the table itself then lists end-use energy quantities according to a variety of housing categories, including:

- Census division (South Atlantic; East South Central; and West South Central)

- Climate region (Very cold/cold; Mixed-Humid; Mixed-dry/Hot-dry; Hot-humid; Marine)
- Housing unit type (Single-family detached; Single-family attached; Apartments in buildings; Mobile homes)
- Ownership of housing unit (Owned (Single-family, Apartments, Mobile Homes), and Rented (same sub-categories as Owned);
- Year of construction (by decade, plus the five-year period of 2010-2015)
- Total square footage (500 square foot intervals, from "fewer than 1,000" to "3,000 or greater", including "2,000 to 2,499" and "2,500 to 2,999"
- Number of household members (1, 2, 3, 4, 5, 6 or more)
- Main heating fuel (Natural gas, Electricity, Fuel oil / kerosene, Propane)

The underlined values in the list above were those that were sampled for the estimation of annual AC load; however, not every housing category was used in each case. Rather, a specific approach was taken appropriate to the nature of each end-use category, and this is detailed in the relevant sections (Appendix B4). Where "Total square footage" was relevant, the average of the "2,000 to 2,499" and "2,500 to 2,999" intervals was taken to approximate the values for the CSG's 2,500 square foot floor area.

5.2.2 Stage II: Annual DC electric demand, L_D^C

In this stage, the calculation is specific to that of a CSG house, with DC appliances and wiring, and with certain other specific considerations depending on the end-use category (Appendix B4).

In calculating the value of L_D^C for each category, the work of Garbesi et al. was instrumental, providing the energy savings for a wide range of electrical appliances, when standard-technology AC devices are replaced with DC alternatives. For each type of device, the energy savings are split into DC-internal and direct-DC savings [14]. These are summarized in Table 5.3 and are referred to throughout Section 5. Examples of DC-internal savings include Variable Speed Drives (VSDs) and Brushless DC Permanent Magnet (BDCPM) motors in place of standard AC

induction motors, heat pumps in place of electric resistance heaters, and LED or CFL (compact fluorescent lamps) in place of incandescent light bulbs.

In general, the equation to determine the DC demand is:

$$L_D^C = L_A^C(1 - \eta_{int})(1 - \eta_{dir}) \qquad (5.2)$$

where η_{int} and η_{dir} represent the DC-internal and Direct-DC savings, respectively.

Relevant symbols and terms are included in additional nomenclature (Table 5.1).

Table 5.3 - Summary of DC energy savings for various appliance types.

End-use category	DC appliance example	DC-internal energy savings[1]	Direct-DC savings[2]
Central air conditioners	Variable speed compressor fans run by BDCPM	47%	11%
Lighting (incandescent)	CFL or LED bulbs	73%	18%
Electric water heater	Heat hump (BDCPM)	50%	12%
Refrigerators & freezers	Detailed[3]	53%	13%
Space heating	Heat pump	40%	12%
Clothes drying	Heat pump	45%	11%
Electric cooking	Induction cooktop	12%	12%
Dishwasher	DC compatible motor	51%	12%
Clothes washers	BDCPM variable speed	30%	13%
Ceiling fans	BDCPM variable speed	30%	13%
TVs and personal electric devices	None, as these are already DC-internal devices		20%

1. See Table 8 in Garbesi et al. [14]
2. See Table 10 in Garbesi et al. [14]
3. See Table 8 in Garbesi et al. [14].

5.2.3 Stage III: Allocating, or fitting, L_D^C to monthly-hourly resolution.

This process produces the 288 required $H_{m,h}^C$ values of the required hourly-monthly resolution of electrical demand, $H_{m,h}^C$, for each end-use category. Computational methods for each category are:

1. Determining the expected net monthly electric (DC) load for each month, M_m^C, where m represents the month of the year, with m=1 representing January, m=2 February, etc. N.B. at this stage of the computation the D subscript was no longer necessary as all loads were DC; both A and D notations were dropped.

   Methods for this step varied depending on the nature of the end-use category, C, some relying heavily on ambient temperature (SH, SC, WH) when the end-use category is heating or cooling related, and others relying on eQuest use profiles (RF, LI, CD, M).

2. Determining the expected average daily electric load for each month, D_m^C, where:

$$D_m^C = \frac{M_m^C}{n_m} \qquad (5.3)$$

   and where n_m is the number of days in the month (n_1=31 for January, n_2 = 28 for February). The complication of leap years is omitted in this study, in line with such omission in SAM simulations (Section 6).

3. Calculating the expected hourly electric load for each hour of the average day in each calendar month, $H_{m,h}^C$, the indices having the same meaning as with previous parameters.

When steps 1-3 were calculated in part from ambient temperatures at the initial geographic CSG context for this study (Athens, Georgia, USA), the necessary temperature data

were taken from the relevant National Solar Radiation Database (NSRDB) weather data file (Section 5.3). As well as providing standard and reliable data, it allowed for consistency with the supply-side modeling as NREL SAM utilizes the same weather data for its simulations [58].

The desired internal residential temperatures, i.e., the thermostat temperatures, are also required to model the temperature related end-uses. Objective thermostat settings were taken from government agencies and utility providers (Table 5.5) and applied throughout the demand-side model.

Table 5.5 – Recommended thermostat settings from a range of objective sources [59-62]

Time	Winter thermostat settings	Summer thermostat settings
6:00- 8:00 am	68 °F	78 °F
8:00am - 6:00pm	60 °F	85 °F
6:00pm – 10:00pm	68 °F	78 °F
10:00pm – 6:00am	60 °F	82 °F

The time periods that form part of these thermostat recommendations could be re-termed as overnight (10pm to 6am), occupied (6am to 8am and 6pm to 10pm), and unoccupied (8am to 6pm, i.e. working hours), and do not therefore represent weekend conditions in which one might hope the majority of community residents do not have to work. Therefore, to improve the accuracy and validity of the model it was necessary to make a distinction between weekday and weekend thermostat settings, the latter having later waking hours and fewer unoccupied hours. A further level of characterization was applied to consider varying levels of occupancy (lower and higher) for both weekday and weekends (Table 5.6).

Table 5.6 – Index and parameters for week and occupancy characterization

	Lower occupancy (l)	Higher occupancy (h)
Weekday (w)	$\boldsymbol{T^{w,l}}$	$\boldsymbol{T^{w,h}}$
Weekend (e)	$\boldsymbol{T^{e,l}}$	$\boldsymbol{T^{e,h}}$

While weekday lower occupancy would represent the standard conditions indicated (Table 5.5), higher occupancy would represent a household in which at least one member is at home throughout the day. Prevalence parameters are created to represent the proportion of high occupancy houses in weekday and weekend modes, ρ and σ respectively, and for simplicity in initial modeling, both are assigned the neutral value of 0.50, i.e., the initial assumption being an equal split of higher- and lower- occupancy houses within the neighborhood. If this model were to be applied to design a CSG development in a specific location, demographic research into the likely customer base might inform a different value of prevalence parameters. For example, the practice of homeschooling, working from home and the time of year (e.g., during public holidays or school vacations), would increase the value of ρ; a high proportion of retirees in the community would result in higher values of both ρ and σ. The recommended settings for heating and cooling (Table 5.5) were thus adjusted according to the above characterization principles to create eight CSG thermostat profiles (Table 5.7).

For other categories in which demand depends less on temperature than other factors, calculations were derived partly from relative eQuest user profiles (Section 5.4), and for some categories, a combined calculation was used. Further nomenclature, relevant to stage III processes, are included in Appendix B1.

Ambient temperature data is required for modeling energy profiles for temperature-related end-use categories, e.g., to determine how much water needs to be heated from ambient temperature for residential use. This data was taken from the National Solar Radiation Database's (NSRDB) TMY (Typical Meteorological) files. Consistent with the modeling resolution (Section 4), only temperature data from the average solar day is required for this work. The TMY-2019 data for Athens, GA, are summarized in Appendix B2.

Table 5.7 – Thermostat settings for CSG demand-side modeling according to different times and occupancy profiles.

	Day:	Weekday				Weekend			
	Occupancy:	Lower occupancy		Higher occupancy		Lower occupancy		Higher occupancy	
	Parameter:	(1-ρ)		ρ		(1-σ)		σ	
	Heating/Cooling:	H	C	H	C	H	C	H	C
Starting time of interval:	0:00	60	82	60	82	60	82	60	82
	1:00	60	82	60	82	60	82	60	82
	2:00	60	82	60	82	60	82	60	82
	3:00	60	82	60	82	60	82	60	82
	4:00	60	82	60	82	60	82	60	82
	5:00	64	80	64	80	60	82	60	82
	6:00	68	78	68	78	64	80	60	82
	7:00	68	78	68	78	68	78	64	80
	8:00	60	85	68	78	68	78	68	78
	9:00	60	85	68	78	68	78	68	78
	10:00	60	85	68	78	60	85	68	78
	11:00	60	85	68	78	60	85	68	78
	12:00	60	85	68	78	60	85	68	78
	13:00	60	85	68	78	60	85	68	78
	14:00	60	85	68	78	60	85	68	78
	15:00	60	85	68	78	60	85	68	78
	16:00	60	83	68	78	60	85	68	78
	17:00	64	80	68	78	60	85	68	78
	18:00	68	78	68	78	60	82.5	68	78
	19:00	68	78	68	78	64	80	68	78
	20:00	68	78	68	78	68	78	68	78
	21:00	68	78	68	78	68	78	68	78
	22:00	60	82	60	82	60	82	60	82
	23:00	60	82	60	82	60	82	60	82

N.B. gray-shaded cells represent an empty house, blue-shaded cells represent likely sleeping hours, with yellow-shaded representing an occupied and awake house. Red text signifies heating modes, and blue text, cooling modes.

5.3 eQuest model

Although the eQuest energy modeling tool [51] is not suited to providing a detailed model of a DC-only building, it provided hourly and monthly relative use profiles required by Stage III DSM computations (Section 5.2.3) to calculate the monthly and hourly loads. An energy-efficient house was modeled in eQuest (Appendix B3) and the resulting energy model (Figure 5.1), informed the setting of the time-dependent parameters from which $H_{m,h}^{C}$ values were derived.

Electric Consumption (kWh x000)

	Jan	Feb	Mar	Apr	May	Jun	Jul	Aug	Sep	Oct	Nov	Dec	Total
Space Cool	0.06	0.14	0.59	0.97	1.91	2.61	3.30	3.25	2.30	1.15	0.39	0.12	16.78
Heat Reject.	-	-	-	-	-	-	-	-	-	-	-	-	-
Refrigeration	-	-	-	-	-	-	-	-	-	-	-	-	-
Space Heat	0.05	0.02	0.01	-	-	-	-	-	-	-	0.01	0.06	0.14
HP Supp.	1.41	1.42	0.17	-	-	-	-	-	-	0.00	0.35	0.89	4.23
Hot Water	1.69	1.59	1.75	1.65	1.56	1.36	1.29	1.19	1.15	1.27	1.35	1.54	17.38
Vent. Fans	0.24	0.21	0.19	0.17	0.19	0.18	0.20	0.19	0.18	0.18	0.19	0.22	2.34
Pumps & Aux.	-	-	-	-	-	-	-	-	-	-	-	-	-
Ext. Usage	-	-	-	-	-	-	-	-	-	-	-	-	-
Misc. Equip.	1.46	1.31	1.44	1.40	1.46	1.40	1.45	1.45	1.40	1.46	1.40	1.44	17.05
Task Lights	-	-	-	-	-	-	-	-	-	-	-	-	-
Area Lights	0.72	0.63	0.66	0.61	0.62	0.58	0.60	0.62	0.63	0.68	0.68	0.71	7.73
Total	5.62	5.31	4.79	4.80	5.73	6.12	6.83	6.70	5.65	4.74	4.37	4.98	65.65

Figure 5.1 – eQuest energy model

5.4 Demand calculation results by end-use category

Detailed computations of the monthly-hourly demand values, $H_{m,h}^{C}$, were conducted for each of the seven end-use categories. Water heating (WH) was a special category, as this load was modeled as being partially met through roof-top mounted solar water heating panels. Details of this, and each of the end-use computations, are provided in Appendix B4. A summary of the process is provided in Table 5.8, with graphical representations of the computations provided in Figures 5.2 to 5.8.

Table 5.8 – Summary of hourly demand profile computations for each end-use category

End-use category (C)	Standard annual load		DC savings	DC load	Monthly-hourly demand determination
	Value / kWh	Determination	DC-internal; Direct-DC		
Space heating (SH)	3874	RECS-15: electrically heated homes, adjusted for 2,500ft^2 homes	30%; 12%	2046	According to difference in ambient temperatures and thermostat settings
Space cooling (SC)	3087	Average of RECS-15 data for climate, construction year & size.	47%; 11%	1456	
Water heating (WH)	5093	RECS-15: electrically heated homes, adjusted for 4-person household	50%; 12%;	1198	By eQuest use profiles, further reduced by solar heating.
Refrigeration (RF)	850	RECS-15 data for 4-person household size	53%; 13%	345	Monthly and hourly by eQuest use profiles
Lighting (LI)	AC: 515 DC: 713	RECS-15 CE data for 2,500 ft^2 house, split into approx. AC and DC loads.	73%; 13%	699	
Clothes drying (CD)	1055	RECS-15 detailed end-use for 4-person household	45%; 11%	516	Hourly by eQuest use profiles
Miscellaneous loads (M)	1950	Various appliance loads from RECS-15 detailed end-use tables, for 4-person household size	Various	1323	Monthly and hourly demands by eQuest use profiles

The first three categories (SH, SC, WH) have significant seasonal variation and so results for those end-uses are shown at monthly resolution.

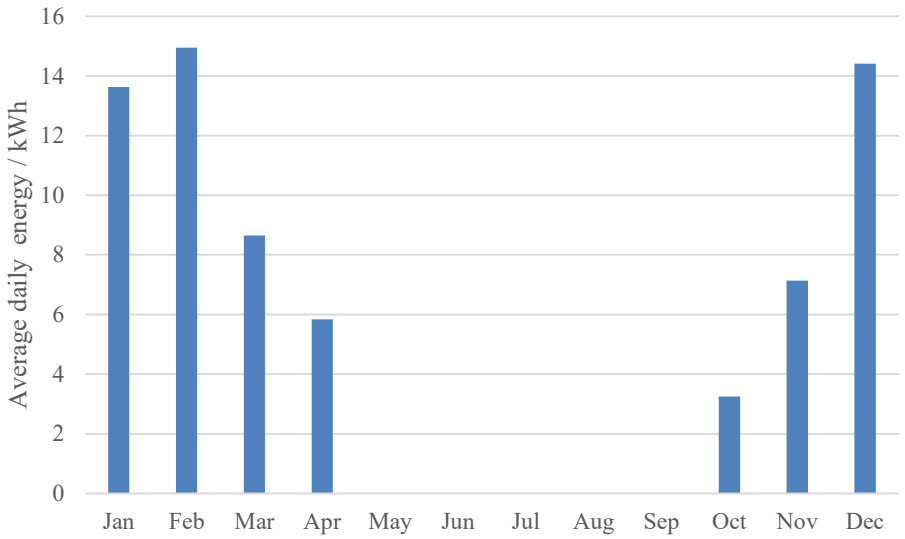

Figure 5.2 – average daily space heating load by month

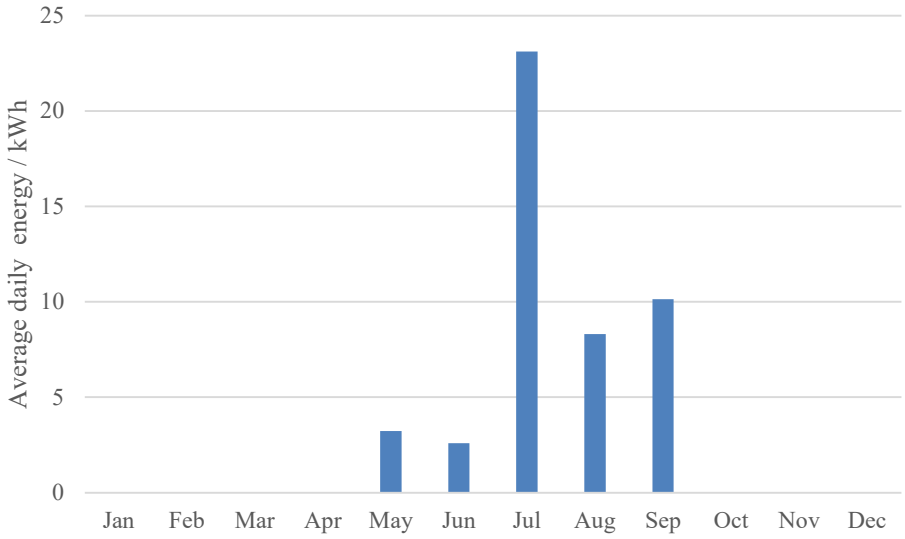

Figure 5.3 – average daily space cooling load by month

The very high cooling load in July compared to other summer months is a consequence of the daytime temperatures reported by NSRDB data (Table B2 in Appendix B2) and the thermostat temperatures as set by the objective sources (Table 5.7). Only daytime temperatures are significant as, at night (from 21:00 to 06:00), the thermostat settings are above ambient

temperatures and no work is done by the space cooling equipment. In July, the average daytime temperature (07:00 to 20:00) is 89.5ºF, significantly above both the 85ºF and 78ºF thermostat settings for low- and high-occupancy households, respectively. Space cooling is active throughout that period in July, and with relatively high consumption values (between 1.63 and 2.73 kWh per house). By comparison, in August, the average temperature in the same interval is only 83.0ºF, crucially between the two thermostat settings, meaning there would be zero cooling load in 50% of the houses in this model, i.e., the low-occupancy houses. Daytime temperatures that cross the threshold of the higher thermostat settings is therefore a significant tipping point, doubling the number of houses that register a cooling load, and introducing a higher cooling load (as this is proportional to the temperature differences between ambient and thermostat) for those extra 50% of houses. Two other unexpected results (the June load being less than May, and August less than September) can be similarly explained. In those months, the active period of space cooling is in a tighter window (11:00 to 17:00) due to lower daytime temperatures overall, and in that period, the average May temperature is greater than the average June temperature (82.7 ºF and 81.6 ºF respectively) and September's is greater than August's (88.3 ºF and 86.8 ºF), which in turn lead to higher temperature differences between ambient and thermostat, and therefore higher cooling loads. As the monthly temperatures are only based on NSRDB for the average solar day of each month, the accuracy of the reported temperature is limited, and an assessment based on each day of the month may give a smoother temperature profile over the year.

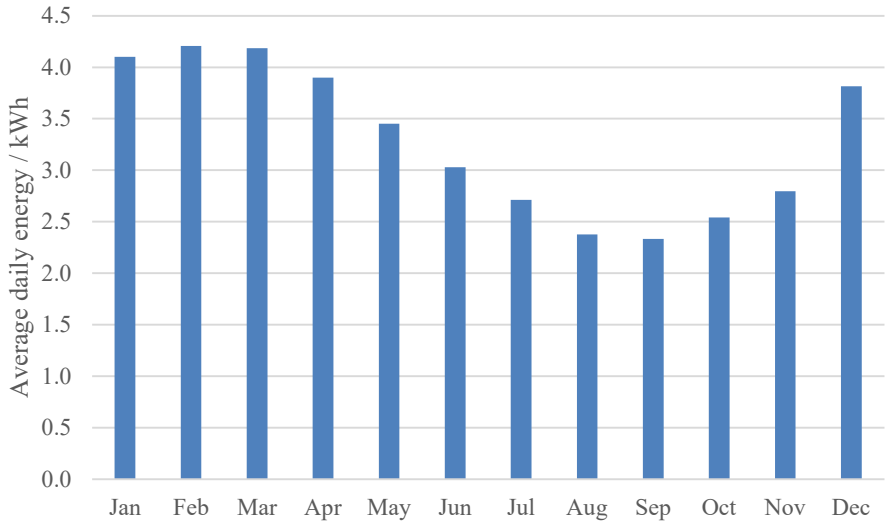

Figure 5.4 - average daily water heating load by month

RF and LI categories have significant monthly and hourly variations, so results for those end-uses are displayed for both resolutions.

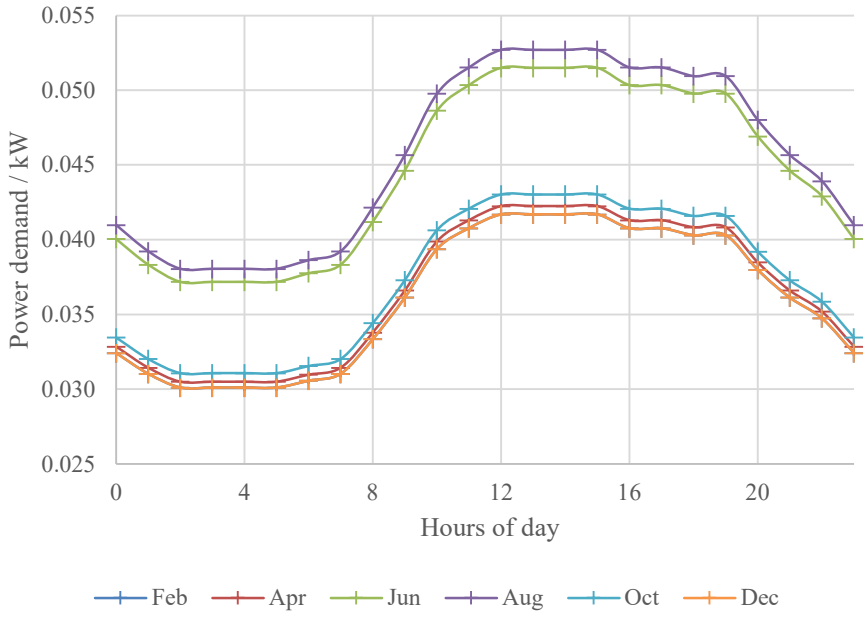

Figure 5.5 – hourly and seasonal variation of refrigeration load

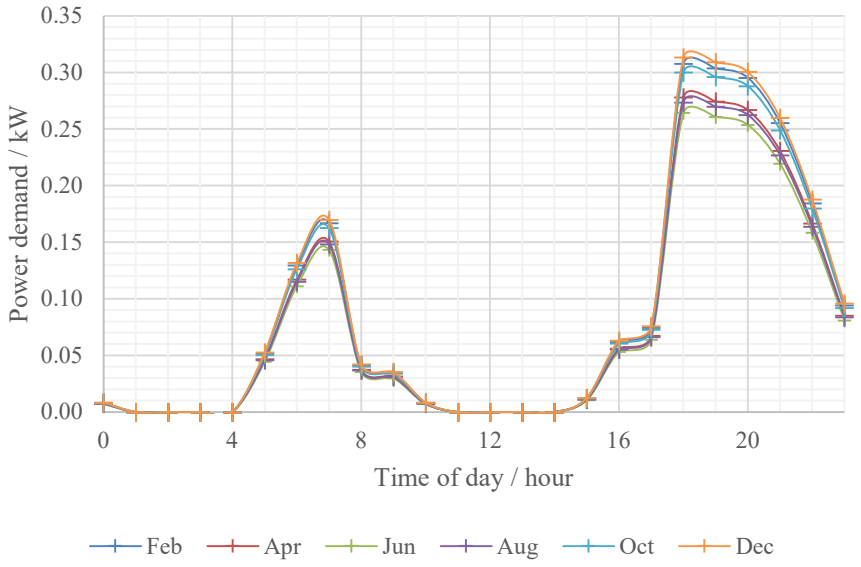

Figure 5.6 – hourly and seasonal variation of lighting load

CD and M have negligible monthly variation and so the demand for those end-uses are shown only at hourly resolution.

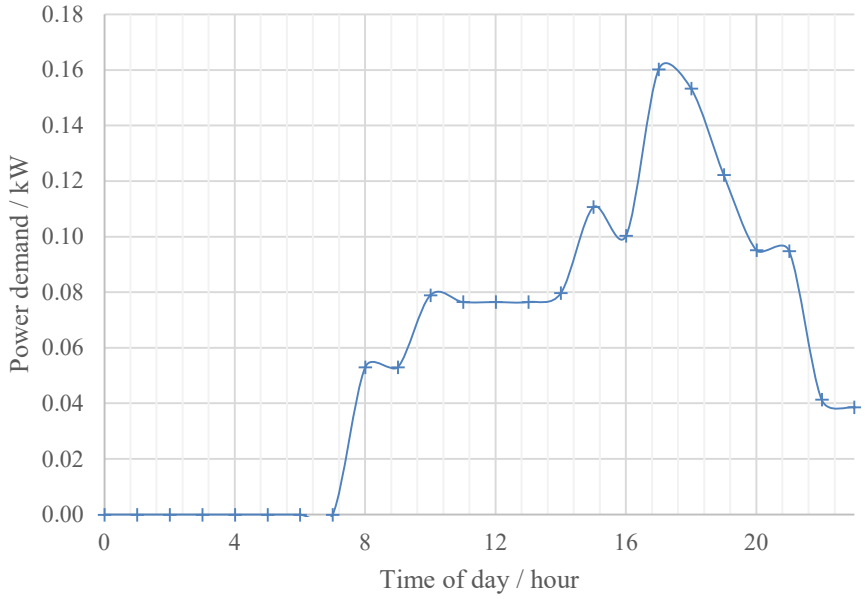

Figure 5.7 – hourly variation of clothes drying load

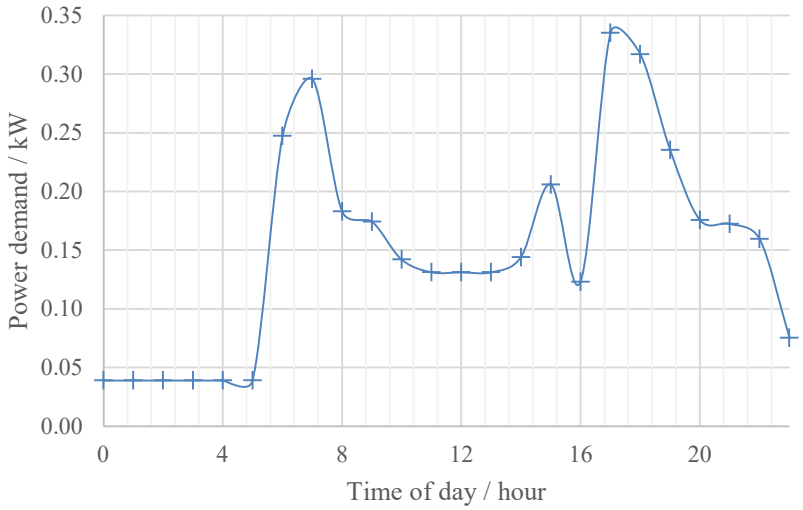

Figure 5.8 – hourly variation of miscellaneous loads

5.5 Total demand profiles for a CSG house

5.5.1 Calculation and evaluation of total demand profiles by category

Once all the monthly-hourly profiles for each of the end-use categories in Appendix B4 were determined, these were then combined to find the total load for each of the 288 monthly-hourly time intervals, $H^T_{m,h}$:

$$H^T_{m,h} = \sum_C^{All\ C} H^C_{m,h} = \left(H^{SH}_{m,h} + H^{SC}_{m,h} + H^{WH}_{m,h} + H^{RF}_{m,h} + H^{LI}_{m,h} + H^{CD}_{m,h} + H^{M}_{m,h}\right) \quad (5.4)$$

Each of the annual category loads and the total CSG load can be compared with averages according to RECS-15 (Figures 5.9a, b). Several aspects combine to provide confidence in the CSG demand-side modeling:

- All categories show energy savings in the CSG model compared to the standard model, as expected.
- The very large proportional differences in space heating and cooling categories are due largely to the significant DC-internal savings for these systems (Table 5.3), 45% and 47% respectively.

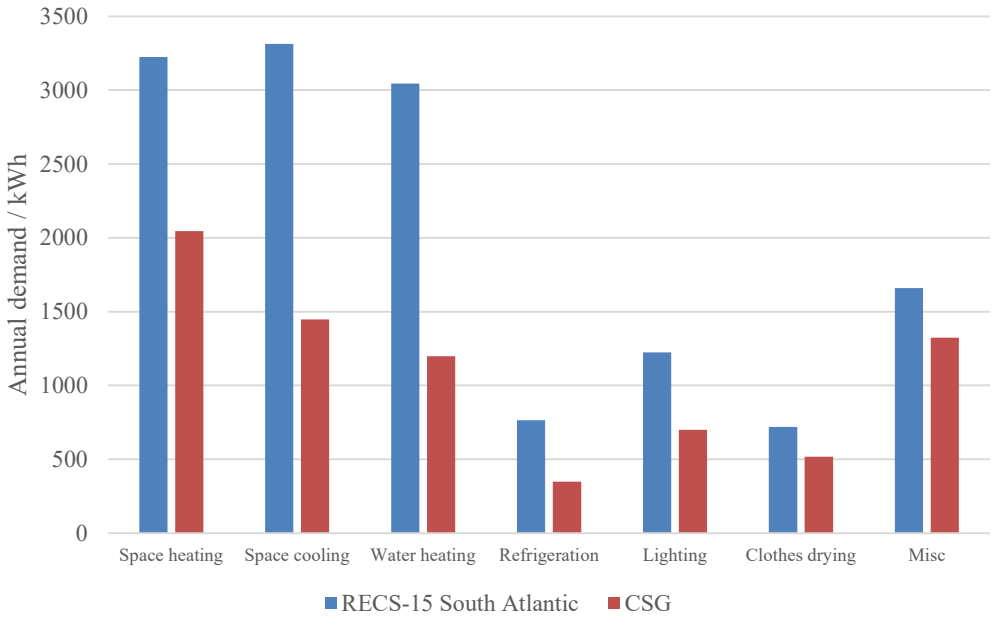

Figure 5.9a – comparison of CSG modeled and RECS-15 reported demand, by end-use category

- The combination of the non-electric savings of a solar water heater and the DC-savings in the air-conditioning system, allow for a 75% reduction of the original demand value standard AC demand for a CSG equivalent and a 61% advantage (1845kWh compared to 3043kWh) over the RECS-15 South Atlantic average.

- The clothes drying in the CSG has less demand than for the South Atlantic average; however, the proportional change is much less than for other categories. As the CSG demand is based upon household size (four-members) the AC standard equivalent load for the CSG was high, and indeed above that of the South Atlantic average (1088kWh comparted to 719kWh). Therefore, although DC savings provide a large decrease in expected demand (51%) the lower DC demand value is proportionally closer to the South Atlantic average than other categories.

- The miscellaneous category is also lower for the CSG DC-only model than the current standard. A significant proportion of the miscellaneous loads are already DC powered (personal electronic devices, entertainment systems) that are already DC-efficient and so the degree of energy savings in this category is limited.

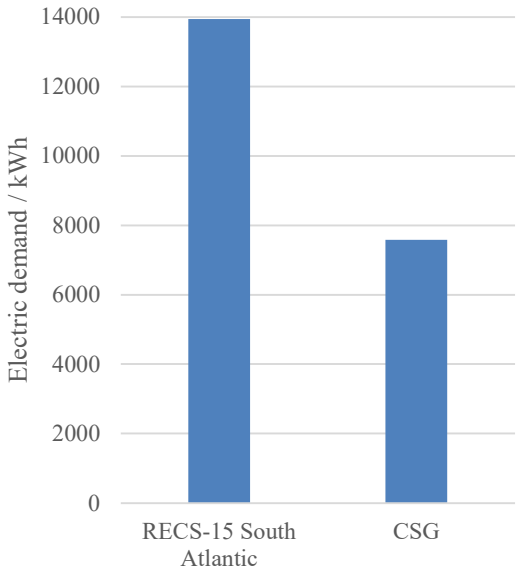

Figure 5.9b – comparison CSG modeled and RECS-15 reported total demand

- Overall there is significant DC savings in the CSG model (less 8000kWh compared to around 14,000 kWh), or 42%. This falls within the 30 to 50% savings for DC appliances as suggested in the work by Vossos et al. [16].

5.5.2 Evaluation of hourly and monthly profiles.

Comparative results for energy demand are difficult to find in the literature as most other studies either do not deal with equivalent systems or provide results with very different levels of resolution. Most are either in locations with very different typical residential energy demands (e.g., located in a less energy-intensive economy than the U.S.) or study systems of a different type or at a different

resolution (e.g., considering commercial energy demand or residential demand aggregated over an entire economy). One study, Lee et al. [63] was the closest that was identified, reporting hourly residential variation for different seasons of the year in Adelaide, Australia (Figure 5.10).

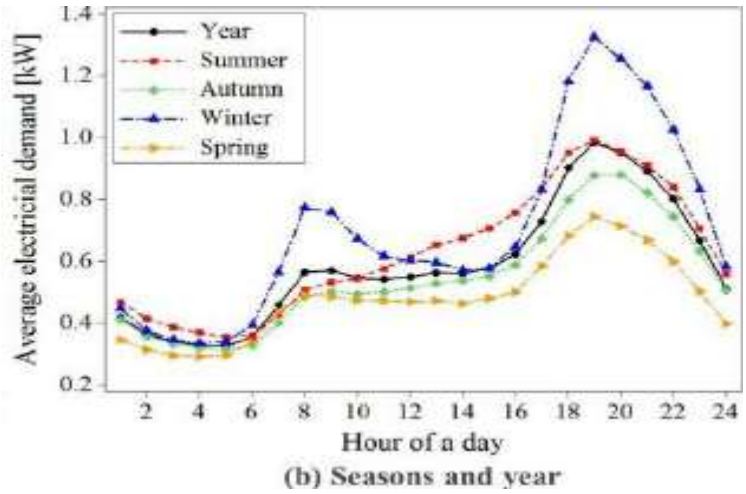

Figure 5.10 – Hourly and seasonal variation of residential loads, as reported by Lee et al. [63]

By comparison, CSG results for total demand are displayed in Figures 5.11 and 5.12a, b.

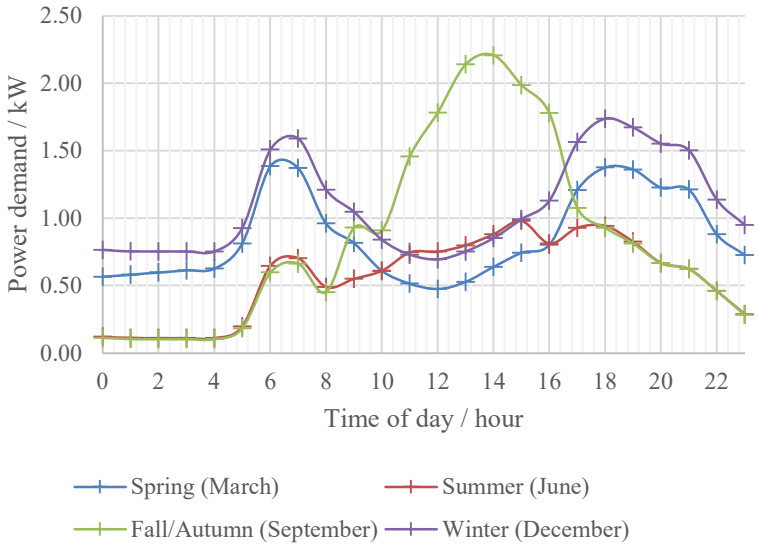

Figure 5.11 – Major seasonal variation in total demand for a CSG house

As with the literature example, there are two main peaks for spring, summer, and winter loads: one in the morning when the household awakes and another in the evening when household members return to the house. Both demand curves show very low overnight values and mid-day values are lower than the peaks but higher than overnight values. These areas of agreement provide significant validation to the DSM.

There are two main differences that should be addressed before the CSG model can be considered valid.

- First, the September curve for the CSG is dramatically different to the Lee et al. study, showing peak demand during the working day. This can be explained by the temperature data for September being significantly (and possibly erroneously) higher than for June (a shortcoming in the model, discussed in Section 9.2) and is higher than that for context of the Lee et al. study.
- Second, the Lee et al. study has larger peaks in the evening than the morning, whereas in the CSG model they are about equal. One possible explanation could be the difference in heating and cooling between the theoretical CSG model and the real study by Lee et al. In the former, thermostat settings and occupancy are considered the same in the morning and the evening leading to similar heating and cooling intensities in those two periods; in reality (the latter), these may differ. A second explanation could be the impact of the benefits of DC savings: if greater peaks in real-context houses occur mostly due to high occupancy, i.e., more people at home using more devices, than the extent of this would be reduced more due to DC savings than the morning peak when fewer appliances may be used (cookers, TVs, washers, etc.).

5.5.3 Evaluation of seasonal variation

The trends in CSG demand from April to September (Figure 5.12a) are expected given the values detailed in Appendix B. In the seasonal warming period from spring to summer, overall loads and mid-day peaks increase due to the increased need for space cooling; this process reverses in the trend from summer to autumn/fall, with the slight anomaly for August to September, due to the temperature anomaly already discussed. At the height of summer, the overall demands are highest,

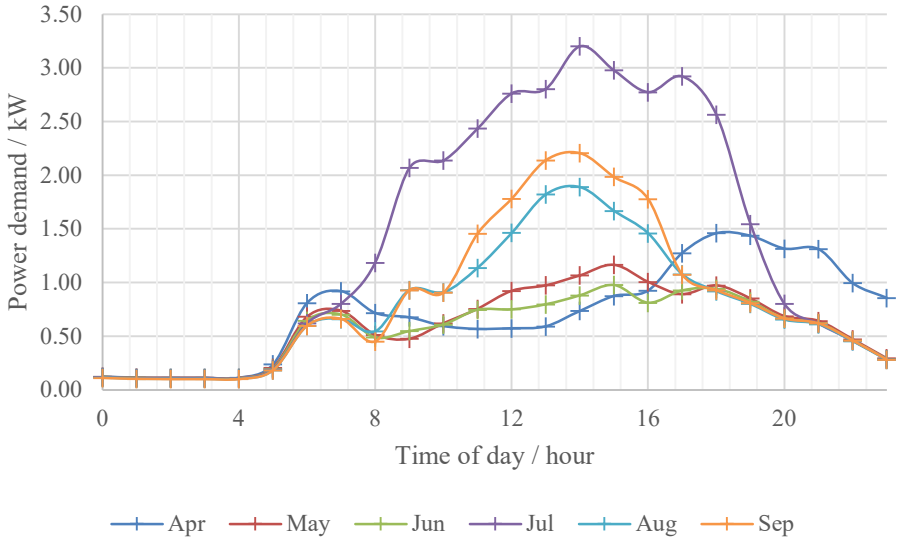

Figure 5.12a – Monthly variation of overall power demand (April to September) for average CSG house

but they are coincident with expected PV generation so meeting that demand should not be overly problematic, and has minimal stress on energy storage systems. Towards the more temperate parts of the year, spring and fall/autumn, the reverse is true: overall demand is less, but its timing provides the main demand for energy storage system to bridge the gap between expected midday PV surpluses and expected evening/morning deficits.

The trend from October through to March (Figure 5.12b) shows a much greater consistency in magnitudes and patterns, which emphasizes the distinct nature of July cooling demands to the general demand: mid-winter heating demands are much less intensive or disruptive to the overall energy demands. This further emphasizes the fact that significant proportional energy savings could be achieved, and significant advantages to CSG energy independence feasibility, if the July peak can be reduced, either through more accurate temperature sampling or through better system design.

The trend through the cooler half of the year is otherwise as expected. With higher demands during the coldest months of the year when space cooling demand is at its highest, and lower demands in the more temperate months in Athens, GA, such as October, November, and March. Months that require heating display the double-hump pattern of morning and evening maxima

unlike the peak cooling month of July as heating demands are greatest in the morning and evening when ambient temperatures are low and occupancy is high.

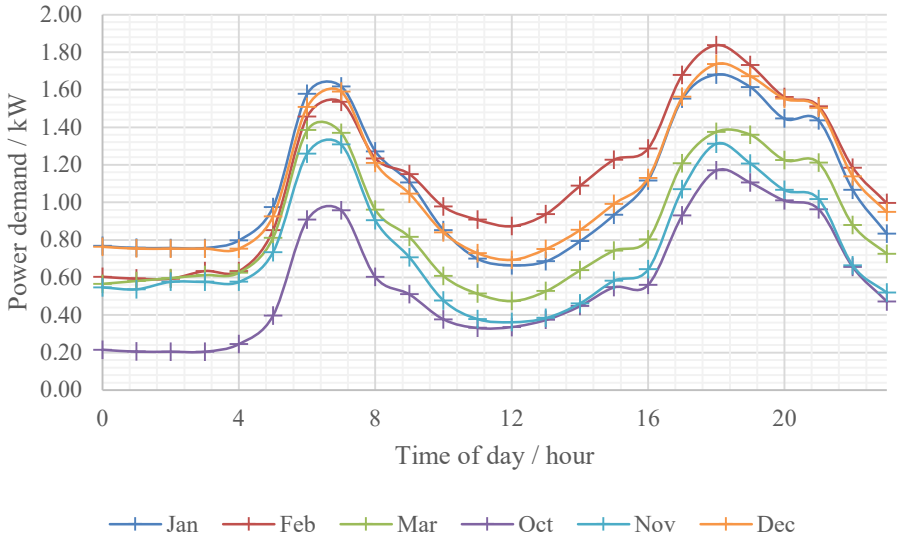

Figure 5.12b – Monthly variation of overall power demand (October to March) for average CSG house

The smooth variation of these patterns on both a daily and seasonal basis, external validation, and their internal consistency, along with the cyclical nature of their daily and seasonal patterns, provides significant confidence in the overall model, albeit with some recognition of the mid-summer differences.

5.6 Application of DSM data

The numerical results from the demand-side model (Table 5.9) are applied, along with the PV supply side modeling results (Section 6) to the overall energy independence feasibility determination (Section 7).

Table 5.9 - Hourly profiles and daily, monthly, and annual totals for an individual household in the community for an average day in the month. The color scale indicates relative magnitude, with the deepest red representing the highest demand, and deepest blue the least.

Month:	Jan	Feb	Mar	Apr	May	Jun	Jul	Aug	Sep	Oct	Nov	Dec
Hour	Electrical demand / kWh											
00:00	0.77	0.60	0.57	0.12	0.12	0.12	0.12	0.11	0.11	0.22	0.55	0.76
01:00	0.76	0.59	0.58	0.11	0.11	0.11	0.11	0.11	0.10	0.21	0.54	0.75
02:00	0.76	0.59	0.60	0.11	0.11	0.11	0.11	0.10	0.10	0.20	0.58	0.75
03:00	0.76	0.63	0.61	0.11	0.11	0.11	0.11	0.10	0.10	0.20	0.58	0.75
04:00	0.80	0.63	0.63	0.11	0.11	0.11	0.11	0.10	0.10	0.25	0.58	0.75
05:00	0.98	0.85	0.81	0.24	0.21	0.20	0.19	0.18	0.18	0.40	0.73	0.93
06:00	1.58	1.46	1.39	0.81	0.68	0.65	0.62	0.60	0.60	0.91	1.26	1.51
07:00	1.62	1.54	1.37	0.92	0.74	0.70	0.80	0.66	0.66	0.96	1.31	1.59
08:00	1.27	1.23	0.96	0.72	0.51	0.49	1.19	0.55	0.45	0.60	0.90	1.21
09:00	1.11	1.15	0.82	0.68	0.48	0.55	2.07	0.93	0.93	0.51	0.71	1.05
10:00	0.85	0.98	0.61	0.60	0.62	0.61	2.14	0.91	0.91	0.38	0.48	0.84
11:00	0.70	0.91	0.51	0.57	0.76	0.75	2.44	1.14	1.46	0.33	0.38	0.73
12:00	0.67	0.87	0.47	0.58	0.92	0.75	2.76	1.46	1.78	0.34	0.36	0.69
13:00	0.69	0.94	0.53	0.59	0.98	0.80	2.80	1.82	2.14	0.37	0.38	0.75
14:00	0.79	1.09	0.64	0.74	1.07	0.88	3.20	1.89	2.21	0.45	0.46	0.85
15:00	0.93	1.23	0.74	0.88	1.17	0.98	2.98	1.67	1.99	0.55	0.58	0.99
16:00	1.12	1.29	0.80	0.93	1.01	0.81	2.78	1.46	1.78	0.56	0.64	1.13
17:00	1.55	1.68	1.21	1.28	0.89	0.93	2.92	1.08	1.08	0.93	1.07	1.56
18:00	1.68	1.84	1.38	1.46	0.97	0.94	2.57	0.92	0.93	1.17	1.31	1.74
19:00	1.61	1.73	1.36	1.44	0.85	0.82	1.55	0.80	0.81	1.11	1.21	1.67
20:00	1.45	1.56	1.23	1.32	0.69	0.67	0.80	0.66	0.67	1.01	1.07	1.55
21:00	1.44	1.51	1.21	1.31	0.64	0.62	0.62	0.61	0.62	0.96	1.02	1.50
22:00	1.07	1.18	0.88	1.00	0.47	0.46	0.46	0.46	0.46	0.66	0.66	1.14
23:00	0.83	1.00	0.73	0.86	0.29	0.29	0.28	0.28	0.28	0.47	0.52	0.95
Daily average total	25.8	27.1	20.6	17.5	14.5	13.5	33.7	18.6	20.5	13.7	17.9	26.2
Monthly total	799	759	639	524	450	404	1046	577	614	426	536	811
Annual total	7585 kWh											

SECTION 6

Supply-side Modeling

6.1 Introduction to PV supply-side modeling.

The supply-side modeling (SSM) process provides an optimized estimate of the monthly-hourly electricity production available for the insolation collected by a one-acre array located in Athens, GA, U.S.A. This was achieved using the National Renewable Energy Laboratory (NREL) System Advisor Model (SAM) (Detailed PV Model module) [58] with weather data from the National Solar Radiation Database's (NSRDB's) Physical Solar Model (PSM) v3 TMY files [64]. Crucially, the temperature data is the same as that used in DSM (Section 5) ensuring the two modeling processes are compatible in that regard.

6.2 Fundamental SAM parameters.

Two basic characteristics of the PV supply were already established (Sections 2 and 4), namely:

- Available array footprint: 1.0 acres, plus space for necessary clear-cutting, battery storage, and power conditioning infrastructure.
- Solar tracking infrastructure would be included to maximize PV output and spread the output across the day, either single-axis or dual-axis solar tracking (SAST or DAST)

In SAM, the array area is not a direct input parameter, but is itself a function of the desired array size (in terms of peak power output) and the Ground Coverage Ratio (GCR), which is the proportion of ground area taken up by the modules to the total ground area used by the array. Therefore, in each simulation iteration, GCR and desired array size values must be carefully entered in SAM to maintain the 1.0-acre array footprint.

When considering single modules, or a low-GCR array of modules, DAST technology provides a distinct energy advantage on clear-sky days; however, this advantage is mitigated once self-

shading effects are considered on more densely packed arrays (Section 2). Further, the SAM version used for modeling work in this study (version 2020.11.29) was only able to compute self-shading effects for "1-axis" and fixed-tilt PV arrays. Therefore, the option of DAST technology in SSM had to be abandoned in favor of more accurate and valid self-shading modeling. The "1-axis" option to refers to a NS-axis (horizontal) SAST.

6.3 Summary of SAM parameter determination.

SAM operates with a range of assumed defaults, thus, the full complexity of the simulation created for this study can be summarized in the specific parameters determined as suitable for the CSG (Table 6.1), with rationale for choices detailed in Appendix C. All parameters not listed in Table 6.1 were simply retained at their default values or settings.

Table 6.1 – Parameter selections for NREL SAM PV simulation

Section	Parameter	Chosen values or type
Solar resource library	Weather file	Athens_GA_PSM3-TMY_60_TMY
Module	Model type	CEC Performance Model with Module Database
Module	Module name	Sunpower SPR-X22-480-COM
Inverter	Inverter name	Schneider Electric Solar Inverters – Inc: Conext Core XC540-NA
AC sizing	Desired array size	309kWdc
	Desired DC to AC Ratio	1
	Estimate Subarray 1 configuration	[Selected]
Tracking & orientation	[Axis selection]	1 Axis
	Tilt	Zero
	Azimuth	180º
	Ground Coverage Ratio (GCR)	0.33
	Tracker rotation limit	40º
	Backtracking	[Enabled]
Array dimensions	Modules along the side of row	2
	Modules along bottom of row	40
	Module aspect ratio	1.7
Snow losses	Estimate Snow losses	[Not enabled]

6.4 SAM simulation output and evaluation.

6.4.1 PV output

SAM simulation produces a wide range of data, of which only Inverter DC input (kW) was necessary in this study. As no inverter is necessary in the CSG concept, sampling its *input* allows us conceptually to eliminate the inverter from the model. By default, SAM exports data for *every hour over 25 years*, i.e., 219,000 values. From this, the hourly data for just the average solar day for each month was extracted, according to the model resolution, for the 25-year extent of the simulation. This resulted in 7200 values (24 hours × 12 days in the year × 25 years). From these a simple average was taken across the 25 years of data for each monthly-hourly value:

$$\overline{S_{m,h}} = \frac{\sum_{y=1}^{25}(P_{m,h})_y}{25} \times (hour) \tag{6.1}$$

Where $P_{m,h}$is the hourly inverter DC input for given month, m, and hour, h, in kW; the y parameter signifies the year in the simulation, and $\overline{S_{m,h}}$is the is the 25-year averaged PV array electrical supply in kWh. The multiplication by the hour ensures dimensional balance. This produces 288 monthly-hourly values of $\overline{S_{m,h}}$ (Table 6.2).

The daily average supply, $\overline{D_m^{CSG}}$ for each month recorded in Table 6.2 was estimated with:

$$\overline{D_m^{CSG}} \approx \left(\sum_{h=0}^{23} \overline{S_{m,h}}\right) \tag{6.2}$$

These data are represented in Figure 6.1.

6.4.2 Evaluating the general trend of results

Several factors provide confidence in the PV model. Zero night-time PV generation and the general trend of near-midday peaks are basic requirements for confidence in the model and are seen in the results (Table 6.2). Further, PV generation starts earlier and finishes later in mid-summer compared to mid-winter. Midday values vary further with greater intensities generally recorded in summer months than in winter months.

Table 6.2 – Simulated PV output for the average solar day in each month, with color scale to indicate the relative scale of each value. The deeper the red, the greater the output; and blue represents zero output, i.e., hours of darkness.

Month:	**Jan**	**Feb**	**Mar**	**Apr**	**May**	**Jun**	**Jul**	**Aug**	**Sep**	**Oct**	**Nov**	**Dec**
Hours	Hourly PV supply / kWh											
0:00	0.0	0.0	0.0	0.0	0.0	0.0	0.0	0.0	0.0	0.0	0.0	0.0
1:00	0.0	0.0	0.0	0.0	0.0	0.0	0.0	0.0	0.0	0.0	0.0	0.0
2:00	0.0	0.0	0.0	0.0	0.0	0.0	0.0	0.0	0.0	0.0	0.0	0.0
3:00	0.0	0.0	0.0	0.0	0.0	0.0	0.0	0.0	0.0	0.0	0.0	0.0
4:00	0.0	0.0	0.0	0.0	0.0	0.0	0.0	0.0	0.0	0.0	0.0	0.0
5:00	0.0	0.0	0.0	0.0	0.0	0.0	0.0	0.0	0.0	0.0	0.0	0.0
6:00	0.0	0.0	0.0	0.6	65.7	78.3	54.7	14.2	4.0	0.0	0.0	0.0
7:00	0.0	1.6	39.0	34.5	209.4	124.3	81.9	87.7	117.5	10.3	13.6	0.0
8:00	33.6	57.6	185.8	12.0	341.6	288.7	79.1	230.9	263.4	69.6	69.6	87.9
9:00	102.1	65.6	226.2	86.0	372.7	238.1	346.8	237.7	342.4	329.6	280.3	225.5
10:00	33.9	226.6	231.9	145.9	332.5	299.0	355.2	295.7	343.7	332.5	127.5	278.5
11:00	78.7	232.0	271.3	161.6	281.8	180.8	357.9	321.1	208.4	323.4	220.1	260.4
12:00	89.8	231.1	239.1	291.9	379.7	370.0	356.6	314.7	338.1	319.9	263.1	249.9
13:00	55.3	290.7	201.3	399.2	379.2	321.8	357.7	312.9	339.8	325.9	270.9	261.7
14:00	86.6	354.2	186.6	406.2	376.9	220.5	354.3	317.1	225.2	336.5	280.5	279.3
15:00	39.7	125.9	168.6	403.7	368.4	34.2	347.8	242.9	341.4	313.5	215.1	210.7
16:00	28.2	243.1	178.6	349.0	336.8	232.7	327.1	69.0	256.3	173.9	80.2	72.2
17:00	2.1	73.5	92.8	193.2	210.1	170.8	226.0	137.9	111.6	26.4	0.0	0.0
18:00	0.0	0.0	4.0	34.5	67.0	78.9	92.9	35.0	2.7	0.0	0.0	0.0
19:00	0.0	0.0	0.0	0.0	0.0	2.5	3.1	0.0	0.0	0.0	0.0	0.0
20:00	0.0	0.0	0.0	0.0	0.0	0.0	0.0	0.0	0.0	0.0	0.0	0.0
21:00	0.0	0.0	0.0	0.0	0.0	0.0	0.0	0.0	0.0	0.0	0.0	0.0
22:00	0.0	0.0	0.0	0.0	0.0	0.0	0.0	0.0	0.0	0.0	0.0	0.0
23:00	0.0	0.0	0.0	0.0	0.0	0.0	0.0	0.0	0.0	0.0	0.0	0.0
Daily average / kWh	550	1902	2025	2518	3722	2640	3341	2617	2895	2562	1821	1926
Monthly total / MWh	17.1	53.3	62.8	75.5	115.4	79.2	103.6	81.1	86.8	79.4	54.6	59.7
Annual total	868.5 MWh											

6.4.3 Anomalous results

The monthly variation in PV supply (Figure 6.1) shows some unexpected results, most notably the lack of a single clear mid-summer peak. The oscillation in supply between April and October is unexpected, unlikely, and represents a limitation in the model. Given that the daily average supply values are simply a sum of the hourly supply values for the average solar day in the month (Equation

6.2), the monthly anomalies can be explained directly from the hourly results in Table 6.2. For example, the values for 15:00 in June and 16:00 in August show large reductions in PV output compared to the hours immediately before and after.

$\overline{D_m^{CSG}} \approx \left(\sum_{h=0}^{23} \overline{S_{m,h}}\right)$

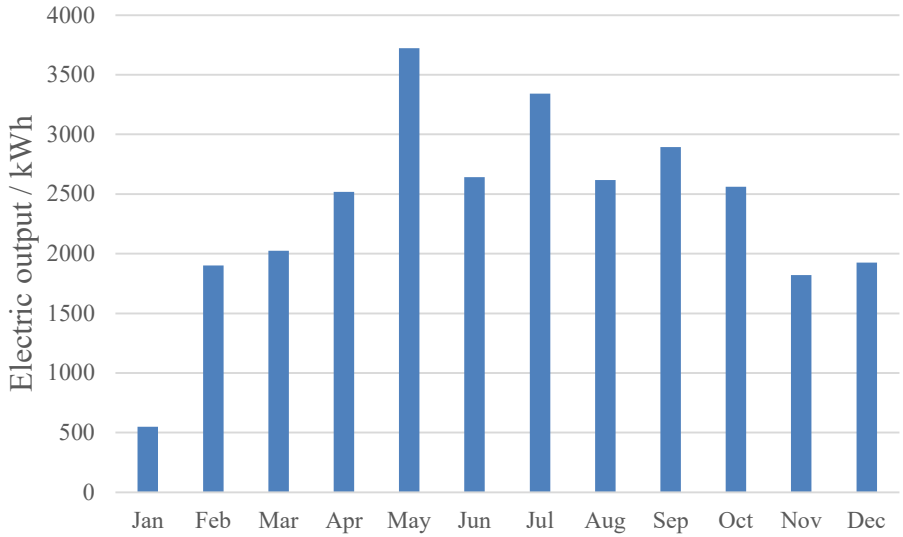

Figure 6.1 - Average daily PV supply from CSG array

Other unusual results occur at 08:00 in April, 11:00 in September, 10:00 in November, and all of these anomalies are consistent over the 25-year NSRDB weather file that provides the irradiance and ambient temperature data from which SAM simulates the results. If these anomalies, and others of smaller magnitude, were replaced with values follow the general trend, then the suppressed daily averages in April, June, and August would be increased to values that would produce a more expected and consistent curve with a mid-summer peak. The likely external-shading causes for the NSRDB/TMY data anomalies are discussed further in Section 9, but it should be noted that any errors do not undermine the validity of any determination that energy independence is feasible for the CSG, as these anomalies appear to reduce PV output below their expected values, thereby working against the viability of the CSG.

A further anomaly is the pronounced reduction in PV supply for January compared to December and February. Whilst low outputs during winter is expected, the degree of the drop-off is surprising. The low PV supply result could be due to high levels of typical cloud cover in January, rather than any anomalous data, especially as there are reduced PV values across the day for January. Without any clear indication to the contrary, the January data is considered accurate, again with the recognition that any errors work against the viability of CSG energy independence by suppressing the PV supply and therefore strengthening any positive assessment of energy-independent feasibility.

6.4.4 Application of SSM data

The results from the SSM (Table 6.2) are applied along with DC-only DSM data (Section 5) to determine the feasibility of energy independence in the CSG (Section 7),

SECTION 7

Electricity demand and supply reconciliation.

In Section 7.1, the 288 monthly-hourly results from the DSM and SSM procedures in Sections 5 and 6 respectively are combined to determine the energy difference between supply and demand, for varying community size, N, at different resolution scales. The role and limitation of the battery bank is considered in Section 7.2 before the assessment of the feasibility of energy independence for the CSG concept in Section 7.3.

7.1 Calculating energy difference with uncertainty analysis.

Total CSG demands (DSM), for N houses, and community supply (SSM) are reconciled to determine the feasibility of community energy independence. The two controlling parameters affecting potential independence are the number of houses and total battery storage capacity. Assuming no computational error, the energy surplus or deficit (energy difference) in the community is:

$$E_{m,h} = S_{m,h} - \left(NH^{T}_{m,h}\right) \tag{7.1}$$

where $S_{m,h}$is the PV supply (kWh) from the array at a given month, m, and hour, h (Table 6.2), $H^{T}_{m,h}$ is the electric load for one CSG house (kWh) at the same month-hour (Table 5.9), and N is the number of houses. In order to satisfy and engage householders, it is recommended that live values of $S_{m,h}$ and $E_{m,h}$, along with $H^{T}_{m,h}$ for their own house, be provided to teach household. As well as providing a general interest point for involved community members, this could, combined with home energy management systems, inform and equip homeowners to control their consumption at crucial times to aid community energy independence.

Prudence dictates that several factors of safety be considered, and error margins applied to calculations, to ensure that the feasibility of energy independence is adequately tested. The

uncertainties are analyzed and applied in three separate categories: demand-side, supply-side, and battery modeling uncertainties.

Demand-side modeling (Section 5) included three main sources or processes. EIA data allowed the estimation of standard AC electrical consumption in an equivalent existing house. The data is based on very large sample sizes, providing confidence in the accuracy of the reported figures; slight inaccuracies may exist from the sampling methods applied in Section 5. An error of 5% is assigned to this data. Any error in the eQuest energy profiles would have a much lower impact on the demand-side model, mostly applied to hourly rather than seasonal variations, so an error of only 2% is assigned to that data. The DC-only energy savings process is based upon the work by Garbesi et at. [14] which is considered highly accurate given the range and depth of data. Given its significant impact on the demand-side results, the error assigned to that data is 5%, bringing the demand-side modeling error total to 12%.

In the Supply-side modeling (Section 6), the assigned error for NSRDB weather data is zero, as any error in insolation (caused by panel shading) would work against the viability of system energy-independence. The NREL SAM simulation covers a wide range of possible factors and no further variables have been identified that could be included. Therefore, a low 2% error is assigned, sufficient to cover any small inaccuracies in the simulation. The transmission of electricity has not yet been included in this model. Modern DC transmission, especially over shorter distances, is highly efficient (Section 2), giving confidence that local transmission of DC electricity from the CSG PV array to the houses within the community should not exceed the average of 5% transmission losses that exist in the U.S. grid [65]. A 5% error margin is therefore applied to the transmission of electricity as a conservative estimate, resulting in a 7% error margin overall for supply-side modeling.

The battery modeling process contains no source-data from which errors may propagate, but the process requires an error margin to account for battery depth of discharge. Based on a desired 80% depth of discharge, battery capacity would have to be 25% larger that the calculated

energy storage capacity for effective storage. Given the potentially serious nature of the electricity supply failing, this error margin is doubled, to 50%. An error margin of this scale is assumed to also take care of charging and discharging rates, and self-discharging rates. This error only affects the battery sizing stage of the modeling process.

A summary of error margins is provided in Table 7.1.

Table 7.1 - Summary of error-margins for the various modeling processes and their totals.

Stage	Source / Process	Assigned error
Demand modeling	EIA data	5%
	eQuest energy profiles	2%
	DC-only energy savings	5%
Subtotal error margin for demand-side modeling, α_D:		**12%**
Supply modeling	NSRDB data	0%
	SAM simulation	2%
Transmission	Transmission losses	5%
Subtotal error margin for supply-side modeling, α_S:		**7%**
Battery modeling	Whole battery process	50%
Subtotal error margin for battery modeling, α_B:		**50%**

Applying the error margins for supply-side and demand-side modeling independently to the calculation of hourly energy surplus requires the following enhancement to Equation 7.1:

$$E_{m,h} = (1 - \alpha_S)S_{m,h} - (1 + \alpha_D)\left(NH^T_{m,h}\right) \quad (7.2)$$

where $\alpha_S = 0.07$ and $\alpha_D = 0.12$ (Table 7.1).

Applying the battery error margin to results requires that the final battery capacity value be increased by 50%, ($1-\alpha_B$); however, this adjustment is not made until Section 7.3.3 in order that the sensitivity of the system to battery capacity can be explored further.

When Equation 7.2 is applied to all values of m and h, $E_{m,h} > 0$ represents an energy surplus and $E_{m,h} < 0$ is a deficit. An exemplar table of results of $E_{m,h}$ for N = 60 homes for a 25-year average of each month-hour (288 total) is included in Appendix D1. During deficits, the community uses the community battery at a rate of $NH_{m,h}^{T}$ for that hour. Increasing N therefore decreases surpluses and leads to increasing deficits.

The average daily energy difference, D'_m, for a month, m, of the year is:

$$D'_m = \sum_{h=0}^{23} E_{m,h} \tag{7.3}$$

and the total monthly energy difference, E_m, is

$$E_m = D'_m \times n_m \tag{7.4}$$

where n_m is the number of days in the month, m (n_m =31 for m=1; n_m =28 for m=2), as in Section 5, and the total annual difference, E_{Annual}, is:

$$E_{Annual} = \sum_{m=1}^{12} E_m \tag{7.5}$$

Applying equations 7.2 to 7.5 for increasing values of N until $E_{Annual} < 0$ provides the result that the CSG development of 95 houses is the largest community that still produces an annual surplus of energy. Any larger community could not possibly exist off-grid over the whole year, as it would produce an annual energy deficit. Hourly, average daily, monthly and annual values of energy difference for N=95 and N=96 (producing an annual deficit) are provided in Tables 7.2 and 7.3.

Table 7.2 – values of energy surplus (positive values) or deficit (negative values) for N = 114. All hourly values are in units of kWh to the nearest kWh, with the color scale representing the degree of surplus (deeper red for higher surplus) and or deficit (deeper blue for deeper deficit). Average daily, monthly cumulative, and annual cumulative surpluses are included in the bottom rows with units (kWh or MWh) specified for each.

Hours	Jan	Feb	Mar	Apr	May	Jun	Jul	Aug	Sep	Oct	Nov	Dec
00:00	-82	-64	-60	-13	-13	-13	-13	-12	-12	-23	-58	-81
01:00	-81	-63	-62	-12	-12	-12	-12	-11	-11	-22	-57	-80
02:00	-81	-63	-64	-12	-12	-12	-12	-11	-11	-22	-61	-80
03:00	-81	-68	-65	-12	-12	-12	-12	-11	-11	-22	-61	-80
04:00	-85	-68	-67	-12	-12	-12	-12	-11	-11	-26	-61	-80
05:00	-104	-91	-86	-25	-22	-21	-20	-20	-20	-42	-78	-98
06:00	-168	-155	-147	-86	-12	4	-15	-50	-60	-97	-134	-160
07:00	-172	-162	-110	-66	116	41	-9	11	39	-92	-127	-169
08:00	-104	-78	71	-65	263	216	-53	157	197	1	-31	-47
09:00	-23	-61	124	8	296	163	102	122	220	252	185	98
10:00	-59	107	151	72	243	213	103	178	223	269	68	170
11:00	-1	119	198	90	182	89	74	177	39	265	164	165
12:00	13	122	172	210	255	264	38	137	125	262	206	159
13:00	-22	171	131	308	249	214	34	97	88	263	211	163
14:00	-4	214	106	299	237	111	-11	94	-25	265	212	169
15:00	-62	-13	78	282	218	-72	6	48	106	233	138	90
16:00	-93	89	81	226	206	130	9	-91	49	102	6	-53
17:00	-163	-110	-42	44	100	60	-101	14	-11	-74	-114	-166
18:00	-179	-196	-143	-123	-41	-27	-187	-65	-96	-125	-140	-185
19:00	-172	-184	-145	-153	-91	-85	-162	-85	-86	-118	-128	-178
20:00	-154	-166	-130	-140	-73	-71	-85	-70	-71	-108	-113	-165
21:00	-153	-161	-129	-140	-68	-66	-66	-65	-66	-103	-108	-160
22:00	-113	-126	-94	-106	-50	-49	-49	-48	-49	-70	-71	-121
23:00	-89	-106	-77	-91	-31	-31	-30	-30	-30	-50	-55	-101
D'_m/ kWh	-2230	-1114	-311	483	1915	1023	-482	453	516	921	-209	-993
E_m / MWh	-69.13	-31.19	-9.64	14.49	59.37	30.69	-14.94	14.04	15.47	28.54	-6.26	-30.77
E_{Annual}	0.65 MWh											

Table 7.3 – values of energy surplus (positive values) or deficit (negative values) for N = 96. All hourly values are in units of kWh to the nearest kWh, with the color scale representing the degree of surplus (deeper red for higher surplus) and or deficit (deeper blue for deeper deficit). Average daily, monthly cumulative, and annual cumulative surpluses are included in the bottom rows with units (kWh or MWh) specified for each.

Hours	Jan	Feb	Mar	Apr	May	Jun	Jul	Aug	Sep	Oct	Nov	Dec
00:00	-83	-65	-61	-13	-13	-13	-13	-12	-12	-23	-59	-82
01:00	-82	-64	-63	-12	-12	-12	-12	-11	-11	-22	-58	-81
02:00	-81	-64	-64	-12	-12	-12	-12	-11	-11	-22	-62	-81
03:00	-81	-68	-66	-12	-12	-12	-12	-11	-11	-22	-62	-81
04:00	-86	-68	-67	-12	-12	-12	-12	-11	-11	-26	-62	-81
05:00	-105	-92	-87	-26	-22	-21	-21	-20	-20	-43	-79	-100
06:00	-170	-157	-149	-87	-12	3	-16	-51	-61	-98	-135	-162
07:00	-174	-164	-111	-67	115	40	-10	11	38	-93	-128	-171
08:00	-106	-79	69	-66	262	216	-54	156	196	0	-32	-48
09:00	-24	-63	123	7	295	162	100	121	218	252	185	97
10:00	-60	106	150	72	242	212	100	177	222	269	67	169
11:00	-2	118	197	89	181	88	71	176	37	265	164	164
12:00	12	121	171	210	254	263	34	135	123	261	206	158
13:00	-22	170	130	308	248	214	31	95	86	263	211	163
14:00	-5	212	105	299	236	110	-15	92	-28	265	211	168
15:00	-63	-15	77	281	217	-74	3	46	104	233	137	89
16:00	-94	88	80	225	205	129	6	-93	47	101	5	-54
17:00	-165	-112	-44	43	99	59	-104	12	-12	-76	-115	-168
18:00	-181	-198	-144	-125	-42	-28	-190	-66	-97	-126	-141	-187
19:00	-174	-186	-146	-155	-92	-86	-163	-86	-87	-119	-130	-180
20:00	-155	-168	-132	-142	-74	-72	-86	-71	-72	-109	-115	-167
21:00	-154	-163	-130	-141	-69	-67	-66	-66	-67	-104	-109	-162
22:00	-115	-127	-95	-107	-51	-50	-49	-49	-50	-70	-71	-122
23:00	-90	-107	-78	-92	-32	-31	-31	-30	-30	-51	-56	-102
D'_m/ kWh	-2259	-1144	-334	463	1899	1008	-520	432	493	905	-229	-1022
E_m / MWh	-70.03	-32.04	-10.36	13.90	58.87	30.24	-16.11	13.39	14.78	28.06	-68.65	-31.68
E_{Annual}	-7.84 MWh											

7.2 Battery efficiency and storage

If $E_{Annual} > 0$, community energy independence may be possible depending on the efficacy of the battery pack and the nature of the energy surpluses including: 1) that surpluses are sufficiently high enough to meet demands after battery charging and discharging losses and 2) that sufficient battery storage is available to accommodate the deficit at each hour of the day for each day of the

year. Energy independence of the CSG concept is considered feasible when, over a year, there is a net surplus ($E_{Annual} > 0$) and these additional conditions are met.

Round-trip efficiencies vary between 80% for lead-acid batteries [66, 67] and 95% for lithium-ion batteries. Round-trip efficiency is conservatively assumed to be 80%. The battery storage energy change, ΔB, is limited by the maximum energy storage capacity of the batteryB^{max} but increases proportional to the energy surplus and charging efficiency and, decreases proportional to the energy deficit and the inverse of the discharging efficiency,

$$\Delta B_{m,h} = \begin{cases} E_{m,h} \times \eta_{Ch}, & when\ E_{m,h} > 0\ and\ B_{m,h} < B^{max} \quad (7.6a) \\ 0 & when\ E_{m,h} > 0\ and\ B_{m,h} = B^{max}\ or\ E_{m,h} = 0 \quad (7.6b) \\ E_{m,h} \times \dfrac{1}{\eta_{Dis}}, & when\ E_{m,h} < 0 \quad (7.6c) \end{cases}$$

An exemplar of battery energy storage for each 288 month-hour interval for N=60 is shown in Appendix D2.

7.3 Feasibility of energy independence.

7.3.1 Conditions for feasibility

The CSG is energy independent if the PV supply (SSM) and battery storage is able to meet electric demand (DSM) at all hours of the year; i.e.,

i. $$(1 - \alpha_S)S_{m,h} > (1 + \alpha_D)\left(NH^T_{m,h}\right), \text{ or} \quad (7.8a)$$

ii. $$(1 - \eta_{Dis})B_{m,h} > (1 + \alpha_D)\left(NH^T_{m,h}\right) \quad (7.8b)$$

for all values of *m* (1 to 12) and *h* (0 to 23).

The battery energy storage, $B_{m,h}$, at the end of each month-hour interval,

$$B_{m,h} = B_{m,h-1} + \Delta B_{m,h} \quad (7.9)$$

with $B_{m,h-1}$ equal to zero, initially.

7.3.2 Start date of analysis.

For the conditions in Section 7.3.2 to be met throughout the year for the largest possible size of community, it is important to begin the assessment of those conditions at an appropriate date. Energy independence of the community is only possible when there is sufficient energy surplus stored in the battery bank during earlier months of the year-round assessment to meet the deficit in later months, and the degree of surplus and deficit depends on the number of houses in the community. Therefore, for each month, there exists a value N_D, the maximum number of houses for which there is a daily average surplus ($D'_m > 0$) produced for that month (Table 7.4).

Table 7.4 – maximum size of community for average daily energy surplus for first four months of the year.

Month	**N_D**
January	21
February	70
March	98
April	144

For January to February, average daily surpluses are only possible with N_D less than the maximum possible for annual energy surplus (N=95 houses). However, the annual surplus for March with N=95 is minimal and leads to system failure in year-round analysis. To ensure the maximum possible value of N for energy independence, the year-round assessment should start April, and nine a.m. is the first hour of the average day in April in which a surplus is recorded, so the year-round assessment should start at m,h = 4,9.

7.3.3 Off-grid feasibility assessment.

a) Maximum community size

Applying Equations 7.1 to 7.7 and 7.8 for all 288 monthly-hourly values for the year, starting at m,h = 4,9, for varying values of N, allows for the two feasibility conditions (Equations 7.8a and 7.8b) to be assessed and the maximum possible value of N for energy independence to be found. Applying all the equations and considerations from Section 7.3, initially with N=95, results in

system failure at 18:00 on the average solar day in January (Appendix D3). At that point, the battery charge is depleted to 39.9 kWh, insufficient to meet the hourly community deficit of 191.6 kWh.

The value of N is therefore iterated down until the CSG PV-battery system supplies enough energy for the full year, which is found at N=83. This is one of the main results of this work, in answer to the research question and represents the largest possible community size, 83 that can exist off-grid. A summary of the iteration in N, along with the failure points for values of N above 83, are provided in Table 7.5.

Table 7.5 – Summary of iteration to determine the maximum value of *N*, that allows energy independence.

N, size of community	Failure point	
	Month	Hour
95	Jan	17:00
90	Feb	03:00
85	Mar	04:00
84	Mar	06:00
83	N/A	N/A

Throughout this stage of the assessment, B^{Max} is set to an arbitrarily high value (10^6 kWh) in order that the battery capacity be effectively removed from the computation (determining the required battery capacity occurs in the next stage).

b.) Determining required battery storage.

To find the maximum effective battery capacity, the year-round assessment was repeated with same start-point (m,h = 4,9) and community size (N=83) that achieved energy independence, but with decreasing values of B^{max}. When the battery capacity was set at the arbitrarily high value of 10^6kWh, the maximum reported charge in the battery bank was 5880kWh; however, even that is unnecessarily high as a considerable excess charge remains at the end of the year under those conditions. Iterating B^{max} down further, the maximum effective battery charge is shown to be

5736kWh for the N=83 size community. A summary of hourly surplus or deficit, and energy storage values, at these conditions, for selected hours of the year, is included in Table 7.5.

Table 7.6- First and last 20 iterations of year-round assessment of hourly surplus and battery charge for **N=83** and $\mathbf{B^{max}}$ **= 5736 kWh** to test for energy-independence. (The other results are removed for brevity).

Month	Hour	Hourly surplus / kWh	Charge or discharge of battery bank	Energy storage / kWh	Month	Hour	Hourly surplus / kWh	Charge or discharge of battery bank	Energy storage / kWh
Apr	9	17.0	Charge	15.2	Mar	13	138.1	Charge	905.5
Apr	10	80.4	Charge	87.0	Mar	14	114.1	Charge	1007.6
Apr	11	97.4	Charge	174.1	Mar	15	87.7	Charge	1086.0
Apr	12	218.0	Charge	369.0	Mar	16	91.5	Charge	1167.8
Apr	13	316.2	Charge	651.6	Mar	17	-26.0	Discharge	1138.8
Apr	14	309.3	Charge	928.1	Mar	18	-124.1	Discharge	999.9
Apr	15	294.1	Charge	1191.1	Mar	19	-126.5	Discharge	858.5
Apr	16	238.5	Charge	1404.3	Mar	20	-114.0	Discharge	731.0
Apr	17	61.1	Charge	1458.9	Mar	21	-112.6	Discharge	605.0
Apr	18	-103.8	Discharge	1342.8	Mar	22	-81.8	Discharge	513.5
Apr	19	-133.7	Discharge	1193.2	Mar	23	-67.5	Discharge	438.0
Apr	20	-122.5	Discharge	1056.2	Apr	0	-11.5	Discharge	425.1
Apr	21	-122.1	Discharge	919.7	Apr	1	-10.7	Discharge	413.2
Apr	22	-92.6	Discharge	816.1	Apr	2	-10.6	Discharge	401.4
Apr	23	-79.8	Discharge	726.9	Apr	3	-10.6	Discharge	389.5
May	0	-11.3	Discharge	714.2	Apr	4	-10.6	Discharge	377.7
May	1	-10.5	Discharge	702.4	Apr	5	-22.2	Discharge	352.9
May	2	-10.4	Discharge	690.7	Apr	6	-74.7	Discharge	269.3
May	3	-10.4	Discharge	679.1	Apr	7	-53.4	Discharge	209.6
May	4	-10.4	Discharge	667.4	Apr	8	-55.5	Discharge	147.4

Under these conditions, the system remains self-sufficient for the full year assessment. Even though the last 16 hourly values (from 17:00 in March to 8:00 in April) all show energy deficit and battery discharge, there remains sufficient battery charge to meet the hourly energy deficit, ensuring independence through to the end of the year period. If the maximum battery capacity were reduced by just 1kWh, the subsequent compound losses of that extra 1kWh through round-trip inefficiencies brings the failure point forward to 7 a.m. on the average solar day in March (Appendix D4)

Applying the 50% error margin (Section 7.3.1) to the battery capacity value for N=83, produces a safe value of B^{max} = 8604 kWh. All further reported battery capacity values will be those *with the error margins applied.*

7.4 Iterating assessment for a range of community sizes.

Maximizing house numbers in the CSG development maximizes economies of scale to decrease per-household costs of the PV array and electrical distribution system. However, the larger the community size, the larger the battery storage requirement, with associated financial and environmental impacts. These impacts could outweigh the benefits of low PV costs per household that come with increased community size, favoring a more modestly sized CSG development. Therefore, the battery sizing process (Section 7.3.4, part b) was iterated for community sizes, varying from 50 to the maximum size of 83, applied under the conditions of the calculated error margins (Section 7.3.1). The numerical results of this iteration are included in Appendix D and summarized in Figure 7.1 and 7.2.

The trend displayed in Figure 7.1 is non-linear, with the rate of increase itself gradually increasing with N. This is emphasized in Figure 7.2, which displays the increasing ratio B^{max}/N, i.e., the gradient of the curve in Figure 7.1. The significance of these results is discussed further in Sections 8 to 10.

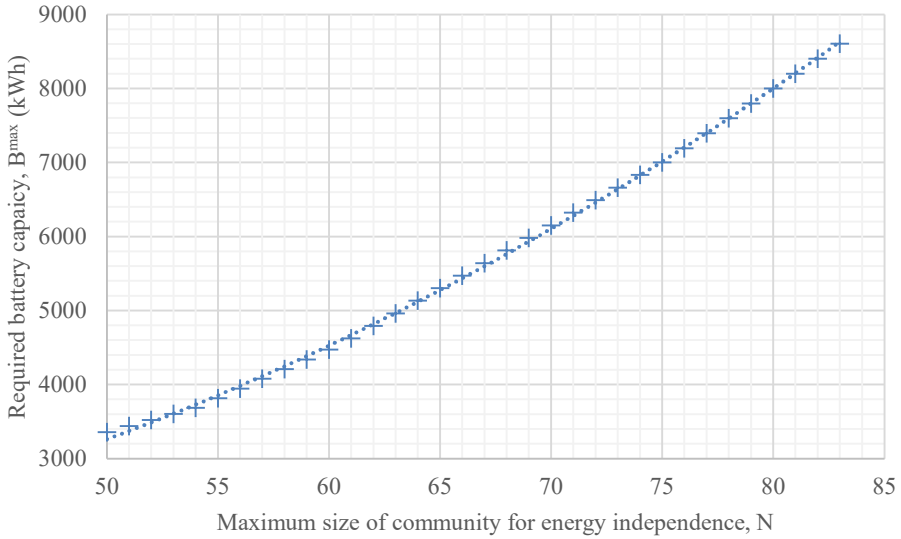

Figure 7.1 – Relationship between required battery capacity, and size of CSG community

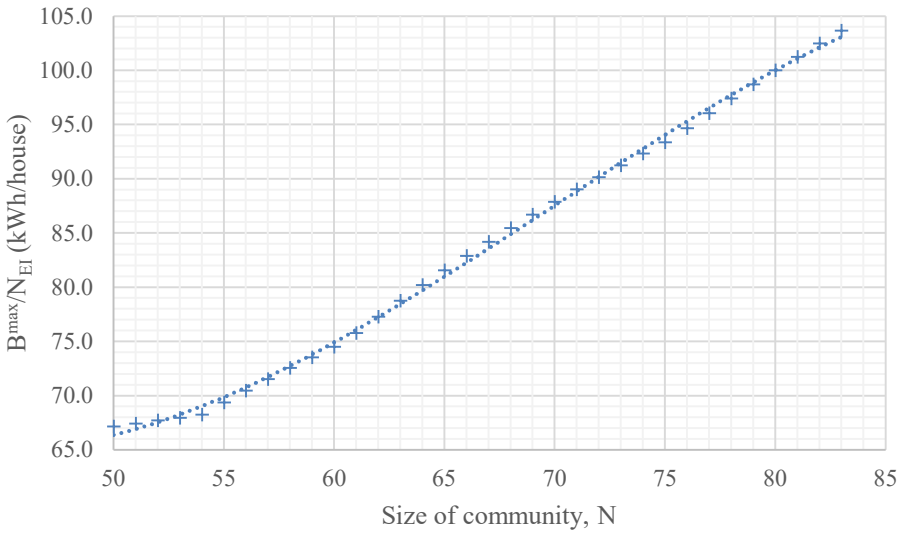

Figure 7.2 – increasing battery requirements per house for an increasing size of CSG community. N.B. this is equivalent to the gradient of Figure 7.1

SECTION 8

Results

The hourly and average daily results from the modeling processes in Section 7 are represented in Section 8.1 and assessed for their reliability and their impact upon the required battery capacity. In Section 8.2 schematic and material specifics for the proposed CSG design are specified. Section 8.3 explores the relationship between community size and required battery capacity.

8.1 Hourly and monthly variations in energy difference.

In Section 7.3.3 it was found that an off-grid CSG community could contain a maximum of 83 houses. Applying Equation 7.2 to that situation produces hourly energy difference (surplus and deficit) values for this maximum-sized community which are broadly in line with expectations. The hourly variations for the average solar days in March and October are displayed in Figures 8.1a,b as examples of clear, sustained daytime surpluses and night-time deficits.

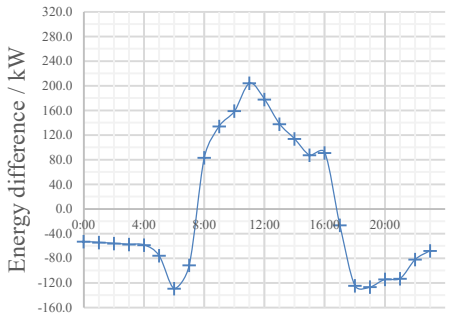

Figure 8.1a – March.

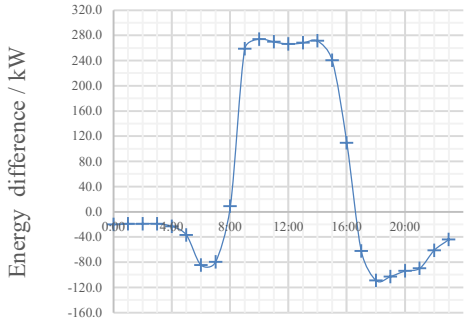

Figure 8.1b - October

Hourly energy difference variations in CSG for 83 houses at two points of the year, demonstrating expected sustained periods of surplus and deficit.

Figures 8.2a, b display expected differences in energy difference results between winter and summer.

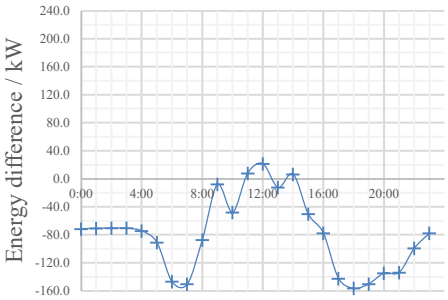

Figure 8.2a – January

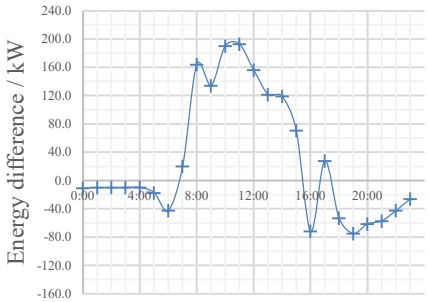

Figure 8.2b - August

Hourly energy difference variations in CSG for 83 houses in winter and in summer, demonstrating expected differences in overall surplus and deficit.

These trends are generally as expected, with surpluses during daylight hours, deficits overnight and the degree of surplus and demand varying with season according to expected solar radiation.

However, in other months there are significant anomalies in the hourly results; those for June are presented as examples in Figure 8.3a, along with the PV output from the CSG array for the same month, in Figure 8.3b.

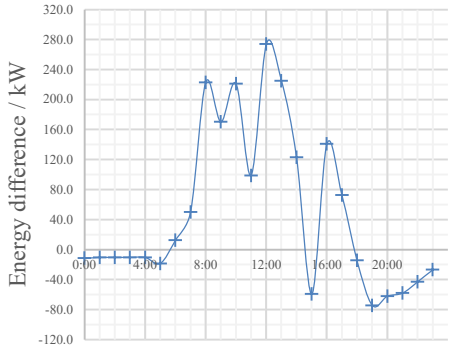

Figure 8.3a – CSG energy difference

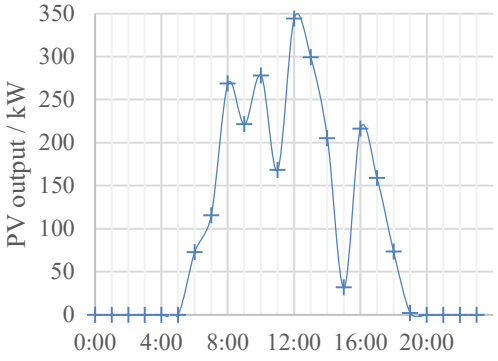

Figure 8.3b – PV output

Comparison of CSG energy difference (for 83 houses) and PV output from the CSG array for the month of June, demonstrating the coincidence of the anomalous variations.

This exact coincidence of the variation between energy difference and supply in Figure 8.3a, b highlights the extent of impact of anomalies in the PV output upon CSG energy differences. The likely cause (external shading) is discussed and possible improvements are explored in Section 9. Significantly for the results, the inaccuracies in the modeled PV supply does not negatively affect the reliability of the off-grid feasibility assessment: the inaccuracies exclusively reduce the supply, effectively raising the bar for CSG off-grid feasibility. In other words, if energy independence can be established for the CSG under these conditions of limited PV supply, then the community should be able to exist off-grid with a more accurate and realistic supply.

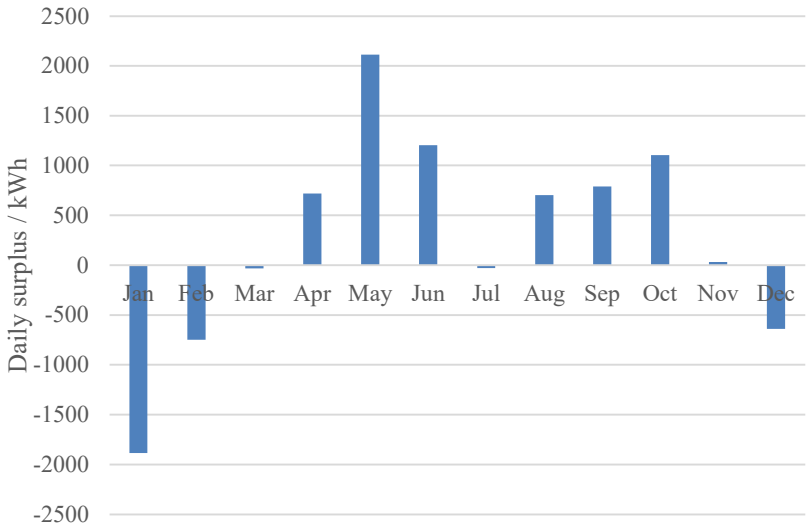

Figure 8.4 – Daily average energy differences (surplus) for each month, for N=83

The hourly values can be summed to give the average daily energy difference for each month (Figure 8.4), which will allow some further assessment of model reliability and will also help inform the role of the battery bank. Note that the error margins from Section 7.4.1 have already been applied to limit the size of any surpluses and extend the deficits, so no error bars are appropriate or applied to this figure.

Several aspects of the results in Figure 8.4 give confidence in the results, namely:

i. The greatest surpluses occur in temperate months when space heating and cooling loads are low and insolation is relatively high, with good sky clarity.

ii. There is much lower excess energy (i.e., there are energy deficits) in July and the winter months, when space heating and cooling loads are greatest.

iii. The winter loads produce a greater energy deficit than July as the latter's load is almost met by higher insolation, whereas the high loads in winter occur when solar radiation is at its lowest levels.

iv. There is generally a smooth variation of energy differences between months.

The pronounced jump in energy difference between July and its neighboring months is initially unexpected given the generally high temperatures throughout the summer in Athens, Georgia. However, this result can be explained by the generally high thermostat settings in the summer compared to the ambient daytime temperatures in those months (which range between 78 and 83ºF, except for July, in which the recorded ambient temperature (90ºF in the TMY data) is significantly above the thermostat setting (Section 5).

The sustained period of negative energy difference from November through to March reinforces the expectation that a high battery capacity is required to store the significant energy excesses over the summer to meet the winter deficits, along with the small deficit in July. Significantly, the battery charging should start in April, when energy surpluses are first recorded, to be able to store enough energy over the summer months of plenty to meet the winter demands.

8.2 Proposed CSG design.

The modeling processes in Sections 5-7, with appropriate error margins, have demonstrated, in response to the research question, that community scale energy independence *is feasible* in the given context of Athens, Georgia, USA, for a community of up to 83 houses when powered by a system of an SAST NS-axis PV array, with a 1.0-acre footprint, and an 8604kWh central battery

bank. A proposed schematic design is provided in Figure 8.5 along with a list of its materials in Table 8.1.

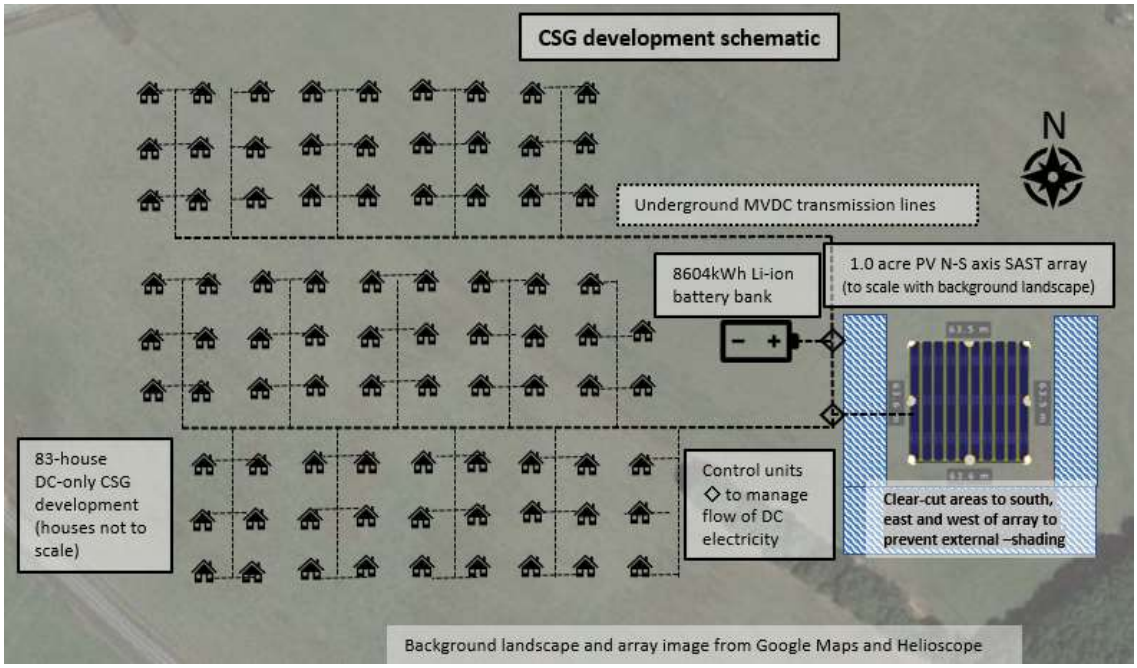

Figure 8.5 – schematic of proposed CSG development design. The housing development is not to scale with the PV array; it does represent a grid layout along north-south and east-west lines to allow for energy efficient design and south-facing rooftops for solar water heating panels.
Most significantly, there is no connection to the external grid, and thus no need for inverter hardware, or point of common control between AC grid and DC microgrid.

Significantly, this community size is 39% larger than the 62-house comparison Reynold's Landing development [13], despite the latter not aiming for energy independence but remaining connected to the utility grid. The DC-only energy savings of 42% over an equivalent AC standard house is mostly responsible for this achievement. While the solar-tracking technology, DC-wiring, and large battery bank of the CSG design will add capital and maintenance costs (Section 9), this work demonstrates the in-principal viability of 100% renewable energy supplied distributed generation (DG) at the community scale, and at a high standard of living (Section 5). These results therefore argue for investors and developers, such as those involved in the Smart Neighborhoods (Section 1), continuing to pursue DG models, but to enhance such developments by scaling generation to the community level and doing so isolated from the utility grid.

Table 8.1 – Summary of system characteristics and materials for the proposed CSG design.

General house construction	Standard energy-efficiency design features of secure thermal envelope and maximized daylighting.
Solar water heating panels	Heliodyne Inc. Gobi 408 013, $3m^2$, on south-facing roofs of all CSG houses.
DC-only features	Houses wired with DC-only systems according to standardized $380V_{DC}$ transmission to houses and 48VDC and $12V_{DC}$ supply within each house [16]. Appliance details can be found in the work by Garbesi [14].
PV modules - make	Sunpower SPR-X22-480-COM.
PV modules - dimensions	1.1272m × 1.91625m (area of $2.16m^2$).
Row number / module allocation	1,120 modules in 10 rows on a north-south axis. 112 modules per row.
Module configuration in each row	Portrait orientation, 2 modules along the side and 56 modules along the bottom of each row.
Row spacing	6.39m
Solar tracking technology and range of motion	Single-axis solar tracking at zero tilt, 40^o range of motion
Estimated PV installation costs	$522,830 (produced by SAM simulation in Section 6)
Total battery capacity required	8,604 kWh, including 50% error margin
Example make of batteries and number required	299 x Outback Power's SystemEdge 830 BLU-300 AFCI (28.8kWh). [68]

Of the materials listed in Table 8.1, the solar water heating panels and PV modules are those selected within the NREL SAM program, producing suitable and sufficient output in this work to enable off-grid feasibility for the CSG system; higher performance or more available options may be selected for any specifically designed CSG development, although the impact on the size and configuration of the PV array should be considered. The suggested battery system is a popular option for residential off-grid applications; however its off-the-shelf unit cost is prohibitively high, with the required 299 units costing approximately $4.6million. Any real

development would likely utilize a purpose-designed battery bank for the community size and would likely enjoy far greater economies of scale. Nevertheless, this demonstrates the economically restrictive nature of battery storage and alternatives are discussed in Section 9.

8.3 Relationship between community size and required battery capacity.

In Section 7 the modeling process was extended to examine the relationship between the community size, N and the required community battery capacity, B^{max}, for $50 \leq N \leq 83$ (Figure 7.1). Further, the ratio of B^{max}/N, the gradient of Figure 7.1, was determined for the community size range $50 \leq N \leq 83$ (Figure 7.2).

The increasing value of the B/N ratio establishes the non-linear response between B and N, which may explained be by two effects that increasing N has upon the system. The first effect is that an increase in the number of houses increases the load at each hourly interval, which increases the size of all energy deficits. This increases the total energy that must be stored in the surplus months, thereby increasing the required B^{max} value. The second effect is that an increased hourly demand reduces the magnitude of all surpluses, meaning that a larger proportion of the surplus needs to be stored when they occur (the intensity of storage requirements increase). Together, these factors produce a relationship in which B^{max} increases at a greater rate than N.

By analogy, a land with long periods of drought and sudden rains would require larger reservoirs to collect rainwater when the crucial greatest rains occur; small reservoirs would lose much of the greatest rains as they would exceed the reservoir capacity at that point, yet later rains may not be enough to fill the remaining reservoir space. This is illustrated further through examining the transition from N=50 to N=51 in the CSG development.

When N=50, B^{max} (before applying the 50% error-margin) is 2238kWh, resulting in a B/N ratio of 44.76 kWh/house. Under these conditions, the battery charge is limited by its maximum capacity at eight points in the year-round assessment, the latest of which is 16:00 on the average solar day in December (interval 200 in Figure 8.5). Thus, the stored 2238kWh at that point limits the available energy to meet the subsequent deficits until the end of the year-round

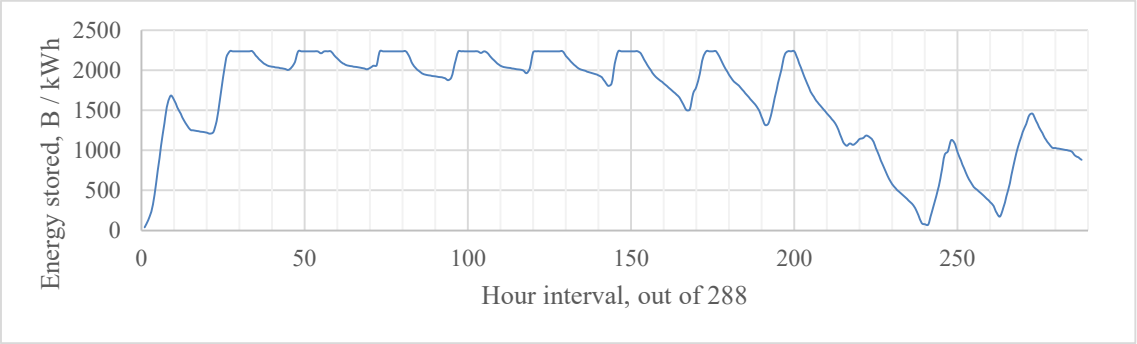

Figure 8.5 – energy stored in battery bank, B, as a function of hourly intervals over the year-long assessment, for a suitably sized CSG battery. The eight periodic flat tops between interval 27 and interval 200 represent maximum charge points, where the battery capacity has limited the total stored energy. Despite battery charge almost being expended at interval 241 (February, 09:00, at which B = 74.0 kWh) it is enough to supply the energy deficit at that hour, -3.4 kWh. The next hour (February, 10:00) is a surplus hour which helps the battery recharge and sustain the system till the end of the year.

assessment, at 08:00 on the average solar day in April (Figure 8.5), at which point the charge is 881 kWh and the system survives off-grid.

If N is increased to 51, and B^{max} is *only increased proportionately* to N, from 2238 to 2283 kWh, there is still sufficient PV supply for the maximum capacity to be achieved at the same point, 16:00 on the average solar day in December, despite all loads increasing. However, the subsequent energy deficits, between 16:00 in December and 08:00 in April, are greater, and the energy surpluses are lower, draining the battery quicker and causing system failure at 07:00 on the average solar day in February when the 87.6 kWh of battery storage is insufficient to overcome the 86.2kWh of deficit once discharge losses are considered (Table 8.2). Increasing the battery capacity *only proportionately* to N maintains the last point of maximum charge, but the increased demands after that point drain the battery at a faster rate than the smaller community size. Therefore, increasing N requires a greater-than-proportional increase in battery capacity, in this case to 2292 kWh (before applying error-margins).

Table 8.2 – summary of battery capacity, charges, and ratios with community size for the transition between N = 50 and N=51. Results here demonstrate the need for battery capacity per house to increase at a greater-than-proportionate rate.

N	B^{max}	B/N	End point	E at end point	B at failure
50	2238 kWh	44.76 kWh/house	08:00, April (successfully off-grid)	-29.0 kWh	880.6 kWh
51	2283 kWh	44.76 kWh/house	07:00, February (system failure)	-86.2 kWh	87.6 kWh
51	2292 kWh	44.94 kWh/house	08:00, April (successfully off-grid)	-29.8 kWh	830.4 kWh

The relationship between N and B^{max} has two further complications. The first is a recession of the maximum charge point and is evident in the transition from N=54 to N=55. At N=54, with a suitable B^{max} = 2457 kWh, maximum charge is achieved at the same point as with lower community size (16:00 in December); however, when the community is increased to N=55, the community load on the PV array is increased sufficiently that the 16:00 in December interval becomes an energy deficit, rather than surplus hour, discharging the battery rather than charging it at that point. Therefore, when N is increased to 55, the point of maximum charge (equal to B^{max} = 2543kWh) is pushed back to the previous hour, 15:00 in December. This extends the period over which the peak charge must meet continued community deficits, requiring a greater increase in battery capacity than when N was increasing from 50 to 54, in part to meet the needs of greater loads, and in part to do so for a longer period. Therefore, when increasing the community size from 54 to 55 houses, there is a discontinuous increase in the required battery capacity, from 55kWh per additional house, to 86kWh per additional house (83 to 129 kWh per house, respectively, once error-margins are applied), (Figure 8.6).

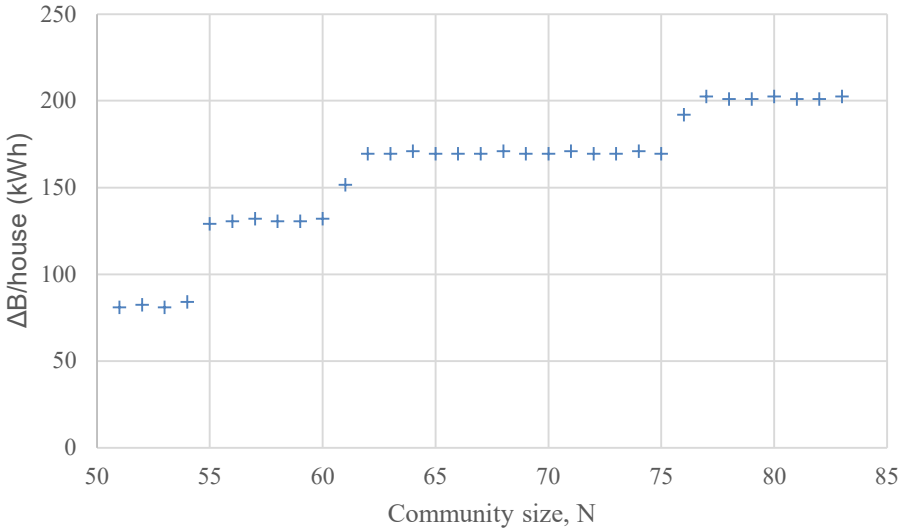

Figure 8.6 – discontinuities in the increasing battery capacity per household increase, arising from the recession of battery maximum charge point. The transition in N from 54 to 55 corresponds 16:00 in December becoming an energy deficit hour under the increased load pushing back the to the maximum battery charge point receding by one hour to 15:00. Transitioning N from 60 to 61 causes the maximum charge point to recede from 15:00 in December to 16:00 in November, and N=75 to N = 76 corresponds to a shift from 16:00 in November to 16:00 in October.

The upper values of N for each of these discontinuities (54, 60, 75, and 83 houses) represent significant cut-off values for any possible developer. I.e., if one is considering building a CSG development of 50 houses, one would be better placed to build 54 since the extra four houses would further spread the cost of the PV array installation without increasing the average required battery capacity per house ratio. However, increasing the community size to 55 would be disadvantageous, decreasing the per-household PV array costs only slightly whilst creating the distinct step-up in battery costs per household.

Calculating 288 values of battery charge for each of the N values that correspond to the start of each consistent battery demand section in Figure 8.6 (N = 50, 55, 62, 77), produces the graphs displayed in Figure 8.7, which provides further insight into the non-linear relationship between N and B. Each of the transitions from one of the N values to

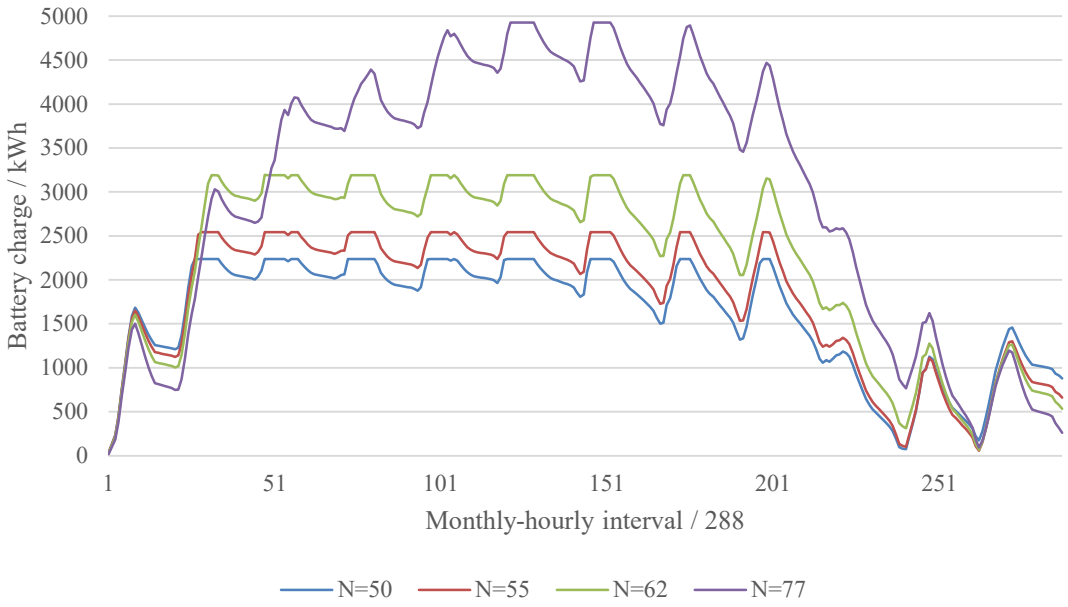

Figure 8.7 – Varying battery charge through the year for CSG developments at sizes that correspond to significant discontinuous increases in required battery capacity, and with battery capacities set to their appropriate, required amounts. These battery capacities can be recognized by the flattened tops of the charge curves. The B^{max} values for the four community sizes are 2238, 2543, 3194, and 4930 kWh respectively (prior to the application of error margins).

the higher ones displayed in Figure 8.7 corresponds to a change in the latest hour interval that records the maximum battery charge, from interval 200 (at 2238 kWh for N = 50) to interval 199 (2543kWh for N = 55), to interval 176 (3194 kWh for N = 62) to interval 152 (4930 kWh for N = 77). The effect of this is to extend the period of time in the end of the year-round assessment in which the remaining energy deficits need to be met by the excess stored in the battery, therefore increasing that amount that is stored, e.g., increasing the required battery capacity. Further, the magnitude of the negative gradient of the battery discharge increases with each step up of N (see from 200th interval onwards in Figure 8.7), representing a increased discharge rate of the battery bank beyond the peak charge point. Through extrapolation, it is evident that a larger maximum charge is required maintain positive battery charge for the remainder of the year.

The final main aspect of the relationship between N and B relates to the maximum community size, N = 83. At that size, B^{max} = 5736 kWh (before applying the error-margin). Increasing B^{max} by any size does not enable an off-grid 84-house community as there is insufficient solar resource to provide an annual energy surplus for that size community. Thus, 83 is the maximum size for energy-independence of a CSG development.

SECTION 9

Discussion

The significance of the overall results is discussed in Section 9.1, before considering limitations of the CSG concept and avenues for its improvement in Section 9.2. Lastly, wider applications are explored in Section 9.3

9.1 Overall results

After considering uncertainties and applying factors of safety to the model (Section 8.4), the upper limit of the community size, 83, represents a cautious reduction on the 95 house community that produces an annual energy surplus. However, the fact that such a community can be energy-independent from the grid and at a size 39% larger than existing residential communities such as Reynold's Landing is encouraging: if Reynold's Landing is economically viable with 62 houses, it is reasonable to expect the CSG would also be economically viable. The installation cost of the PV array (Table 8.1) is, when shared between the 83-house community, $6,299 (Equation 9.1) - only a fraction of a cost of a detached family house in the region, and that cost could be spread over the expected 25-year lifetime of the array – this comes to $21/month for each household. Thus, the result of the primary aim of this study is a positive one: the CSG concept can feasibly be energy-independent, and at a scale that allows the PV array to be affordable with suitable financing options.

However, as the larger communities require disproportionately large battery capacities, the PV-array economies of scale may be dwarfed by the increased battery costs. Detailed battery technology choice, selection, and costing falls beyond this work, and would be required by later

studies to determine the optimum CSG development size. Alternatively, secondary generation options may be considered (Section 9.3).

9.2 Limitations and avenues for improvement.

While a range of opportunities exist to develop this work in terms of expanding the model to other regions or improving its resolution, three significant limitations exist in the model's current form.

9.2.1 Accuracy: dependence on the average solar day and NSRDB data.

As outlined throughout this study, the model is based heavily upon the energy demand and supply for the average solar day of the month (Section 4). The accuracy of the model is limited by this approach: if either the demand or the supply model is slightly incorrect for one hour, it affects the model for a whole month. Two factors restrict the negative effects of this: first, that the errors in the solar radiation database tend to under-report the available solar radiation and, second, that error margins have been included to help prevent over-estimation in feasible community size. Together these should protect the validity of the overall feasibility judgment; however, they increase the theoretical burden on the required battery capacity, B. A more parsimonious, and realistic, estimation of B would require a greater temporal resolution through the demand-side and supply-side models, ideally increasing from every hour of every average solar day of a month (288 values in a year) to every hour of each day of the year (8760 values in a year), a 30.4-fold increase.

Such an increase should not be a problem for the supply-side model. The SAM output already provides values for every day of the year, for 25 years of weather and solar radiation data. Current supply-side modeling samples the 288 monthly-hourly values for 25 years (7200 values in total); if an updated supply-side model sampled the 8760 hourly values for an entire year for just 5 years this would require analysis of 43,800 hourly values of PV supply: approximately a six-fold increase over the current model, but certainly within computational capacities. Indeed, it

may prove quicker as the data to be discarded are more conveniently arranged (years 1-20 of the TMY data) rather than being interspersed among the currently used average solar day data.

Applying this increased resolution to the demand-side model could prove a greater challenge. The temperature-related demand models (space heating, space cooling, water heating, and refrigeration) would need developing to include temperature data for each day of the year; a detailed but certainly highly possible task. However, the monthly variation of other end-use categories is determined by the eQuest user-profiles which have no greater seasonal resolution. In order for demand- and supply-side modeling to have equal resolution (without which the improved supply-side resolution is meaningless), an alternative means of determining seasonal variation in residential energy loads will be required. One has not been identified as part of this study; doing so would be a first step in developing the accuracy of the CSG concept beyond the current average solar day dependency.

Regardless of how data is sampled from the TMY files, the solar radiation values supplied by NSRDB include anomalous dips (Section 8.2) which are almost certainly unrepresentative of the insolation in that region. Future work should consider how to correct for these errors, either by acquiring more representative date from the same or another source, or by adjusting the data, explicitly, to smooth out the anomalous points.

9.2.2 Relevance: considering the increasing demand from electric vehicles (EVs)

The RECS-15 data does not contain any assessment of EV demand as an end-use category. EVs are increasingly popular [69], and with greater societal and governmental push for their uptake, the pressure on electric generation could be severe. Currently, around 37% of all U.S. energy expenditures are on transportation; even if just 10% transfers from fuel-based to electric propulsion, that would represent almost a 25% increase in total residential energy consumption [70]. The CSG concept's value would be enhanced if it could meet the demand of EV charging at individual households.

Two means of expanding the model present themselves: first, simply expanding the size of the PV array; second incorporating rooftop-PV arrays for the households that with to charge an EV at home. The former has an in-principal challenge of fairness: if only some households run an EV, then they would receive a disproportionate benefit from the array – in that case, either there would have to be increased HOA costs for such households (allowing them access to a higher proportion of the array's output), or an internal marked would need to be created by which units of electricity are purchased from the central array. The number of households using EVs would either have to be accurately predicted or carefully controlled to ensure that centralized PV array is built to a suitable size: too small and it will fail in terms of delivery; too large and it might fail financially. Such matters would need to be assessed for EV charging from the central array. The increased demands upon the CSG concept is not simply in terms of PV array area, but also battery sizing. EV charging demand is likely to be greatest overnight, requiring additional battery capacity, in addition to greater PV area, to bridge the energy gap between daytime generation and nighttime demand.

An alternative means to meet this demand in an equitable manner could be through individual households, that wish to run an EV, incorporating their own rooftop-PV systems to supplement their draw from the community array. Being financed and operated separate from the community system allows more freedom for the individual householder, as well as greater synergy for the EV system being used (for example, the AC system of a Tesla EV, rooftop PV, and battery system [71-73]). The analysis required for such work would therefore be to ascertain if there is enough south-facing rooftop on each house to provide both the electric energy required to run an average EV year-round and the extra electric energy required to meet the shortfall in water heating energy if the solar water heating panels (Section 5.4) need to be relocated to the North-facing roof (receiving less solar energy).

9.2.3 Sensitivity and resilience: dependence on reasonable consumer behavior and the potential demand for energy backup

The DSM is considered to be accurate and reliable given the nature of the outputs modeled and the correspondence with broader energy analysis. There is confidence that this modeling represents a realistic prediction of likely residential electricity demand, and, with the addition of the error margins (Section 8.4), the projected community size and feasibility should be sound. However, the presence of just one unpredictable or unreasonable householder could critically undermine CSG feasibility through intensive energy use at a tipping-point in the surplus and deficit variations in the PV supply. Increased resilience could be achieved by increased generation capacity. One option for this is to add rooftop PV modules (as with EV charging); another could be to include a supplementary generator in the community.

Supplementary or back-up generators have a distinct advantage of dispatchability, that is the ability for the generator to be activated and varied according to need, unlike PV supply. This provides a further significant advantage to the resilience of the CSG concept. The increase in weather unpredictability due to climate changes, the impact of forest fires upon PV generation [74], or the unlikely event of PV module failure could all leave the CSG with unpredicted energy shortfalls; considering this, it would not be unreasonable for developers or householders to demand that the community include such a dispatchable fuel-based generation capacity.

If such a generator were based on renewable natural gas (RNG) or other biofuel, rather than fossil-based natural gas or diesel, then near carbon-neutral generation would still be possible, aligning closely with the sustainable aims of the CSG project. The economic, technologic, and environmental viability of such a system would depend on the distances between the proposed CSG development and the local RNG / biofuel sources, and the nature of their production. It would be inadvisable if such fuel consumption impacted negatively on agricultural land-demands due to its production methods, or if transportation of the fuel supply results in unacceptably high carbon emissions. However, if it is possible to source such fuels without these shortcomings, then this would provide the CSG concept with much improved resilience to internal and external stressors.

Another advantage of including dispatchable generation could be a significantly reduced battery requirement and even a reduction in PV array size. If nighttime demands, and other periods of sustained deficit, could be supplied directly by fuel-based generators, then significantly less battery energy storage would be required to bridge energy gaps. The saved material and embedded energy costs may outweigh the environmental costs of renewable fuel consumption. If carefully integrated, the fuel-based generation could be built into a combined heat and power (CHP) facility on the community level, providing the energy for space heating and thus dramatically reducing the electric demand in winter months. Simple quantitative analysis projects the following potential energy generation and storage advantages through incorporation of a CHP facility, compared to a baseline of no CHP integration (Table 9.1):

Table 9.1 – summary of possible quantitative energy and material advantages arising from the integration of a biofuel supplied combined heating and power plant

Means of advantage	Electrical demand per house / kWh	Maximum N	Battery capacity requirements (with 50% error margin)
None	7585	83	8604 kWh total 104 kWh/house
CHP facility providing space *heating* loads in energy deficit months (November through to March).	5815 (23.3% reduction)	105 (26.5% increase)	3215 kWh total 38.7 kWh/house
CHP facility meeting winter electrical power deficits[1]	5815 (23.3% reduction)	105 (26.5% increase)	2472 kWh total 29.8 kWh/house

1. The determination of the timing of minimal supplementary electrical power provision from the CHP plant requires a trial-and-error approach using equations 7.6 to 7.9, but the overall required power provision is low, only occurring at critical intervals, often just before a return to energy surplus at daylight hours. In the case of 105 houses and 1648 kWh total battery capacity (before applying 50% error margin), supplemental energy is required for just 9 out of the 288 monthly-hourly intervals, occurring between 06:00 and 08:00 in October, between 21:00 and 23:00 in January, and between 04:00 and 09:00 in February. Scaling these intervals and the energy requirements for the number of days in the month, this results in an expected 264 hours (out of 8760 in a year) and 4156 kWh of supplemental electrical energy requirements provided by the CHP plant. The 4156 kWh represents the energy generation end-product; the actual volume, mass, and energy content of the fuel would depend on various factors, including the efficiency of the CHP generator and of a rectifier to convert the generated AC electricity into DC, to be compatible with the CSG system.

The advantages listed in Table 9.1, in terms of reduced energy demand per house, the resultant increase in maximum community size, and decreased battery capacity requirements, are those arising from the separate heating and electric generation functions of a CHP generator, as

the combined benefit has not been modeled. In reality, the heating function during the winter months would provide extra electrical energy potentially increasing N and decreasing the battery capacity requirements further; modeling this would likely require a detailed engineering design and resulting calculations and was therefore considerably beyond the scope of this work, but presents a promising option for future study..

9.3 Other future work

In addition to the points in Section 9.2, some further options exist for future work.

9.3.1 Apply the model to other locations.

The CSG concept is intended to have wide, even global, application, and so a primary priority for further application is to apply this model to other geographic and socio-economic contexts. It is suggested that this happens in two stages:

Stage 1: application to other locations in the U.S.

By locating the first wider-context within the U.S. maintains a low burden on the demand-side modeling. Comfort levels and general use levels can be treated the same as in the test-case, TMY data files from NSRDB will be available in a broad range of locations, and RECS-15 (or more up-to-date equivalents) would provide sufficient and suitable data for detailed modeling. Supply-side modeling with SAM will also be straightforward if the location is suitably close to a U.S. city with an available TMY file. The methodology for the synthesis stage should not require change.

Stage 2: applications beyond the U.S.

Significant adaptations for each country, and for significant socio-economic variations within a country, will be required but the general methodology will be broadly the same. In terms of the fundamental assumptions, the available size of array, available type of modules and tracking technology, and the desired size of house within the community should be re-appraised. In order to favor the possibility of energy independence, the size of each house should be sensibly

scaled down if there is less communal area for the central PV array, of if only lower performance PV technology is available.

For the demand-side modeling itself, a country- or region-specific alternative to the EIA RECS data should be sought in order to determine the suitable end-use categories to model and to estimate the standard AC equivalent loads. The Garbesi et al. data [14] should be broadly applicable although some sensitivity should be afforded to the availability of such technology in each location: a tailored approach should be taken, for example, BDCPM motors may not be available for heat pumps, but space heating or space cooling may simply be unnecessary or not expected in certain locations. Suitable energy use profiles for daily and seasonal variations may be required to replace those provided by eQuest. It may be necessary to determine these from direct observation, or a suitable estimation may be applied.

An alternative to the NREL SAM model would have to be found, unless a compatible equivalent to TMY files exist for the given location, which could then simply be applied to the SAM simulation.

9.3.2 Explore different energy storage options.

Alternative battery options should be considered for each location so the ideal technology is applied for the given local temperatures and possible maintenance available. However, with the burgeoning field of energy storage research, several broader options exist, and many more may be developed, that diversify away from chemical energy. In addition to the possibility of providing enhanced performance, such technologies also reduce the intensive global demands upon highly sought-after chemicals and minerals (e.g. lithium and cobalt) and reduce the CSG development's dependence on such expensive and possibly unreliable sources. Some of these other technologies include:

- Hydrogen fuel cells
- Compressed Air Energy Storage (CAES)
- Pumped Storage (PS) of water

- Super-capacitors
- Mechanical flywheels

Each of these should be assessed on a broad basis, including overall capacity (in kWh), charging and discharging rates, performance under varying weather conditions, mechanical and electrical reliability, synergy with otherwise DC-only systems, material availability, technological maturity, safety concerns and the available engineering, scientific, and operational expertise to ensure safe and effective operation of the energy storage option.

9.3.3 Examine the suitability of seasonal and dual axis tracking for the PV array.

Seasonal (EW-)axis and dual-axis solar arrays were not included in this study simply as the available version of SAM at the time of the start of research did not offer, or appear to offer, self-shading simulation for those technologies. If later a version of SAM, or alternative PV modeling software, does offer accurate modeling of such solar trackers, the PV output should be modeled first to see if they offer an energy advantage in a given location, and second to determine which is most suitable.

9.3.4 Broadening the renewable energy supply mix

Although this would constitute a significant departure from a primary element of the CSG concept, it may be appropriate in certain locations to consider additional distributed energy sources that could supplement and synergize well with PV generation. The immediate problem with other energy sources is that they do not generally generate DC electricity directly, and so AC/DC rectifiers would need to be included in the design, increasing the material and maintenance demands. However, if an energy source is chosen that complements the intermittency of solar radiation well, e.g., wind energy, its shortcomings may be worth the more consistent and overall, more reliable energy generation. With technology such as the Invelox wind compressor [75], there are possibilities of significant alternative renewable energy production on the community scale.

9.3.5 Considering other solar technologies.

Further to previous options, some other solar options may exist for communities of a smaller size than that proposed in the existing CSG concept. Concentrated photovoltaics (CPV) and dish-Sterling concentrated solar power (CSP) use mirror- or lens-based optical concentration to increase the power density of solar generation. The former generates DC electricity in a similar way to regular PV but requires solar cells that can operate at a much higher temperature than standard PV modules; the latter generates AC electricity through a Sterling engine which therefore has an inbuilt hybridization potential with RNG as a supplementary dispatchable energy source (although, as with wind energy, AC rectification will be required for the Sterling engine).

SECTION 10

Conclusion

This study has found that, when DC-only electricity is applied to residential systems (in generation, in transmission, and in DC-only appliance utilization), that suitably large communities can be energetically sustained by solar-tracking PV arrays without the need to depend on external supply from the utility-grid. In the test case examined in this study, 83 family residences (detached, 2,500 sq ft houses) could be sustained year-round by a 1.0 acre north-south aligned single-axis solar tracking array, (with additional space for sufficient clear-cutting to prevent external shading); however, this is at the high material cost of an 8,604 kWh central battery bank, heavily favoring the incorporation of supplemental power generation to lower the required energy storage. When applying this concept to locations other than this test case (Athens, Georgia, U.S.A.), careful re-evaluation of the likely residential energy demands, PV supply profile, and most appropriate energy storage systems would be necessary. Significant opportunities for technological development have been identified, including the possibility of alternative energy storage options, the incorporation of an RNG-based CHP micro-plant to reduce PV array size and battery requirements, and the addition of supplemental rooftop-PV to individual households to allow for EV charging. Several further model improvements and expansions are suggested, including improvements to resolution and accuracy by modeling supply and demand for each day of the year, rather than the average solar day. The final resolution improvement offers further opportunity in reducing the calculated battery requirements.

References

1. EnergySage. [cited 2021; Available from: https://news.energysage.com/solar-trackers-everything-need-know/.

2. SolarPowerWorld. 2016 [cited 2021; Available from: https://www.solarpowerworldonline.com/2016/05/advantages-disadvantages-solar-tracker-system/.

3. Administration, U.S.E.I. [cited 2021; Available from: https://www.eia.gov/energyexplained/electricity/electricity-in-the-us.php.

4. Business, N.E. [cited 2021; Available from: https://www.nsenergybusiness.com/news/fossil-fuels-energy-mix-2040/.

5. Energy, I. [cited 2021; Available from: http://insideenergy.org/2015/11/06/lost-in-transmission-how-much-electricity-disappears-between-a-power-plant-and-your-plug/.

6. Raman, P., et al., *Opportunities and challenges in setting up solar photo voltaic based micro grids for electrification in rural areas of India.* Renewable and Sustainable Energy Reviews, 2012. **16**(5): p. 3320-3325.

7. Prinsloo, G., A. Mammoli, and R. Dobson, *Customer domain supply and load coordination: A case for smart villages and transactive control in rural off-grid microgrids.* Energy, 2017. **135**: p. 430-441.

8. Energy, U.S.D.o. [cited 2021; Available from: https://www1.eere.energy.gov/solar/pdfs/distributed_pv_system_design.pdf.

9. World, R.E. [cited 2021; Available from: https://www.renewableenergyworld.com/solar/pv-durability-and-reliability-issues/.

10. Aboubakr El Hammoumi, S.M., Abdelaziz El Ghzizal, Abdelilah Chalh, Aziz Derouich, *A simple and low-cost active dual-axis solar tracker.* Energy Science and Engineering, 2018.

11. Sidek, M.H.M., et al., *Automated positioning dual-axis solar tracking system with precision elevation and azimuth angle control.* Energy, 2017. **124**: p. 160-170.

12. Laboratory, T.N.R.E. [cited 2021; Available from: https://www.nrel.gov/docs/fy12osti/52978.pdf.

13. Power, A. *Smart Neighborhood*. [cited 2021; Available from: https://apcsmartneighborhood.com/reynolds-landing-at-ross-bridge-smart-neighborhood-i-alabama-power/.

14. Garbesi, K., *Catalog of DC Appliances and Power Systems*. 2012: Lawrence Berkeley National Laboratory.

15. Justo, J.J., et al., *AC-microgrids versus DC-microgrids with distributed energy resources: A review.* Renewable and Sustainable Energy Reviews, 2013. **24**: p. 387-405.

16. Vossos, V., K. Garbesi, and H. Shen, *Energy savings from direct-DC in U.S. residential buildings.* Energy and Buildings, 2014. **68**: p. 223-231.

17. Agency, T.I.E. [cited 2021; Available from: https://www.iea.org/countries/united-states.

18. MacKay, D.J., *Sustainable Energy - Without the hot air*. 2009, United Kingdom: UIT, Cambridge.

19. Abusharkh, S., et al., *Can microgrids make a major contribution to UK energy supply?* Renewable and Sustainable Energy Reviews, 2006. **10**(2): p. 78-127.

20. Hirsch, A., Y. Parag, and J. Guerrero, *Microgrids: A review of technologies, key drivers, and outstanding issues.* Renewable and Sustainable Energy Reviews, 2018. **90**: p. 402-411.

21. Green, M., *Community power.* Nature Energy, 2016. **1**(3): p. 16014.

22. Planas, E., et al., *AC and DC technology in microgrids: A review.* Renewable and Sustainable Energy Reviews, 2015. **43**: p. 726-749.

23. Warneryd, M., M. Håkansson, and K. Karltorp, *Unpacking the complexity of community microgrids: A review of institutions' roles for development of microgrids.* Renewable and Sustainable Energy Reviews, 2020. **121**.

24. Ton, D.T. and M.A. Smith, *The U.S. Department of Energy's Microgrid Initiative.* The Electricity Journal, 2012. **25**(8): p. 84-94.

25. Rajanna, S. and R.P. Saini, *Development of optimal integrated renewable energy model with battery storage for a remote Indian area.* Energy, 2016. **111**: p. 803-817.

26. Agency, I.E., *Africa energy outlook. A focus on the energy prospects in sub-Saharan Africa. .* World Energy Outlook Special Report. , 2014: p. p. 1-237.

27. Gandini, D. and A.T. de Almeida, *Direct current microgrids based on solar power systems and storage optimization, as a tool for cost-effective rural electrification.* Renewable Energy, 2017. **111**: p. 275-283.

28. Alstone, P., D. Gershenson, and D.M. Kammen, *Decentralized energy systems for clean electricity access.* Nature Climate Change, 2015. **5**(4): p. 305-314.

29. McHenry, M.P. and D. Doepel, *The 'low power' revolution: Rural off-grid consumer technologies and portable micropower systems in non-industrialised regions.* Renewable Energy, 2015. **78**: p. 679-684.

30. Mehra, V., R. Amatya, and R.J. Ram, *Estimating the value of demand-side management in low-cost, solar micro-grids.* Energy, 2018. **163**: p. 74-87.

31. Ashourian, M.H., et al., *Optimal green energy management for island resorts in Malaysia.* Renewable Energy, 2013. **51**: p. 36-45.

32. Aghamolaei, R., M.H. Shamsi, and J. O'Donnell, *Feasibility analysis of community-based PV systems for residential districts: A comparison of on-site centralized and distributed PV installations.* Renewable Energy, 2020. **157**: p. 793-808.

33. Monadi, M., et al., *A communication-assisted protection scheme for direct-current distribution networks.* Energy, 2016. **109**: p. 578-591.

34. George, K., *DC Power Production, Delivery and Utilization (White Paper)*. 2006.

35. Letschert, V., et al., *Energy efficiency – How far can we raise the bar? Revealing the potential of best available technologies.* Energy, 2013. **59**: p. 72-82.

36. Singh, G.K., *Solar power generation by PV (photovoltaic) technology: A review.* Energy, 2013. **53**: p. 1-13.

37. Chang, T.P., *Performance study on the east–west oriented single-axis tracked panel.* Energy, 2009. **34**(10): p. 1530-1538.

38. Chin, C.S., A. Babu, and W. McBride, *Design, modeling and testing of a standalone single axis active solar tracker using MATLAB/Simulink.* Renewable Energy, 2011. **36**(11): p. 3075-3090.

39. Dakkak, M. and A. Babelli, *Design and Performance Study of a PV Tracking System (100W-24Vdc/220Vac).* Energy Procedia, 2012. **19**: p. 91-95.

40. Díaz-Dorado, E., et al., *Optimal distribution for photovoltaic solar trackers to minimize power losses caused by shadows.* Renewable Energy, 2011. **36**(6): p. 1826-1835.

41. Fathabadi, H., *Novel high efficient offline sensorless dual-axis solar tracker for using in photovoltaic systems and solar concentrators.* Renewable Energy, 2016. **95**: p. 485-494.

42. Fernández-Ahumada, L.M., et al., *A novel backtracking approach for two-axis solar PV tracking plants.* Renewable Energy, 2020. **145**: p. 1214-1221.

43. Ghosh, H.R., N.C. Bhowmik, and M. Hussain, *Determining seasonal optimum tilt angles, solar radiations on variously oriented, single and double axis tracking surfaces at Dhaka.* Renewable Energy, 2010. **35**(6): p. 1292-1297.

44. Lave, M. and J. Kleissl, *Optimum fixed orientations and benefits of tracking for capturing solar radiation in the continental United States.* Renewable Energy, 2011. **36**(3): p. 1145-1152.

45. Li, Z., X. Liu, and R. Tang, *Optical performance of inclined south-north single-axis tracked solar panels.* Energy, 2010. **35**(6): p. 2511-2516.

46. Njoku, H.O., *Upper-limit solar photovoltaic power generation: Estimates for 2-axis tracking collectors in Nigeria.* Energy, 2016. **95**: p. 504-516.

47. Quesada, G., et al., *Tracking strategy for photovoltaic solar systems in high latitudes.* Energy Conversion and Management, 2015. **103**: p. 147-156.

48. Şenpinar, A. and M. Cebeci, *Evaluation of power output for fixed and two-axis tracking PVarrays.* Applied Energy, 2012. **92**: p. 677-685.

49. Yao, Y., et al., *A multipurpose dual-axis solar tracker with two tracking strategies.* Renewable Energy, 2014. **72**: p. 88-98.

50. Beckman, J.A.D.a.W.A., *Solar Engineering of Thermal Processes*. Fourth ed. 2013: Wiley.

51. Energy, U.S.D.o. *eQuest*. [cited 2021; Available from: https://doe2.com/equest/.

52. Administration, U.S.E.I. *Electricity use in homes*. [cited 2021; Available from: https://www.eia.gov/energyexplained/use-of-energy/electricity-use-in-homes.php.

53. Agency, U.S.E.P. *Electricity Customers*. [cited 2021; Available from: https://www.epa.gov/energy/electricity-customers.

54. Administration, U.S.E.I. *Residential, consumption*. [cited 2021; Available from: https://www.eia.gov/consumption/residential/.

55. Administration, U.S.E.I. *Residential Energy Consumption Survey, 2015*. 2015 [cited 2021; Available from: https://www.eia.gov/consumption/residential/reports/2015/overview/.

56. Administration, U.S.E.I. *Housing Characteristics Tables*. 2015 [cited 2021; Available from: https://www.eia.gov/consumption/residential/data/2015/index.php?view=characteristics.

57. Administration, U.S.E.I. *Consumption and Expenditure Tables*. 2015 [cited 2021; Available from: https://www.eia.gov/consumption/residential/data/2015/index.php?view=consumption#by%20end%20uses.

58. Laboratory, N.R.E. *System Advisor Model*. [cited 2021; Available from: https://sam.nrel.gov/.

59. ASHRAE. *Technical resources - residential*. [cited 2021; Available from: https://www.ashrae.org/technical-resources/residential)

60. Energy, D.o. *Thermostats*. [cited 2021; Available from: https://www.energy.gov/energysaver/thermostats#:~:text=In%20the%20summer%2C%20you%20can,at%20home%20and%20need%20cooling

61. EnergyStar, U.S.D.o.E.-. *Heating and cooling guide*. [cited 2021; Available from: https://www.energystar.gov/ia/partners/publications/pubdocs/HeatingCoolingGuide%20FINAL_9-4-09.pdf.

62. Power, G. *Save money and energy*. [cited 2021; Available from: https://www.georgiapower.com/residential/save-money-and-energy/home-energy-efficiency-and-savings/energy-efficiency-tips.html.

63. Lee, S.W., David; Saman, Wasim, *Electricity Demand Profile of Australian Low Energy Houses.* . Energy Procedia, 2014. **62**.

64. Laboratory, N.R.E. *NSRDB data - TMY download*. Available from: https://developer.nrel.gov/docs/solar/nsrdb/psm3-tmy-download/.

65. Administration, U.S.E.I. *Frequenty Asked Questions - transmission*. Available from: https://www.eia.gov/tools/faqs/faq.php?id=105&t=3.

66. Energy, H. *Battery roundtrip efficiency*. [cited 2021; Available from: https://www.homerenergy.com/products/pro/docs/latest/battery_roundtrip_efficiency.html.

67. Energy, W.P. *How three battery types work in grid scale energy storage systems*. [cited 2021; Available from: https://www.windpowerengineering.com/how-three-battery-types-work-in-grid-scale-energy-storage-systems/.

68. Electric, S. [cited 2021; Available from: https://www.solar-electric.com/outback-power-se-420blu-300afci-grid-tie-off-grid-energy-

system.html?msclkid=514df21edac01078cb7f92aac374fe13&utm_source=bing&utm_medium=cpc&utm_campaign=Shopping%20-%20All%20Products&utm_term=4588536901185459&utm_content=All%20Products.

69. CNN. *EV battery waste*. 2019 [cited 2021; Available from: https://www.cnn.com/2019/11/06/business/electric-vehicles-battery-waste-scn/index.html.

70. Administration, U.S.E.I. *US Energy facts*. 2021 [cited 2021; Available from: https://www.eia.gov/energyexplained/us-energy-facts/.

71. Tesla. *Solar roof*. [cited 2021; Available from: https://www.tesla.com/solarroof.

72. Tesla. *Solar panels*. [cited 2021; Available from: https://www.tesla.com/solarpanels

73. Tesla. *Powerwall*. [cited 2021; Available from: https://www.powerwall2.com/about

74. Science, C., *Forest Fire impact on Solar PV*.

75. Engineering, W. *The wind turbine has been reinvented and it is 600% more efficient than current design*. 2014 [cited 2021; Available from: https://wonderfulengineering.com/the-wind-turbine-has-been-reinvented-and-is-600-more-efficient-than-current-design/.

Appendices

Appendix A: Estimated PV array size for comparative site at Reynold's Landing

Information on the PV grid of Reynold's Landing is taken from ariel images available on Google Maps (co-ordinates 33.403476, -86.877239) and the measurement tools available on that platform. The array's immediate footprint, the smallest area encapsulating the PV rows themselves, is approximately 4,033m^2, is very close to 1 acre (4,047m^2), in the shape of a parallelogram, slanted from the north-south axis (Figure A1).

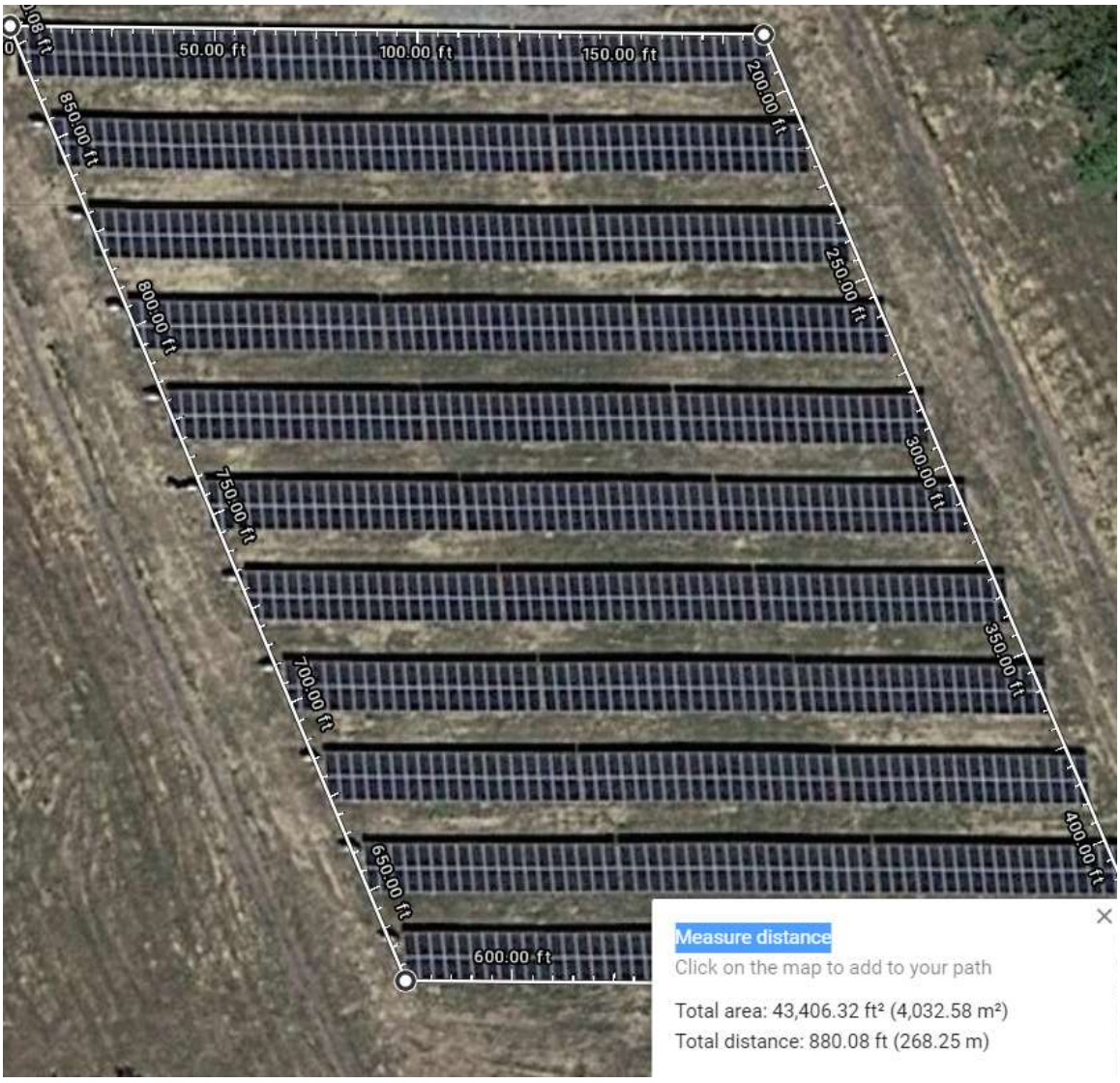

Figure A1 – ariel image and area estimation of the PV array at Alabama Power's Reynold's Landing development, performed with Google Maps.

Appendix B1: Nomenclature used for demand-side modeling processes (Table B1).

Table B1 - List of nomenclature symbols and meanings used in Stage II and III DSM processes (Allocating annual DC loads to monthly-hourly demand profiles)

Symbol	Unit[1]	Description	Calculation / values
h		Hour of the day, starting at value h, i.e. h=0 is from midnight to 01:00	0≤h≤23
m		Month of the year	1=Jan, 2 =Feb, etc
n_m		Number of days in a given month, m	n_1=31, n_2=28, etc
z		Specific day that relative use profile applies.	
$T_{m,h}^{Th}$	°F	Hourly temperature setting of thermostats for given month, m, of the year. The superscript *Th* is replaced with occupancy parameters: see Tables 5.6 and 5.7	
$T_{m,h}^{amb}$	°F	Hourly external ambient temperature at CSG location for a given month, m, of the year. Superscripts and subscripts follow those for $T^{Th.}$	Values from TMY data, Appendix B2
$\Delta T_{m,h}$	°F	Hourly temperature difference between T^{amb}, at the given CSG location and, T^{Th}, at given month, m, and hour, h. Superscripts and subscripts follow those for $T^{Th.}$	$\Delta T_{m,h} = T_{m,h}^{Th} - T_{m,h}^{amb}$
ρ		Ratio of higher occupancy of CSG house during the working week, set at 0.50 by default	
σ		Ratio of higher occupancy of CSG house during the weekend, set at 0.50 by default	
α_m	°F	Aggregate of the hourly temperature difference, ΔT_{mh}, over a 24 hour day in a given month, m.	$\alpha_m = \sum_{h=0}^{23} \Delta T_{mh}$
β_m	°F	Aggregate of the hourly temperature difference, ΔT_{mh}, for a given month, m	$\beta_m = \alpha_m \cdot n_m$
γ	°F	Aggregate of the hourly temperature difference, ΔT_{mh}, over the year	$\gamma = \sum_{m=1}^{12} \beta_m$
e_H	kWh·°F^{-1}	Specific energy of the heating demand, i.e., the element of electrical demand in kWh for each degree Fahrenheit difference of heating for a one-hour period	$e_H = \frac{E_D^C}{\gamma}$
$\varepsilon_{h,z}^C$	No unit	Relative hourly electric load, for hour, *h,* of the day, relative to the entire day's load.	
$\varepsilon_{T,z}^C$	No unit	Total of relative hourly electric load from eQuest, *T* representing total rather than being a variable.	$\varepsilon_{T,z}^C = \sum_{h=0}^{23} \varepsilon_{h,z}^C$
$r_{h,z}^C$	No unit	Ratio of hourly ε value to the total for that category C and z value.	$r_{h,z}^C = \left(\frac{\varepsilon_h}{\varepsilon_T}\right)^{C,z}$
q_m^C	No unit	Relative monthly electric load, from eQuest model, for month, *m*, of the day, relative to the entire year's load.	
q_T^C	No unit	Total of relative monthly electric load from eQuest, *T* representing total rather than being a variable.	$q_T^C = \sum_{m=1}^{12} q_h^C$
s_m^C	No unit	Ratio of monthly q value to the total for that category C.	$s_m^C = \left(\frac{q_m}{q_T}\right)^C$
$H_{m,h}$	kWh	Hourly energy consumption for a given hour, h, in a given month, m	Depends on the computational method appropriate to end-use category
M_m	kWh	Monthly electrical consumption for heating for given month, m	
D_m	kWh	Average daily electrical consumption for heating in a given month, m	$D_m = \frac{M_m}{n_m}$

Appendix B2 Monthly-hourly temperatures for the average solar day from TMY data

Table B2 – Hourly reported TMY temperature for the average solar day in each month

Starting time of hourly interval	Jan	Feb	Mar	Apr	May	Jun	Jul	Aug	Sep	Oct	Nov	Dec
0:00	32.0	39.2	40.8	62.6	57.2	68.0	71.6	69.8	68.0	55.4	41.0	32.0
1:00	32.0	39.2	39.7	62.6	55.4	68.0	69.8	69.8	66.2	55.4	41.0	32.0
2:00	32.0	39.2	39.0	62.6	55.4	68.0	69.8	69.8	66.2	55.4	39.2	32.0
3:00	32.0	37.4	38.3	62.6	55.4	66.2	69.8	69.8	66.2	55.4	39.2	32.0
4:00	30.2	37.4	37.8	62.6	55.4	66.2	69.8	68.0	66.2	53.6	39.2	32.0
5:00	30.2	35.6	37.2	62.6	57.2	68.0	71.6	68.0	66.2	53.6	39.2	32.0
6:00	30.2	35.6	38.3	62.6	60.8	71.6	75.2	69.8	68.0	53.6	39.2	32.0
7:00	32.0	35.6	42.3	60.8	66.2	75.2	78.8	73.4	71.6	55.4	41.0	32.0
8:00	33.8	35.6	47.3	57.2	73.4	77.0	84.2	78.8	77.0	59.0	46.4	35.6
9:00	39.2	37.4	51.8	57.2	77.0	78.8	89.6	82.4	82.4	62.6	53.6	41.0
10:00	44.6	39.2	55.2	55.4	80.6	80.6	91.4	84.2	84.2	66.2	59.0	44.6
11:00	50.0	41.0	58.1	55.4	82.4	82.4	93.2	86.0	87.8	68.0	64.4	48.2
12:00	51.8	42.8	60.3	55.4	84.2	82.4	95.0	87.8	89.6	69.8	66.2	50.0
13:00	53.6	42.8	61.2	57.2	84.2	82.4	95.0	89.6	91.4	71.6	68.0	50.0
14:00	53.6	41.0	61.0	55.4	84.2	82.4	96.8	89.6	91.4	69.8	68.0	50.0
15:00	51.8	39.2	60.3	53.6	84.2	82.4	95.0	87.8	89.6	68.0	66.2	48.2
16:00	44.6	37.4	58.3	51.8	82.4	80.6	93.2	86.0	87.8	66.2	60.8	42.8
17:00	39.2	33.8	54.0	50.0	77.0	78.8	91.4	80.6	80.6	60.8	55.4	37.4
18:00	39.2	32.0	51.3	46.4	71.6	77.0	87.8	77.0	75.2	57.2	51.8	35.6
19:00	37.4	32.0	47.3	42.8	68.0	73.4	82.4	75.2	71.6	55.4	51.8	33.8
20:00	37.4	32.0	45.9	41.0	66.2	73.4	78.8	75.2	71.6	53.6	51.8	32.0
21:00	35.6	32.0	44.4	39.2	66.2	71.6	77.0	75.2	69.8	53.6	51.8	32.0
22:00	35.6	30.2	43.0	37.4	64.4	71.6	75.2	73.4	69.8	51.8	51.8	32.0
23:00	37.4	30.2	41.7	35.6	64.4	71.6	75.2	73.4	68.0	51.8	50.0	32.0
0600-1800 average	43.7	38.5	54.0	56.0	78.1	79.6	89.9	83.0	83.5	64.3	57.4	42.7
1800-0600 average	34.3	34.7	42.2	51.5	61.4	70.3	74.9	72.1	68.8	54.4	45.7	32.5

All temperatures were reported in Celsius in the TMY files but were converted to Fahrenheit for presentation here for easier comparison with recommended thermostat settings in the U.S. context. The last two lines report the average day time (6a.m. to 6p.m.) and average overnight (6p.m. to 6 a.m.) temperatures. The daytime temperatures are represented according to month in Figure B1.

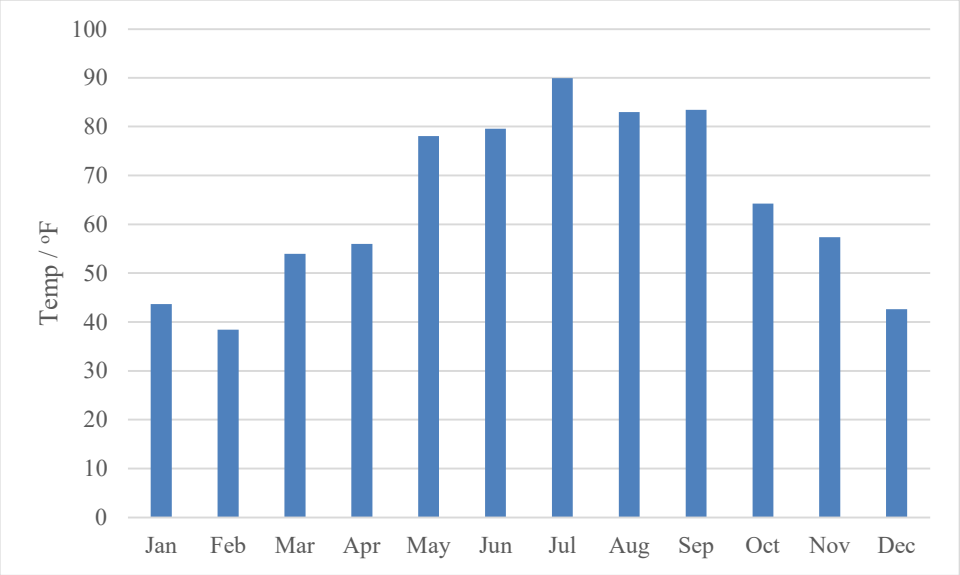

Figure B1 – average daytime temperatures for the average solar day in each month, as reported in TMY data

Appendix B3 Basic features of CSG house in eQuest model.

As a fundamental basis of the CSG model, certain house characteristics are defined: it is a detached, two story, family house (4 member household), set on an east-west axis with a significant south-facing roof and floor area of 2,500 square feet (Section 2). Broadly speaking these characteristics were entered into the eQuest model which provided relative-use profiles on daily and weekly bases.

The eQuest modeling inputs are summarized in Table B3. Not all screen numbers were presented on the wizard so should not be expected here (for example, the wizard jumped straight from screen 1 to screen 3, screen 2 only being visible dependent on certain screen 1 choices). Only the changes to defaults are included in Table B3.

Table B3 – non-default parameters entered into eQuest model for determining basic CSG house model			
Screen: content	Parameter	Setting	Comments
1: General information	Climate zone	3B – warm dry	Close correspondence to climate zone in RECS
	Building area	2,700ft^2	An error in comparison to RECS-15 approach but adapted on the next page
	Heating equipment	DX coils (heat pump), ground loop.	Heat pump is equivalent technology to CSG concept; ground loop is not included in CSG but its presence here will help keep heating load low as DC-only heat pump will in CSG house
	Building type	Multifamily	Single-family option not available on this version. This may have an impact on the model in terms of the inaccuracy of the relative use profiles.
3: Building footprint	Plan North	North	Allows for South-facing roof for PV – also affects daylighting and passive heating.
	Dimensions	60ft x 40 ft	Changes house size to 2,400 sq ft; now below target size (an error) but should have negligible effect on relative use profiles
4: Building envelope construction	Roof surfaces	Wood advance frame 24 in o.c. construction Steel finish 6in polyisocyanurate (R-42) exterior insulation No batt or rad barrier	Maximizing insulation for secure thermal envelope along lines of modern high performance building construction.
	Above grade walls	R-15 Batt additional insulation 1 in Polyisocyanurate (R-7) interior insulation.	
5: Building interior construction	Top floor ceiling	Drywall finish.	
	Other fall ceilings	R-21 Batt insulation.	Maximizing insulation for a secure thermal envelope.
	Vertical walls	R-13 Batt insulation.	
6: Exterior doors	Doors by orientation	North, South, West: 1 each East: zero.	Doors required on main faces of building (North and South); additional door on West to allow in evening Sun in .
	Door construction	Wood, solid core flush, 1-3/4 in.	Maximizing insulation.
7: Exterior windows	Glass category	All changed to Triple Low-E.	Maximizing insulation.
8: Exterior window shades and blinds	Overhangs	Selected for all windows. Shade depth calculated to 3.52m	Maximizing daylighting but minimizing passive heating.

	Window blinds / drapes	Type set to Horizontal blinds – light color.	
	Season definitions	Maximum three seasons selected and set to defaults, with Fall/Spring at all dates outside season 2 and 3; Season 2 (Summer) from May 1 to Sep 30; Season 3 (Winter) set from Dec 1 to Feb 28.	
9 Roof skylights	Skylights	Default (o) retained.	To avoid passive heating.
10: daylight zoning	Daylit area method:	Simplified (Wizard only).	
	Sensor 1:	Dimming 30% light (30% pwr).	
12: Top floor daylighting	Daylit area method:	Simplified (Wizard only).	
13: Season definitions	Observed holidays	[Deselected]	Designed for commercial buildings, so unnecessary.
	Season description	Typical use through year.	Selected as the only option.
	Number of seasons	Default value (1) retained.	This screen determines building operations rather than climate.
14: Building operation schedule	Weekdays	Set to unoccupied during working day (7am to 5pm).	This large simplification step does introduce some inconsistency with DSM.
	Weekends	Set to "open 24 hours".	
15: Activities areas allocation	Main screen	Default values retained.	No informed need to change.
	Occupancy profiles	No input: these profiles are treated as an output, Table 5.2b.	These profiles are taken and used partly to inform user profiles throughout Section 5.
17: Non HVAC end-uses to model		Exterior lighting removed.	Not included as part of the model
18: Interior lighting loads to profile		Defaults retained.	No informed need to change.
20: Cooking loads and profiles	Energy intensity	11.9W/ft^2	Max power: 4.8kW https://www.hunker.com/12196042/how-many-watts-does-an-electric-stove-use Floor area: (0.15x2,700ft^2) = 450 ft^2. Energy intensity = 4800W/450ft^2
21: Self contained refrigeration loads and profiles	Energy intensity	0.48W/ft2	No informed need to change.
22: Miscellaneous loads and profiles		Default values retained.	No informed need to change.
28: Domestic water heating hourly profiles		Default values retained.	No informed need to change. SAM provide d hourly profiles.
29: HVAC system definitions	Heat Pump source	Ground loop	A means to minimize heating demand although not included in overall load estimation
30: HVAC zones: Temperature and Air zones		Defaults retained	No informed need to change.
32: Packaged HVAC equipment		Defaults retained	No informed need to change.
34: HVAC system fans		Defaults retained	No informed need to change.

35: HVAC System # 1 Fans schedule	Weekends	Switched to 24 hours	Other defaults retained (on at 5pm and off at 7am)
37: HVAC Zone Heating, Vent, and Economizers		Defaults retained.	No informed need to change.
40: GSHP Equipment – loop properties		Defaults retained.	No informed need to change.
48: Non-residential domestic water heating		Defaults retained.	No informed need to change.
50: Electric utility charges	Customer charge	Set to zero.	Fundamental element of model.
52: Fuel utility charges	Customer charge	Set to zero	Fundamental element of model

.

Hourly profiles produced by screens were taken to inform hourly use profiles in Appendix B4.

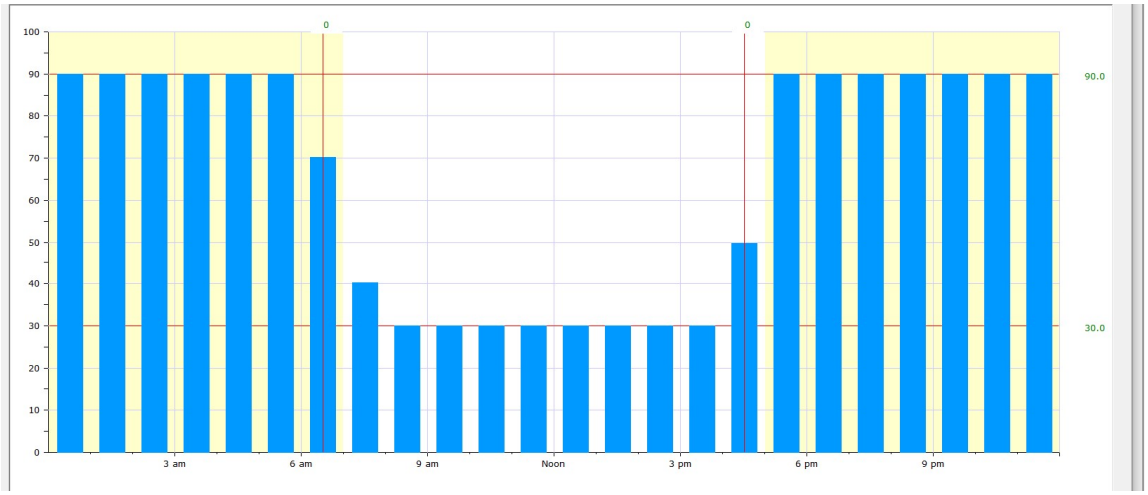

Figure B2 - weekday occupancy profile.

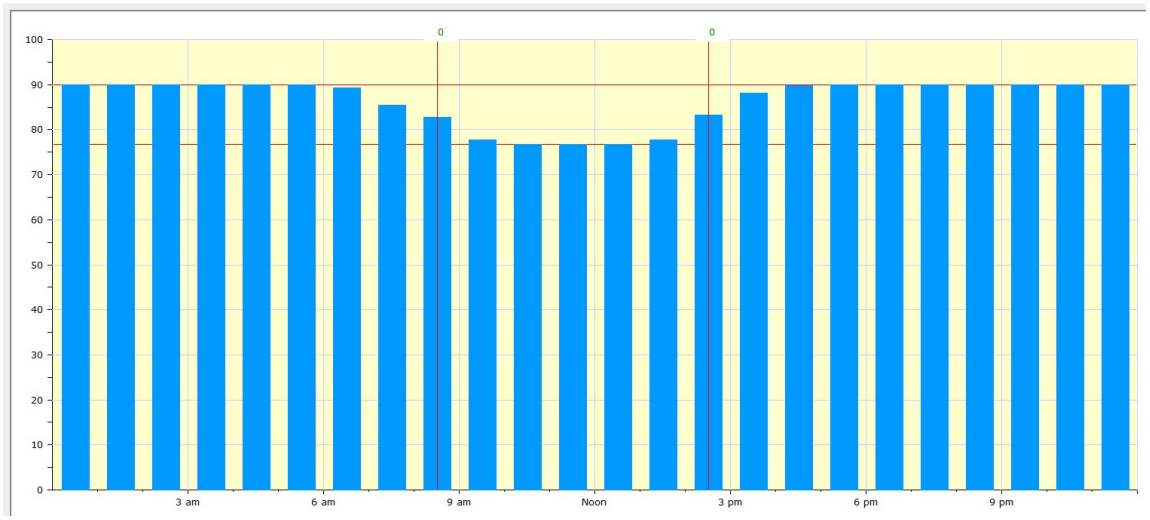

Figure B3 - weekend occupancy profile.

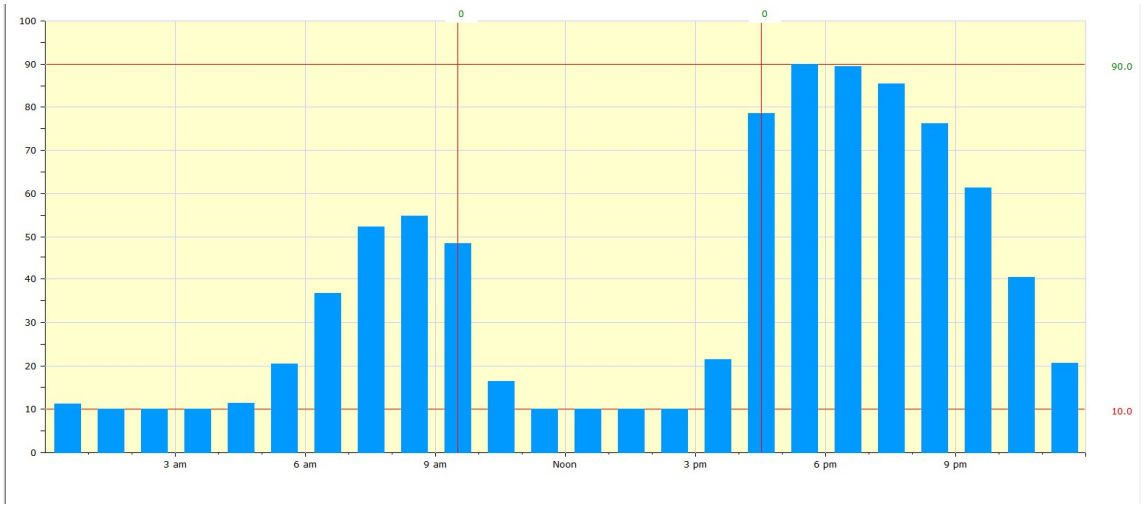

Figure B4 - lighting profile.

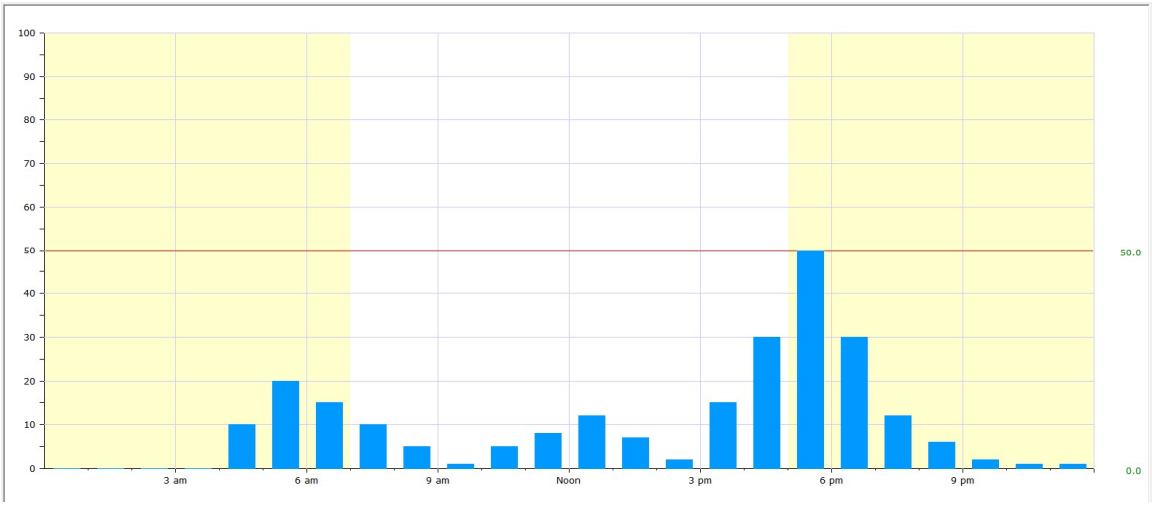

Figure B5 - cooking equipment profile.

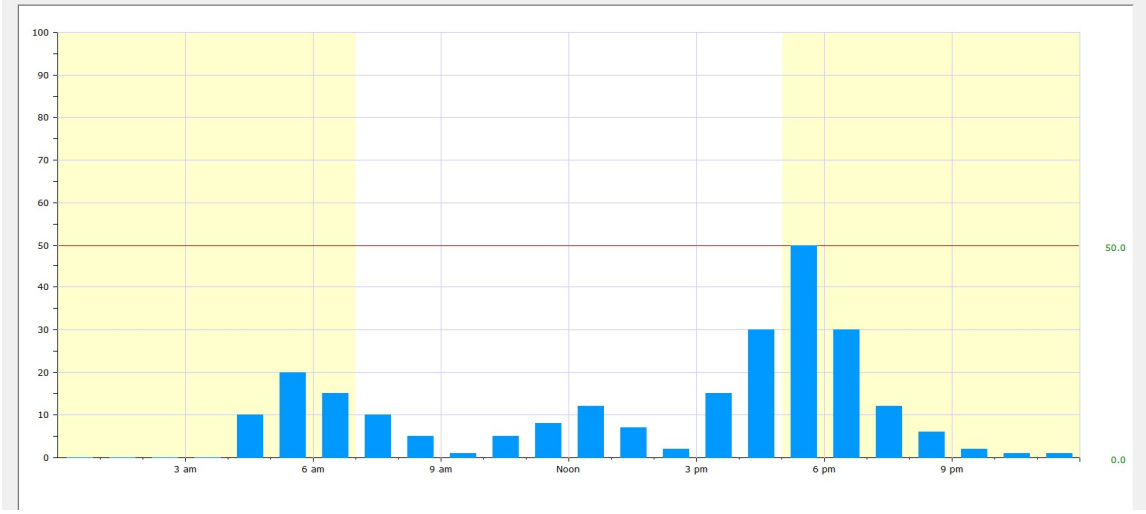

Figure B6 - miscellaneous equipment profile.

Appendix B4: Computation of hourly profiles by end-use categories.

1: Space heating : C = SH

Stage I: $L_A^{SH} = 3874kWh.$

To realize the foundational CSG principle of energy independence, space heating necessarily must be electrical, rather than fueled by natural gas, or other non-electric fuels. The relevant RECS-15 table (CE5.3a) includes "average site energy consumption" for space heating and air handlers for heating under various categories. Total square footage, climate region, and construction year were taken as the three most relevant categories for space heating estimation: the greater the floor area of the house, the greater the volume of air that needs to be heated, the colder the climate, the more heating is required, and the newer the construction, the greater the likelihood of the house being built with a secure thermal envelope. The same reasoning applies for space cooling and thus the same RECS-15 categories are sampled for the equivalent load estimation in that end-use category. Therefore, the weighted average of the heating demand for the house size ranges on either side of the CSG house, 2,500 sq ft, was calculated (Table B4, Equation B1) and then combined in a simple average with the energy demand for houses in the mixed-humid region and 2010-15 construction year range to produce the average space heating demand under standard AC electrical systems (Equation B2).

Table B4 – RECS 15 data for estimation of annual equivalent AC load for SH

RECS-15 Category	Number of houses in category (million)		RECS-15 annual electrical demand for heating / kWh		
	In area range	Total of both ranges	Space heating (general)	Air handlers for heating	Total
2,000 – 2,499 sq ft	4.9	8.2	3618	261	3879
2,500 – 2,999 sq ft	3.3		4051	325	4376
Mixed-humid region	N/A		4354	191	4545
Constructed 2010-15	N/A		2831	168	2999

$$2{,}500 sq\ ft\ house\ estimated\ demand = \frac{(3879kWh \times 4.9) + (4376kWh \times 3.3)}{8.2} = 4079kWh \qquad \text{(B1)}$$

$$CSG\ house\ estimation = \frac{(4079 + 4545 + 299\ )kWh}{3} = 3874kWh \qquad \text{(B2)}$$

Stage II L_D^{SH} = 2046 kWh.

The DC loading for space heating was determined, straightforwardly, from the $\boldsymbol{L_A^{SH}}$ value and the those in Table 5.3 using Equation 5.2:

$$L_D^{SH} = L_A^{SH} \times (1 - \eta_{int}) \times (1 - \eta_{dir}) \quad \text{(B3)}$$

$$L_D^{SH} = 3874kWh \times (1 - 0.40) \times (1 - 0.12) = 2046kWh \quad \text{(B4)}$$

Stage III Fitting annual DC load to monthly-hourly profile for space heating.

In fitting L_D^{SH} to the 288 monthly-hourly values, the first order approximation was made that the work done by the heat pumps in a given hour interval would be proportional to the difference between the thermostat setting temperature, T^{th}, and the ambient external temperature, T^{amb}, at the given hour *h* and month, *m*.

First, ΔT_{mh}, was calculated for the initial CSG location for each hour of the day and month of the year with the following system:

$$\Delta T_{m,h} = \begin{cases} T_{m,h}^{Th} - T_{m,h}^{amb}\ ,\ for\ T_{m,h}^{Th} > T_{m,h}^{amb} & (B5a) \\ 0 \qquad for\ T_{m,h}^{Th} \leq T_{m,h}^{amb} & (B5b) \end{cases}$$

The zero value for when the thermostat is set below the ambient temperature (or if the month is a cooling month, May to September, Section 4) allows for the computation to calculate zero work when the heater is not active.

These calculations were performed once for each of the four *heating* thermostat profiles provided (Table 5.6), and so produce four ΔT profiles (Appendix B2), requiring two superscript indices to the ΔT parameter. The first, *w* or *e*, refers to a temperature difference based on weekday or weekend thermostat profiles, respectively; the second, *h* or *l*, refers to those based on higher or lower occupancy profile; so that, for example, $\Delta T_{11,20}^{w,h}$ would refer to the difference between

ambient and thermostat temperatures for a higher-occupancy house at 8pm on a weekday in November. These four ΔT profiles were sampled in different proportions using Equation B7 to produce a weighted average monthly-hourly temperature difference profile:

$$\overline{\Delta T_{mh}} = \left(\frac{5}{7}\right) \cdot \left\{(1-\rho)\Delta T_{mh}^{w,l} + \rho \Delta T_{mh}^{w,h}\right\} + \left(\frac{2}{7}\right) \cdot \left\{(1-\sigma)\Delta T_{mh}^{e,l} + \sigma \Delta T_{mh}^{e,h}\right\} \quad \text{(B6)}$$

The ratios of 5/7 and 2/7 are self-evidently the ratios for weekday and weekend profiles respectively, with ρ and σ providing sampling ratios for weekday and weekend high occupancy rates (Section 5), at their default values of 0.50 each. These values were computed for each of the 288 monthly-hourly intervals.

Next, the derivative computational parameters (α_m, β_m, γ, e_H, M_m, D_m) were calculated from the $\overline{\Delta T_{mh}}$ values using relevant equations and definitions (Table B1, and these are described as follows:

- To allocate appropriate proportions of the daily energy consumption, these $\overline{\Delta T_{mh}}$ values were summed into the aggregate parameter α_m, specific to each month, m:

$$\alpha_m = \sum_{h=0}^{23} \overline{\Delta T_{mh}} \quad \text{(B7)}$$

- These values vary from one another in part due to the changing ambient temperatures and depending on whether thermostats are in cooling or heating modes. From this α_m parameter, the aggregate hourly temperature difference from the whole month, β, can be calculated by simply multiplying the α parameter by the number of days in that given month:

$$\beta_m = \alpha_m \cdot n_m \quad \text{(B8)}$$

- Considering March (m=3), calculations for α3 and β3 are provided below as an example:

$$\alpha_3 = \sum_{h=0}^{23} \overline{\Delta T_{3h}} = (19.2 + 20.3 + 21.0 + \ldots + 23.6 + 17.0 + 18.3)\ ^oF = 377.6^oF; \quad \text{(B9)}$$

$$\beta_3 = \alpha_3 \cdot n_3 = 377.6\ ^oF \times 31 \text{ days} = 11{,}706.3\ ^oF \quad \text{(B10)}$$

- These β values were summed for the 12 months of the year to give the $\boldsymbol{\gamma}$ parameter, the aggregate hourly temperature difference (between ambient and thermostat temperatures) for the whole year. The annual expected energy demand, L_A, was then divided by γ to give the *specific energy of the heating* parameter, e_H,

$$\gamma = \sum_{m=1}^{12} \beta_m = (18450.3 + 18277.6 + \cdots + 19510.5)^o F = 89322.7F \quad \text{(B11)}$$

$$e_H = \frac{L_A}{\gamma} = \frac{2046\ kWh}{89322.7F} = 0.02290\ kWh \cdot^o F^{-1} \quad \text{(B12)}$$

Equations B7 to B12 were applied to provide necessary parameter values for the CSG space heating months (January to April; October to December, Table B5)

Table B5 – Derived parameters for space heating for relevant months

Month	Jan	Feb	Mar	Apr	Oct	Nov	Dec
α_m/ °F	595.2	652.8	377.6	254.7	141.8	311.4	629.4
β_m/ °F	18450.3	18277.6	11706.3	7640.6	4396.2	9341.1	19510.5
γ	89322.7 °F						
e_H	0.02290 kWh·°F^{-1}						

The final stage in calculating the monthly-hourly demand values is to multiply the specific energy value by the temperature difference value for the given monthly-hourly interval, described and exemplified as follows and summarized in Table B6:

$$H_{mh} = e_H \times \overline{\Delta T_{m,h}} \quad \text{(B13)}$$

Again, considering March as an example, and the 11:00am hour interval:

$$H_{3,11} = 0.02290\ kWh \cdot^o F^{-1} \times 5.9^o F = 0.14\ kWh \quad \text{(B14)}$$

Finally, the internal accuracy of the calculations can be verified by calculating M_m values which in turn can be summed to find a derivative value of L_D^{SH}. This should agree with the value from Stage II.

$$M_m = e_H \times \beta_m \quad \text{(B15)}$$

$$M_m = e_H \times \beta_m = 0.02290\ kWh \cdot^o F^{-1} \times 11706.3kWh = 268.1\ kWh \quad \text{(B16)}$$

$$L_D^{SH} = \sum_{m=1}^{12} M_m = (422.5 + 418.6 + \cdots 213.9 + 446.8)kWh = 2045.5kWh \quad \text{(B17)}$$

The agreement between equations B4 and B17 provides a degree of confidence in the computational method.

The results of equations B16 to B18 were calculated (Table B6) along with daily average space heating loads for each month calculated with equation 5.21.

$$D_m = \frac{M_m}{n_m} \quad \text{(B18)}$$

Space heating DSM output

The average daily loads per month summarized in Figure B7.

Table B6 – space heating loads – all values in kWh												
Month	Jan	Feb	Mar	Apr	May	Jun	Jul	Aug	Sep	Oct	Nov	Dec
$M_{m:}$	422.5	418.6	268.1	175.0	N/A – not heating months					100.7	213.9	446.8
L_D^{SH}:	2046 kWh											
D_m:	13.6	14.9	8.6	5.8	N/A – not heating months					3.2	7.1	14.4

The average daily loads per month summarized in Figure B7.

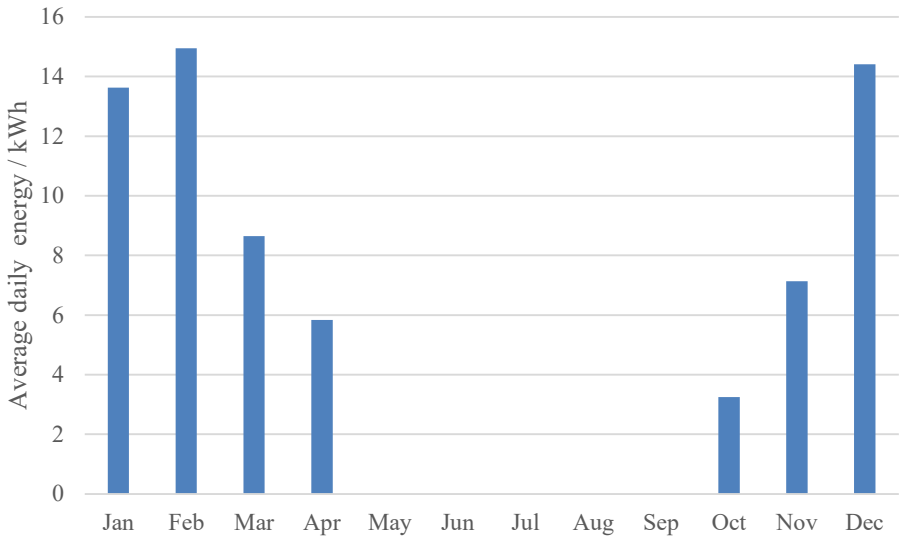

Figure B7 – Average daily space heating load by month.

The seasonal variation (Figure B7) corresponds well to ambient temperatures in the TMY data and the designated thermostat settings (greatest difference between the two values occurring in February). The unexpected result of January's demand being less than either December or February is down to the thermostat settings and occupancy profiles as the temperature difference during heating hours is greatest in the other two months rather than in January, when the average temperature over the entire day is colder. The sudden drop-off and pick-up in April and October

are due to the designation of May to September as non-heating months, which is appropriate for the local climate conditions in Athens, Georgia. If the model had a greater resolution, i.e., modeling more than just the one average solar day in a month, then it is likely that April would show a lower demand and September a non-zero demand.

Daily variations in space heating (Figures B8 a-f) for the six main heating months of the year demonstrate broadly expected results. Demand is greatest at times of highest occupancy when household members are awake (early morning and during the evening), with lower demand during the middle of the day when temperatures are higher and occupancy lower. Further, the overall demand tends to be higher in expected winter months. The slightly unexpected result of February's demand being higher than January's (discussed above in seasonal variation) is demonstrated here by much greater heating during the middle of the day when ambient temperatures are lower than the same times in January. The colder overnight temperatures in January do not affect it demand as space heating is not active at that time.

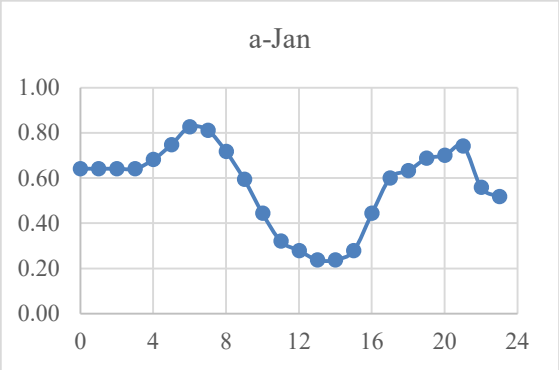

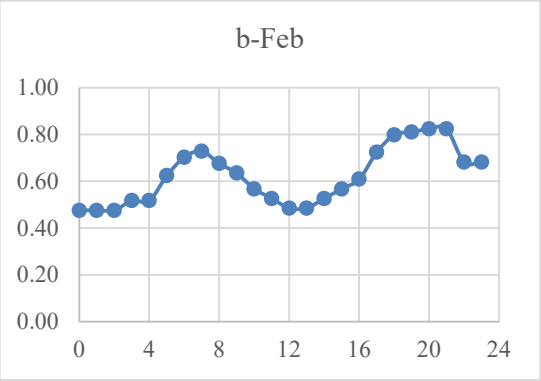

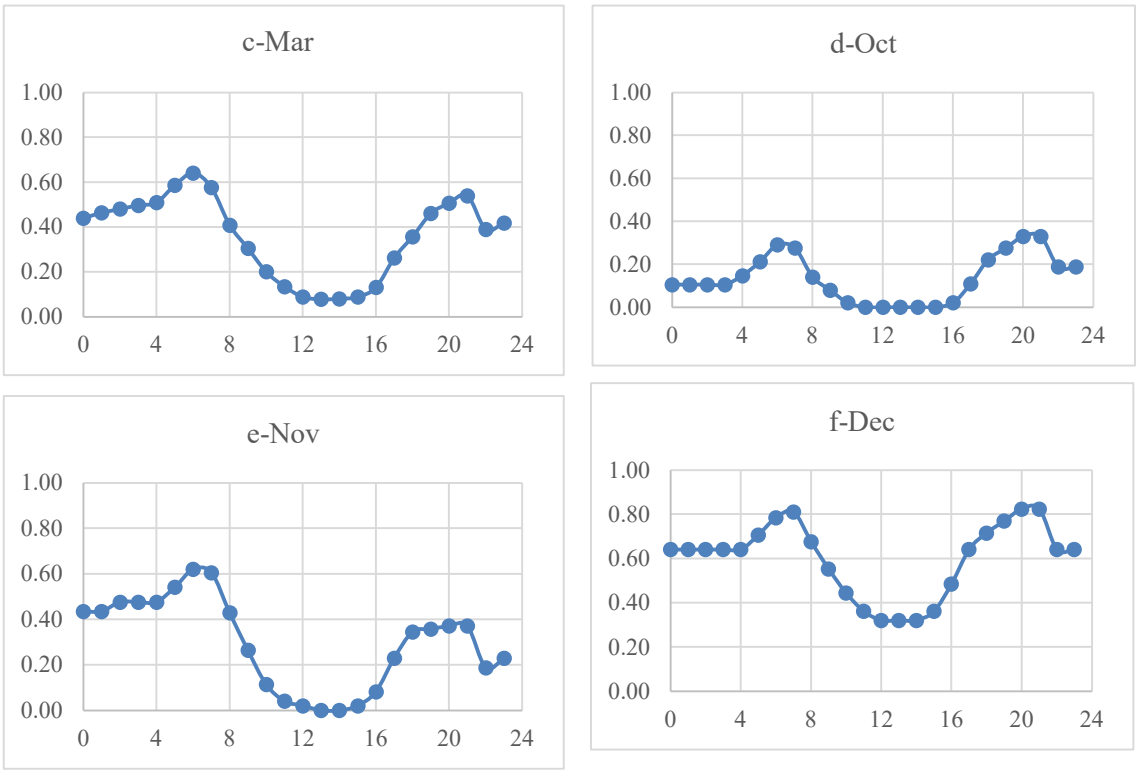

Figures B8 a-f Hourly variation of space heating for average solar days in six space heating months. Vertical axes are all the power rating in kW, the horizontal axes are all time of day, in hours, with the intergral area representing electical energy load, in kWh.

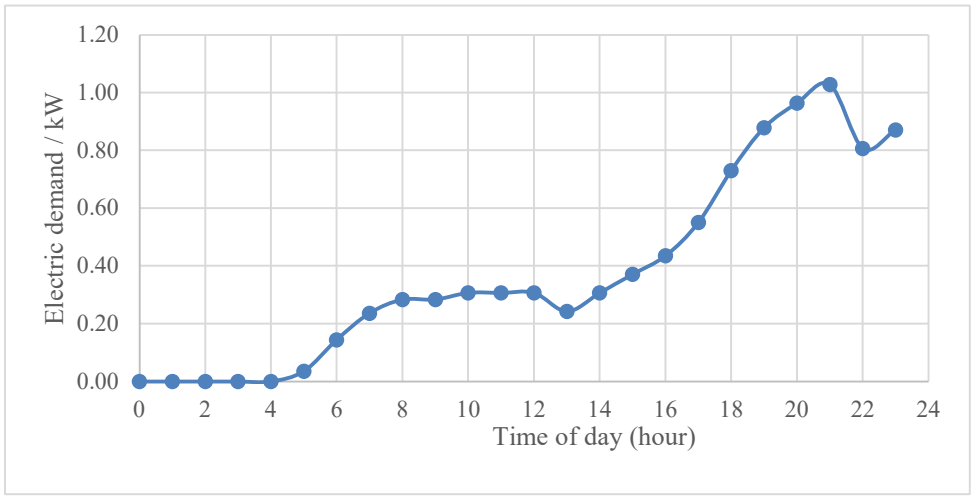

Figure B9 – Hourly variation of space heating load in April

The daily demand curve for April is the most unusual (Figure B9). and appears to be a major factor in the unusual daily variation for the total demand across all categories for that month. On inspection of the TMY data, this appears due to the gradual but significant drop in ambient temperature and the resultant increasing difference between that temperature and the thermostat settings (Figures B10a, b). The inaccuracy between this modeling and reality is likely to lie in the temperatures for the average solar day in April (the 15th day) being used as a representative of the whole. In that sense, the inaccuracy is acceptable: better that the bar be set too high than too low. Regardless, the situation is unavoidable due to the need for consistency between demand-side and supply-side modeling; potential improvements are discussed in Section 9.3.

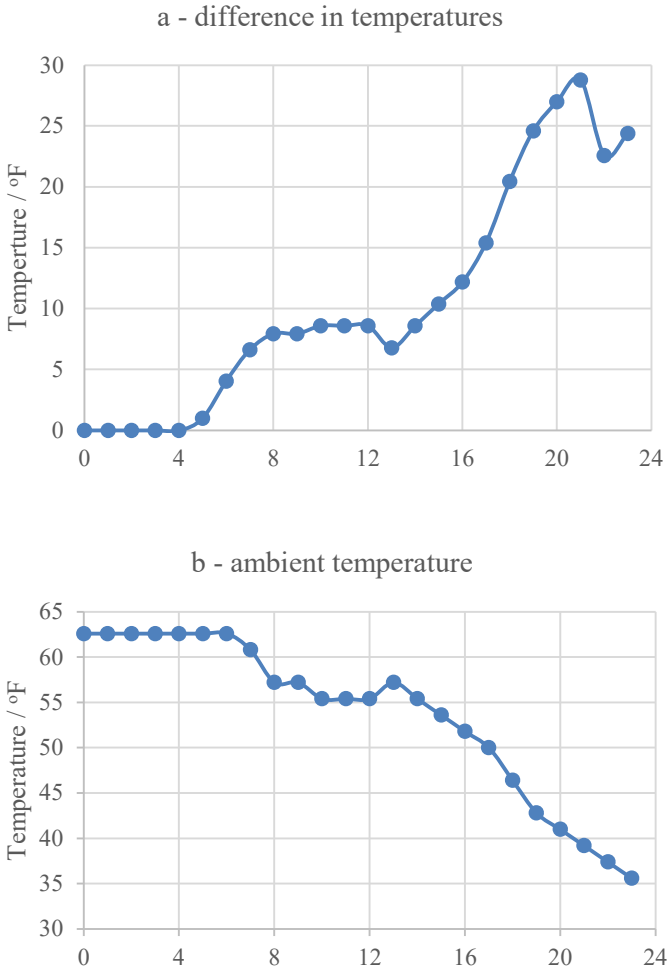

Figure B10a, b – Temperature variations and differences for April for space heating

2. Space cooling (C=SC)

Stage I: L_A^{SC} = 3087 kWh.

Unlike the SH category, RECS-15 does not have a specific category for "electricity as cooling fuel" as all space cooling is electrically powered. Instead, an average of the appropriate type for all the other relevant categories were taken. Table B7 outlines the categories which were considered, the ones chosen to form part of the average calculation, and the reasons why.

Table B7 - Reported energy consumption for air-conditioning (i.e., space cooling) from different housing categories within the South of the U.S., from to the EIA 2015 RECS.

RECS category: specific type	Electrical demand[1] / kWh	Notes	Included
Census division: South Atlantic	3136	This is a very broad category covering a large geographic region and has a low resolution for this model, so this was not included in the average.	
Climate region: Mixed-humid	2257	This category covers a broad range of houses (21.3 million) and is a relevant category with climate, especially humidity, being a prime driver of space cooling load.	✓
Construction year: 2010-2015	2872	This bracket for construction year is the latest available in the RECS model and the energy consumption is considerably lower than other brackets, supporting the general assumption that more modern houses are built with more effective energy efficiency and thermal design.	✓
Housing unit: Single family detached	4132	These categories cover broad geographical and size ranges and as they are considered less important drivers for space cooling and are not included in the average.	
Ownership: owned, single-family	4162		
Area: 2,000 - 2,499 sqft	3928	The CSG floor area of 2,500 square feet lies in the middle of these two ranges, so an average value of 4133 kWh is used for the average calculation.	✓
Area: 2,500 - 2,999 sqft	4338		
Number of household members: 4	3781	Considered less relevant than other factors	
Main heating fuel: electricity	2901	This value is considerably lower than when natural gas is the main heating fuel; however, the connection between the type of heating fuel and the cooling electricity consumption is not immediately obvious.	

Thus, the expected annual AC load for space cooling is calculated from the simple average:

$$L_A^{SC} = \left(\frac{2257+2872+}{3}\right) kWh = 3087kWh \quad \text{(B19)}$$

Stage II L_D^{SC}= 1456kWh.

Using the air-conditioning DC efficiency values (Table 5.3) in the standard DC efficiency calculation gives the following expected DC demand for space cooling:

$$L_D^{SC} = 3087kWh \times (1 - 0.47) \times (1 - 0.11) = 1456kWh \quad \text{(B20)}$$

Stage III Fitting annual DC load to monthly-hourly profile for space cooling.

The process of fitting L_D^{SC} to the 288 monthly-hourly values is essentially the same in form as that for the space heating profiles, with the obvious differences of reversing the temperature difference calculation and decisions (Equations 5.24a, b).

$$\Delta T_{m,h}^{SC} = \begin{cases} T_{amb} - T_{Th}\,, & for\ T_{th} < T_{amb} \quad (B21a) \\ 0 & for\ T_{th} \geq T_{amb} \quad (B21b) \end{cases}$$

Space cooling DSM output

By applying these equations to the cooling columns of the thermostat profiles, Equation 5.9 could then be used to calculate weighted average values of temperature difference. These results were then applied through Equations B18 to B20 to derive the monthly-hourly energy demand profiles for space cooling. These are summarized in Table B8 Figures B11 a-f.

Table B8 – space cooling loads – all values in kWh					
Month	May	Jun	Jul	Aug	Sep
M_m:	100.3	77.8	716.4	257.4	304.2
L_D^{SC}:	1456.1				
D_m:	3.23	2.59	23.1	8.3	10.1

Dividing L_A^{SC}, 3087 kWh**,** by the number of days in the five cooling months (122) gives a simple mean average daily cooling load of 20.2 kWh, suggesting that the pronounced spike in July demand is more a result of especially low cooing demands in July than in other cooling months rather than the July demand being particularly high. The low demands in May, June, August and September are explained by the thermostat settings and ambient temperatures in those months: the former values are reasonably high (78ºF for occupied hours and 85ºF for unoccupied), such that the latter do not trigger the cooling systems to operate, forcing low demands. In contrast, the July daytime temperatures, averaging 89.9ºF, easily exceed the thermostat setting, resulting in an electric demand similar to the standard expected load for normal, existing, houses.

The nature of this cooling demand, though it may be questioned given the pronounced July spike, is predicated on two objective sources: EPA recommended temperatures for the thermostat settings, and NSRDB TMY files for ambient temperatures. Developers for a real residential development may choose to apply more realistic thermostat modeling, but the current temperature data is required for synergy between demand-side and supply-side processes. Improved accuracy may be achieved by expanding both processes beyond average solar day sampling, and this is discussed in Section 9.2.

Apart from the July peak, the data (Figures B11 b-f) appears accurate and valid in terms of the overall magnitude and profile of the demand, with higher daily peaks in warmer months, peaks accentuated in those warmer months, and with peaks around midday. In terms of timing and energy planning, space-cooling presents one of the easier challenges as it is intrinsically linked with expected PV supply in terms of co-incidence: when the sun is "up" and at its greatest intensity, it is supplying heat and electrical energy simultaneously – the electricity for cooling is supplied at the same time it is required, if not necessarily at the same rate.

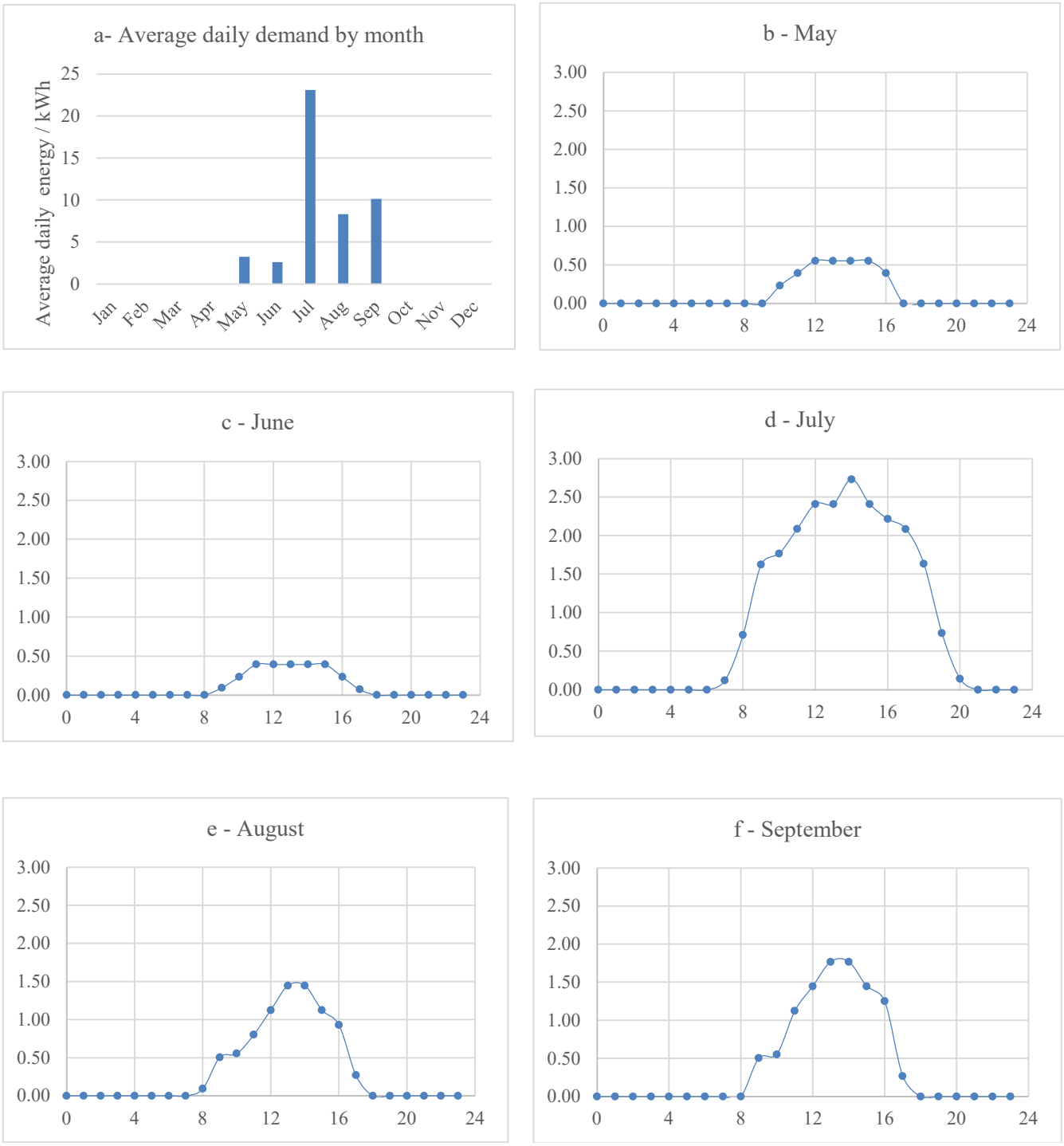

Figure B11 a-f – seasonal (a) and hourly space cooling demands for relevant months (b-f).

3. Water heating (C=WH) with solar thermal panel supply.

The process to determine the monthly-hourly water heating demand is different from that for other categories due to the option of solar water heating. As, in the CSG model, PV modules are placed

on the ground in a centralized location, the rooftops of individual houses are available for standard solar thermal panels (STP) which use the heating component of the Sun's radiation to heat domestic water. The resultant reduction in electrical consumption can be simulated via a module in the same application in SAM that is used to model PV performance. The computation steps for water heating demand are therefore:

- Stage A: estimation of expected annual AC electric demand for current mainstream use.
- Stage B: determine monthly AC electric demand through application of eQuest relative monthly use profile.
- Stage C: simulation of STP contribution to water heating demands on a monthly basis, and calculation of the remaining monthly AC electric demand.
- Stage D: calculation of the expected monthly DC electric demand through DC savings, and from this, expected average daily demand for each month.
- Stage E: computation of monthly-hourly water heating demand by application of eQuest relative hourly use profile.

Stage A Estimating, $L^{WH}{}_{A}$ = 5092 kWh.

Table CE5.3a of RECS-15 provides detailed end-use consumption for water heating in terms of electrical demand. The number of household members was taken as the most significant factor in determining demand for this category, for which the reported value was 4882kWh.

Stage B Determining monthly AC profile.

The eQuest seasonal energy profile (Section 5.4) for the CSG model is applied to determine the monthly AC water heating demand from the annual AC value:

$$s_m^C = \left(\frac{q_m}{q_T}\right)^C \tag{B22}$$

$$M_{m,A}^{WH} = s_{m,}^C \times L_A^{WH} \tag{B23}$$

where q is the eQuest relatively monthly demand as previously defined (Appendix B1).

Table B9 – Water heating demand												
	Jan	Feb	Mar	Apr	May	Jun	Jul	Aug	Sep	Oct	Nov	Dec
q_m	1.69	1.59	1.75	1.65	1.56	1.36	1.29	1.19	1.15	1.27	1.35	1.54
q_T	17.4											
s_m	0.097	0.091	0.101	0.095	0.090	0.078	0.074	0.068	0.066	0.073	0.078	0.089
Annual demand	5092 kWh											
$M_{m,A}$ / kWh	474.4	446.4	491.3	463.2	437.9	381.8	362.1	334.1	322.8	356.5	379.0	432.3

Stage C Simulating solar thermal panel contribution to water heating.

Parameters appropriate to the CSG model (Table B1) were entered into the Solar Water Heating (SWH) module (Distributed, Residential Owner) module of SAM version 2020.11.29.

Table B10 – Parameter values for solar thermal heating panels in NREL SAM simulations		
Parameter	**Value chosen / action taken**	**Explanation**
Weather file	Athens_GA, PSM3-TMY 60	Ensures consistency with other calculations in this study.
Average daily hot water use	Set to 172 kg/day	Value determined by subsidiary calculation and average use data.
Collector area	2.98 m^2	2.98m^2 is the default value, and was selected after sensitivity analysis of increasing collector area on energy savings.
System: tilt	Set to latitude at 34°	This should give optimal performance and is a reasonable value for roof pitch.
System: azimuth	Set to 180°	i.e. South facing roof / panels.
Collector	Heliodyne Inc. Gobi 408 013	Default equipment; no basis for choosing another.

The simulation output from SAM is the electrical demand with, and without, the solar water heating system (Table B11). The calculated values of electrical use both with and without the system are far in excess of any of the household consumption values provided in the EIA RECS 2015 data; given the reliability of the RECS data, the discrepancy is likely an inaccuracy in the SAM simulation of the total consumption values.

Table B11 – Simulation results from SAM model of solar water heating		
	Electrical demand or savings / kWh	
Month	With STP use: μ'_m	Without STP use: μ_m
Jan	566.7	752.2
Feb	463.8	642.4
Mar	451.3	647.8
Apr	446.5	643.8
May	582.4	777.2
Jun	976.4	1151.7
Jul	1423.8	1594.8
Aug	1226.6	1393.4
Sep	852.3	1016.2
Oct	660.4	837.8
Nov	452.0	640.4
Dec	568.3	731.8
Total:	8670.3	10829.3

The purpose of the simulation, for this study, is to determine the amount of heating energy that can be saved through STP utilization and that were easily calculated by:

$$M_m^{STP} = \mu_m - \mu'_m \quad \text{(B24)}$$

These monthly values of energy saved through STP utilization were then used to determine the reduced monthly AC demand for water heating (Table B12)

$$M_{m,R}^{WH} = M_{m,A}^{WH} - M_m^{STP} \quad \text{(B25)}$$

Table B12 – Stage C monthly demands values for WH – all values in kWh												
Month:	Jan	Feb	Mar	Apr	May	Jun	Jul	Aug	Sep	Oct	Nov	Dec
$M^{WH}_{m,A}$	474.4	446.4	491.3	463.2	437.9	381.8	362.1	334.1	322.8	356.5	379.0	432.3
$M^{STP}_{m,}$	185.5	178.6	196.5	197.3	194.9	175.3	171.0	166.8	163.9	177.4	188.4	163.6
$M^{WH}_{m,R}$	288.9	267.7	294.8	265.9	243.1	206.5	191.2	167.3	159.0	179.1	190.6	268.8

Stage D Calculating monthly and daily demand after DC savings.

DC-internal savings of 50% and Direct-DC savings of 12% (Table X) allow the calculation of DC demand on a similar basis as previous categories but at a monthly resolution, with daily demand calculated as previously (Table B13)

$$M_{m,D}^{WH} = M_{m,R}^{WH} \times (1 - \eta_{int}) \times (1 - \eta_{dir}) \quad \text{(B26)}$$

$$D_m^{WH} = \frac{M_{m,D}^{WH}}{n_m} \quad \text{(B27)}$$

Table B13 – Stage D monthly and daily demands for water heating, all values in kWh

Month:	Jan	Feb	Mar	Apr	May	Jun	Jul	Aug	Sep	Oct	Nov	Dec
$M_{m,R}^{WH}$	289	268	295	266	243	207	191	167	159	179	191	269
$M_{m,D}^{WH}$	127	118	130	117	107	91	84	74	70	79	84	118
D_m^{WH}	4.1	4.2	4.2	3.9	3.5	3.0	2.7	2.4	2.3	2.5	2.8	3.8

Stage E Fitting annual DC load to monthly-hourly profile for water heating

When the CSG house is modeled on eQuest (i.e., on the basis of residential use), an hourly hot water use profile is generated with distinctions between weekdays, Saturdays, and Sundays (B14).

Table B14 – hourly user profiles for different points of the week for water heating.			
Time	Weekday	Saturday	Sunday
Parameter:	ε_h^w	ε_h^{Sat}	ε_h^{Sun}
0:00	0.05	0.2	0.2
1:00	0.05	0.2	0.2
2:00	0.05	0.2	0.2
3:00	0.05	0.2	0.2
4:00	0.05	0.2	0.2
5:00	0.2	0.2	0.2
6:00	0.8	0.21	0.2
7:00	0.7	0.3	0.2
8:00	0.5	0.45	0.25
9:00	0.4	0.55	0.3
10:00	0.2	0.55	0.35
11:00	0.2	0.42	0.35
12:00	0.2	0.45	0.4
13:00	0.3	0.65	0.55
14:00	0.5	0.75	0.65
15:00	0.5	0.75	0.55
16:00	0.7	0.65	0.42
17:00	0.7	0.6	0.35
18:00	0.4	0.55	0.35
19:00	0.4	0.5	0.35
20:00	0.2	42	0.35
21:00	0.2	0.35	0.35
22:00	0.1	0.3	0.3
23:00	0.1	0.22	0.25
Total	**ε_T^w =7.55**	**ε_T^{Sat} =51.45**	**ε_T^{Sun} =7.72**

The equation to combine these values with a correct weighting into the final water heating monthly-hourly demand is therefore:

$$H_{mh} = D_m^{WH} \times \left\{ \left(\frac{5}{7}\right)\left(\frac{\varepsilon_{h,w}}{\varepsilon_{T,w}}\right)^{WH} + \left(\frac{1}{7}\right)\left(\frac{\varepsilon_{h,Sat}}{\varepsilon_{T,Sat}}\right)^{WH} + \left(\frac{1}{7}\right)\left(\frac{\varepsilon_{h,Sun}}{\varepsilon_{T,Sun}}\right)^{WH} \right\} \quad \text{(B28)}$$

Results of the computation are summarized in Figures B12-13.

Water heating DSM output

The seasonal results appear broadly and intuitively correct (Figure B12) with the expected average daily electrical energy load dropping gradually from January to August: as the ambient temperature decreases, more overall work needs to be done to heat the water, and as net daily insolation decreases with the seasonal cycle, a greater proportion of that work needs fall upon the electrical heater rather than the solar water heater. While the annual load is less than space heating and space cooling (1291 kWh for water heating compared to 3189 and 1456 kWh respectively), the daily load (varying from 2.5 kWh in Summer to just under 4.5kWh in Winter) are significant and greater than the cooling loads in temperate months. The overall low value of heating (especially compared to the current standard demand) is due to the fact that much of the heating load is taken by the solar water heater, particularly in winter months.

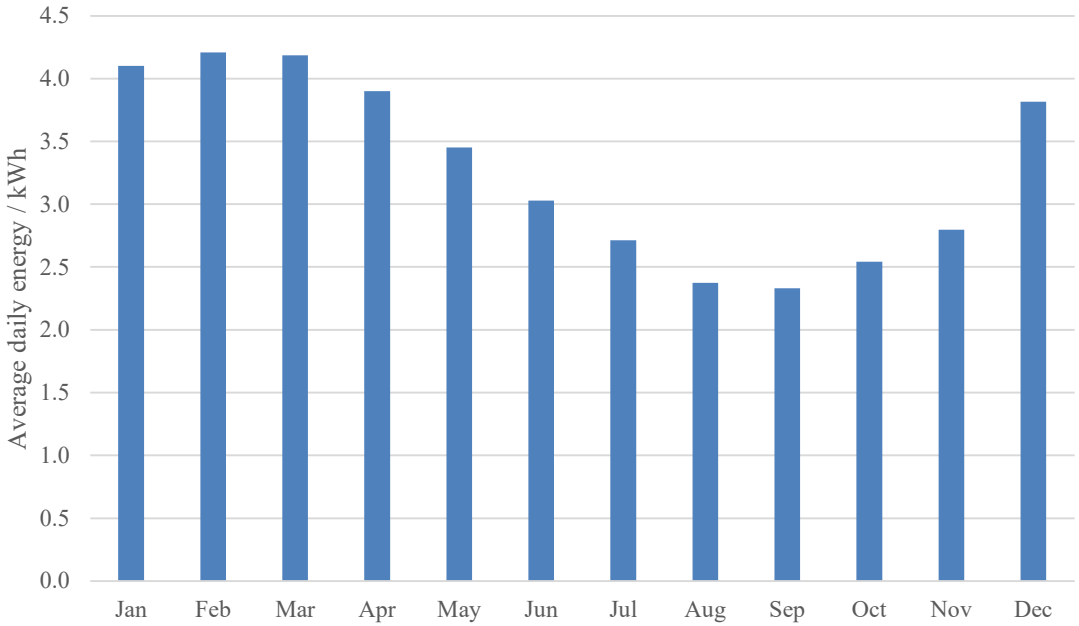

Figure B12 – average daily cumulative water heating loads, by month

The daily profiles (Figure B13) follow a similar shape month by month due to the nature of monthly and hourly demands being sampled from eQuest profiles. The overall magnitudes of the daily

demand, at each hour of the day, follows the pattern of the seasonal variation in demand as may be expected. The maximum values occur at times when peak occupancy coincides when households are awake, i.e., early morning and the evening, as with space heating. In many ways the profiles here are unremarkable and appear trustworthy.

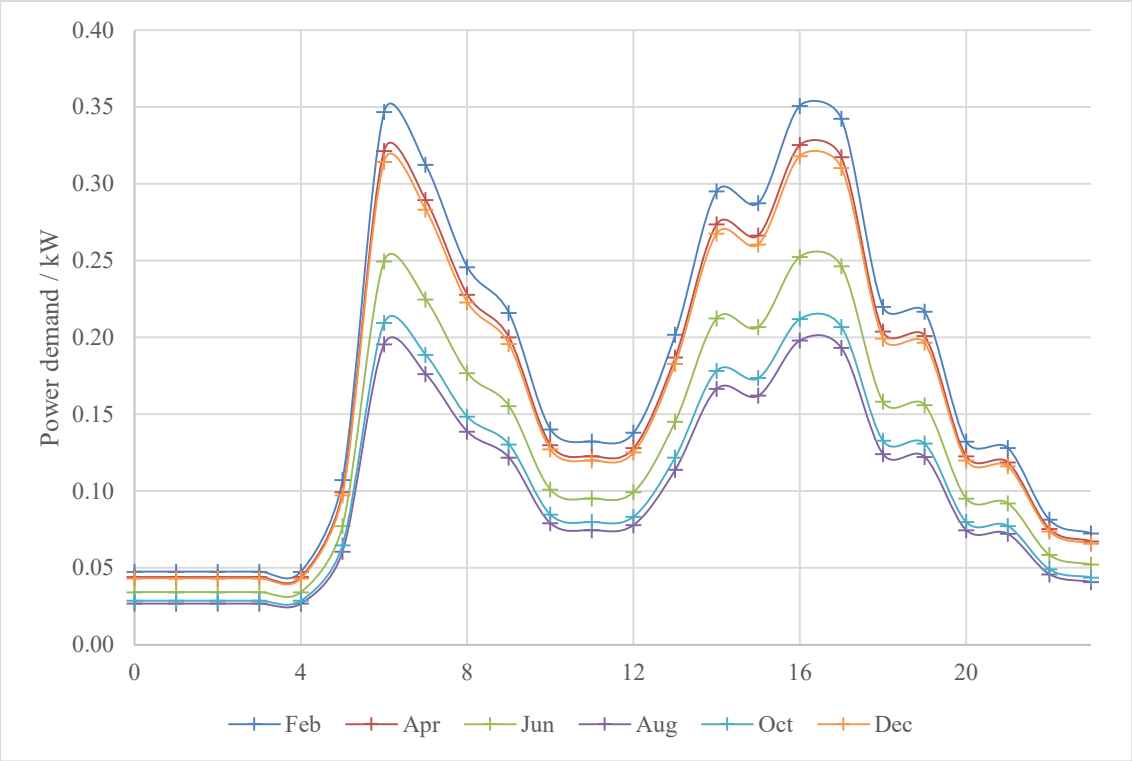

Figure B13 – hourly variations of the day for six months.

4 Refrigeration (C=RF)

Stage I L_A^{RF} = 850kWh.

The Refrigeration category in RECS-15 is considered to include both refrigerator units and freezer units, and the housing category that is most relevant to refrigeration as an end-use is the number of members in the household: the more people in a house the more a refrigerator is likely to be opened, requiring work by the appliance to cool the inflowing air. With the number of house occupants considered to be the primary factor driving refrigeration load, the RECS-15 average refrigeration load for a four-person house, 850kWh, is taken as the AC equivalent.

Stage II L_D^{RF} = 348kWh.

The refrigeration and freezer DC efficiency values from Table 5.3 are the same (53% for DC-internal, and 13% for DC-direct). The standard DC efficiency calculation, Equation 5.2, gives the following expected DC demand for space cooling:

$$L_D^{RF} = 850kWh \times (1 - 0.53) \times (1 - 0.13) = 348kWh \quad \text{(B29)}$$

Stage III Fitting annual DC load to monthly-hourly profile for refrigeration.

The hourly-monthly profile calculations required a split approach: first, an estimation of monthly variation of refrigeration demand by analyzing temperature differences between appliance settings and the internal house temperature; second, fitting the monthly demand to hourly values using the relevant eQuest use profile.

In the first estimation of monthly variation, one simplification was to consider the refrigerator and freezer loads to be equivalent. This may be inaccurate, but in the absence of any data on which to base a more accurate allocation of load and, considering the overall very low load of this category (barely more than 1kWh a day), this was considered an appropriate simplification and approximation.

For each of the occupancy profiles characterized in the space heating and cooling sections, an hourly value of internal house temperature was determined according to the month of the year: for winter (heating) months, then the internal temperature at each hour is set at the higher of ambient temperature and thermostat setting; for summer (cooling) months, it is set to the lower of ambient temperature and thermostat setting; for April and October the internal temperature is set to be the ambient temperature if it falls between the cooling and heating thermostat settings; if it exceeds either than internal temperature is set to the nearest thermostat setting (the cooling value if the

ambient temperature is high, and the heating value if it is low). These four temperature profiles were combined in a weighted average to give the average internal temperature, $\overline{T_{mh}^{Int}}$:

$$\overline{T_{mh}^{Int}} = \left(\frac{5}{7}\right) \cdot \left\{(1-\rho)T'^{wl}_{mh} + \rho T'^{wh}_{mh}\right\} + \left(\frac{2}{7}\right)\left\{(1-\sigma)T'^{el}_{mh} + \sigma T'^{eh}_{mh}\right\} \quad \text{(B30)}$$

where ρ and σ have the same definition and values as previously and the T' parameters indicate the actual internal temperatures in the average CSG house according to the different occupancy profiles.

From this, a simple subtraction for all 288 monthly-hourly allowed the temperature differences to be computed: between the refrigerator setting and the internal temperature ΔT_{mh}^{R}, and between the freezer setting and the internal temperature ΔT_{mh}^{F}:

$$\Delta T_{mh}^{R} = T_{mh}^{Int} - T^{R}; \quad \text{(B31a)}$$

$$\Delta T_{mh}^{F} = T_{mh}^{Int} - T^{F} \quad \text{(B31b)}$$

where T^R is the temperature setting for the refrigerator, and T^F for the freezer unit, 30°F and 0°F respectively.

From these, secondary parameters α_m, β_m, and γ were calculated for refrigerators and freezers separately, using equivalent equations to those in space heating and cooling. The parameters γ^R and γ^F therefore represent the cumulative aggregate temperature differences, in degrees Fahrenheit, between the internal ambient temperature and the refrigerator and freezer unit temperature settings respectively, over the whole year. This was then combined by simple addition into the combined parameter γ^{RF}, which in turn could then be used to divide the $L^{Re}{}_A$ to derive the specific energy of refrigeration value, e^{RF}.

$$\gamma^{RF} = \gamma^{R} + \gamma^{F} \quad \text{(B32)}$$

$$265{,}067.6\ {}^{O}F + 597{,}947.6\ {}^{O}F = 863{,}015.3\ {}^{O}F \quad \text{(B33)}$$

$$e^{RF} = \frac{L_A^{RF}}{\gamma^{RF}} = \frac{365.6kWh}{863{,}015.3\ {}^{O}F} = 0.0004236\ kWh/\ {}^{O}F \quad \text{(B34)}$$

M_m and D_m values were then calculated from β_m, γ, and n_m values using the same methods as space heating and cooling (Section 5.5.1 and 5.5.2), summarized in Table B15.

Table B15 – Refrigeration parameters and energy demand values.												
	Jan	Feb	Mar	Apr	May	Jun	Jul	Aug	Sep	Oct	Nov	Dec
	Refrigerator values											
α_m/°F	618.6	618.6	619.9	632.7	743.3	871.1	936.3	902.1	857.6	653.0	635.4	618.6
γ/°F	265067.6											
eRe	0.0004236 kWh°F^{-1}											
M_m / kWh	8.1	7.3	8.1	8.0	9.8	11.1	12.3	11.8	10.9	8.6	8.1	8.1
D_m / kWh	0.3	0.3	0.3	0.3	0.3	0.4	0.4	0.4	0.4	0.3	0.3	0.3
	Freezer values											
α_m/°F	1530.6	1530.6	1531.9	1544.7	1655.3	1783.1	1848.3	1814.1	1769.6	1565.0	1547.4	1530.6
γ/°F	597947.6											
eRe	0.0004236 kWh°F^{-1}											
M_m / kWh	20.1	18.2	20.1	19.6	21.7	22.7	24.3	23.8	22.5	20.6	19.7	20.1
D_m / kWh	0.6	0.6	0.6	0.7	0.7	0.8	0.8	0.8	0.7	0.7	0.7	0.6

Lastly, from the two respective D_m range of values and the hourly eQuest user profiles for refrigeration (Table B15) the hourly demands, $H^{RF}_{m,h}$, were computed using:

$$H^{RF}_{m,h} = \left(\frac{\varepsilon_h}{\varepsilon_T}\right)^{RF} \cdot (D^R_m + D^F_m) \qquad \text{B35}$$

Table B16 - eQuest user hourly user profile for Refrigeration			
Time (at start of hour interval)	Relative use parameter, ε^{RF}_{h}	Time (at start of hour interval)	Relative use parameter, ε^{RF}_{h}
0:00	0.70	12:00	0.90
1:00	0.67	13:00	0.90
2:00	0.65	14:00	0.90
3:00	0.65	15:00	0.90
4:00	0.65	16:00	0.88
5:00	0.65	17:00	0.88
6:00	0.66	18:00	0.87
7:00	0.67	19:00	0.87
8:00	0.72	20:00	0.82
9:00	0.78	21:00	0.78
10:00	0.85	22:00	0.75
11:00	0.88	23:00	0.70
ε_T:	18.68		

The results of computing Equation B35 are detailed are summarized in Figure B15 and B16.

Refrigeration DSM output

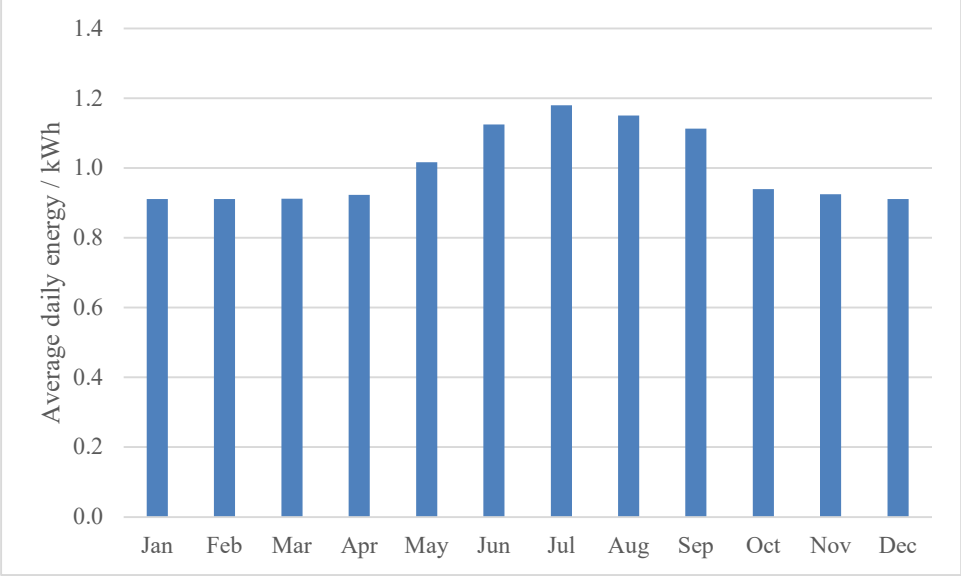

Figure B15 – Average daily refrigeration load

As expected, there is slightly higher demand in summer than in winter months (Figure B15) when the internal temperature, despite the use of space cooling, will be higher. Nevertheless, there

is no great range in absolute value with both summer and winter extremes varying less than 0.2 kWh from 1.0kWh. This variation will likely make a small, but noticeable, impact on the total hourly loading for the CSG house model.

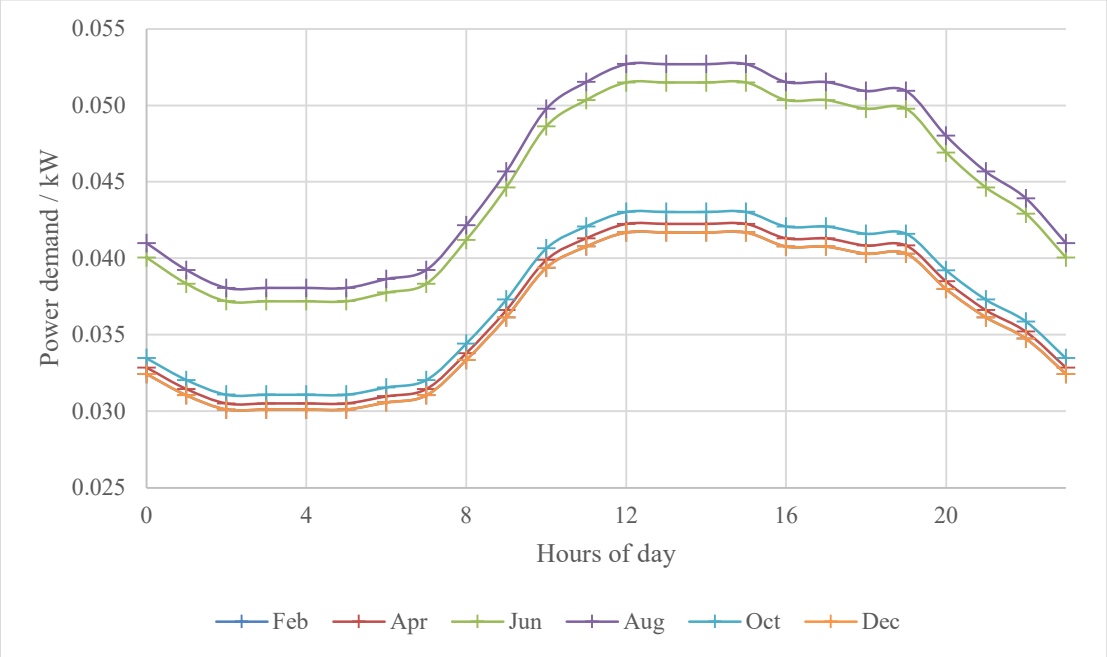

Figure B16 – hourly and seasonal variation in refrigeration load

The results for hourly variation during the day (Figure B16) are reasonable and as may be expected. Given the computational method, the daily demand follows the same variation pattern in each month, with magnitudes grouped tightly by season given the different heating and cooling thermostat settings. There is greater demand during the day when temperatures are higher and the refrigerator unit or freezer unit are being opened and closed mor often than overnight; further, the demands are cyclical with the midnight values matching at either end of the curve. The model here thus appears trustworthy and accurate, and the magnitudes involved should have a small but non-negligible effect on the overall CSG house load.

5 Lighting (C=LI).

Lighting is distinct from the end-use categories in the previous sections for two reasons: first, there is already significant penetration of DC appliances – compact fluorescent lamps (CFLs) and light emitting diode (LED) bulbs - within the lighting category; and second, the hourly use of lighting does not depend directly upon temperature. This required a different approach to determining the expected DC load:

- Stage A: estimating the existing AC and DC lighting loads (separately) for houses that approximate the CSG model. Symbolically, these parameter will have a prime index to differentiate between existing DC loads and calculated total DC load in a CSG house (Stage B).
- Stage B: estimating the total lighting load if the existing AC loads (incandescent bulbs) were changed for DC loads (CFL and LED bulbs).
- Stage C: fitting this total DC lighting load to monthly-hourly demand profiles.

Stage A: $L'^{Li}_{A} = 515$ kWh; $L'^{Li}_{D}=713$ kWh.

In addition to the *Consumption and Expenditures* tables that have already been referenced, EIA RECS surveys also include detailed *Housing Characteristics* (HC) tables. Of these, series five provides a detailed analysis of lighting appliances in terms of: the total number of indoor lightbulbs installed (in a house), the number of incandescent bulbs installed indoors, the number of CFL bulbs installed indoors, and the number of LED bulbs installed indoors. For each of these, the recorded responses are under the categories:

For number of lightbulbs installed
- Fewer than 20
- 20 to 39
- 40 to 59
- 60 to 79
- 80 or more

- *For the type of lightbulbs installed*
- All bulbs are [of that type]
- Most bulbs are [of that type]
- About half of bulbs are [of that type]
- Some bulbs are [of that type]
- No bulbs are [of that type]

These responses are recorded for the various housing categories already covered in previous end-uses, and from these data, an approximation was made split between the lighting load that is AC, 515 kWh, and that which is DC, 713 kWh. House size was considered to be the primary factor

driving lighting demand, so the average demand of the 2,000 to 2,499 square foot and the 2,500 to 2,999 square foot houses (to approximate the 2,500 square foot size of a CSG house), L = 1228 kWh, was used to in determining these values.

Stage B: L_D^{LI} = 699 kWh.

The AC lighting load (514.6 kWh) can be reduced by 73% thanks to internal-DC savings realized by replacing incandescent lightbulbs with energy efficient DC alternatives (CFL or LED bulbs), to give the expected AC to DC load, $L_{A\to D}^{LI}$. The existing DC load clearly does benefit from any further internal-DC savings, so the expected DC load, L_D^{LI}, is the same as the existing load, Li'^{Li}_D.

$$L_{A\to D}^{LI} = (1-\eta_{int}) \times L'^{LI}_A = (1-0.73) \times 514.6\ kWh = 138.9\ kWh \quad \text{(B35)}$$

$$L_D^{LI} = Li'^{LI}_D = 713.4\ kWh \quad \text{(B36)}$$

Thus, the combined DC-internal load was calculated as:

$$L_{DC-int}^{LI} = (L_{A\to D}^{LI} + L_D^{LI}) = (138.9 + 713.4)kWh = 852.3\ kWh \quad \text{(B37)}$$

And from this the Direct-DC load was found to be:

$$L_D^{LI} = L_{DC-int}^{LI} \times (1-\eta_{dir}) = 852.3\ kWh \times (1-0.13) = 698.9\ kWh \quad \text{(B38)}$$

Stage C: Fitting annual DC load to monthly-hourly profile for lighting.

Fitting the annual load to monthly loads was performed using the monthly fitting equations:

$$M_m^{LI} = s_m^{LI} \times L_D^{LI} \quad \text{(B39)}$$

$$s_m^{LI} = \left(\frac{q_m}{q_T}\right)^{LI} \quad \text{(B40)}$$

where s_m^{LI} is the monthly proportion of load to the annual, calculated from q_m, the individual relative monthly use profiles for lighting from the eQuest model (Appendix B.3), and q_T, the annual total of the q_m values. From these, the daily average lighting loads for each month were calculated (Equation B39). The computational results are summarized in Table B17.

Table B17 – Lighting loads												
	Jan	Feb	Mar	Apr	May	Jun	Jul	Aug	Sep	Oct	Nov	Dec
L^{Li}_D	698.9											
q^{Li}_m	0.75	0.65	0.68	0.62	0.64	0.59	0.62	0.64	0.65	0.71	0.7	0.73
s^{Li}_m	0.094	0.081	0.085	0.078	0.080	0.074	0.078	0.080	0.081	0.089	0.088	0.091
M_m / kWh	65.69	56.93	59.56	54.30	56.05	51.67	54.30	56.05	56.93	62.18	61.31	63.94
D_m / kWh	2.12	2.03	1.92	1.81	1.81	1.72	1.75	1.81	1.90	2.01	2.04	2.06

Hourly loads were then determined from Equation 5.43 and the eQuest model's daily use profiles, split according to weekday and weekend (Table B18).

$$H^{Li}_{m,h} = D^{Li}_m \times \left\{ \left(\frac{5}{7}\right)\left(\frac{\varepsilon_{h,w}}{\varepsilon_{T,w}}\right)^{Li} + \left(\frac{2}{7}\right)\left(\frac{\varepsilon_{h,e}}{\varepsilon_{T,e}}\right)^{Li} \right\} \quad \text{(B41)}$$

Table B18 – eQuest hourly profiles for lighting		
Time (starting time of hourly interval)	Hourly profile	
	Weekday $\varepsilon_{h,w}$	Weekend $\varepsilon_{h,e}$
0:00	0.00	0.10
1:00	0.00	0.00
2:00	0.00	0.00
3:00	0.00	0.00
4:00	0.00	0.00
5:00	0.20	0.00
6:00	0.50	0.00
7:00	0.50	0.45
8:00	0.00	0.50
9:00	0.00	0.42
10:00	0.00	0.10
11:00	0.00	0.00
12:00	0.00	0.00
13:00	0.00	0.00
14:00	0.00	0.00
15:00	0.00	0.15
16:00	0.00	0.75
17:00	0.00	0.90
18:00	0.90	0.90
19:00	0.90	0.85
20:00	0.90	0.75
21:00	0.80	0.58
22:00	0.60	0.35
23:00	0.30	0.20
Daily totals: $\varepsilon_{h,z}$	5.60	7.00

Lighting DSM output

The seasonal variation in lighting load (Figure B17) is much less than might be expected. While low absolute changes are unsurprising given the low absolute lighting load, thanks to high performance devices, the very low proportional change in average daily energy between the maximum in January, 2.10 kWh, and June/July, 1.75 kWh (16.7% change from the maximum) is unexpected given the significant difference in daylight hours in the CSG location (Table B19) during hours of high occupancy.

Table B19 – Local sunrise and sunset times at Athens, GA

Dates	Sunrise	Sunset
Dec 21st (approx. winter solstice)	7:35 a.m.	5.29 p.m.
March 21st (approx. spring equinox)	6:35 a.m.	6.46 p.m.
June 21st (approx. summer solstice)	5:23 a.m.	8:28 p.m.
September 21st (approx. autumn equinox)	6:21 a.m.	6.31 p.m.

According to the National Oceanic and Atmospheric Association (NOAA, https://www.esrl.noaa.gov/gmd/grad/solcalc/

Times stated are local Eastern time, not corrected for daylight savings; to do so, one hour should be added to the March, June, and September dates to change to EST.

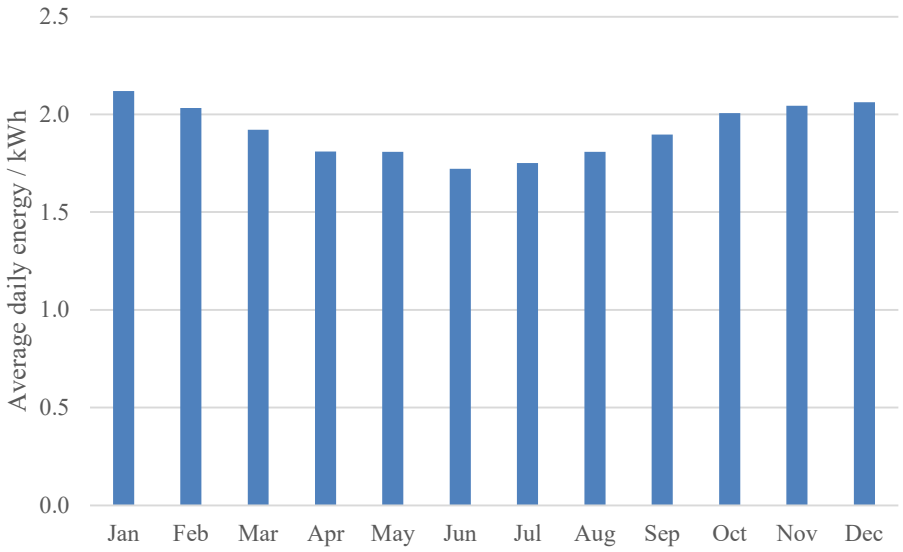

Figure B17 - varying DC lighting load by month in CSG house.

Questions may further be raised by the daily variations for each month (Figure 5.12) which show sharp rises in lighting demand occurring at the same time (5:00pm) throughout the year. This is not surprising given the nature of the computational method – the hourly use profiles were not modulated according to month – but it does demonstrate a shortcoming in the method: a more accurate computation would take daylight hours into consideration and vary the hourly use profiles accordingly. Nevertheless, the error is not considered to be a significant problem for the CSG model overall - the magnitudes are small compared to overall demand (hourly loads not exceeding 0.32kWh at the peak) resulting in a small impact on the overall result and the nature is to over-estimate the lighting demand, strengthening rather than weakening the study's feasibility test.

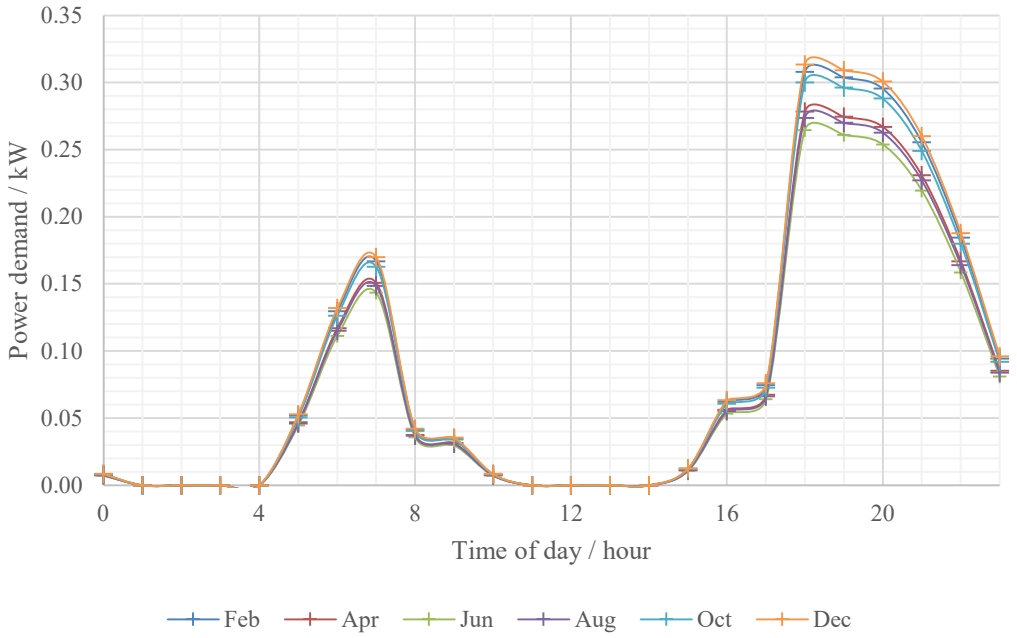

Figure B18 - daily variation in lighting demand for each hour, by month, in CSG house.

6 Clothes drying (C=CD)

The clothes drying end-use category was modeled followed the basic computational methodology.

Stage I L_A^{CD} = 1055kWh.

On the basis that clothes drying demand is primarily driven by the number of members in the household, the RECS-15 data for a four-member household only was considered. Unlike previous categories, clothes drying falls outside the major end-use categories covered by RECS table CE3.4 and rather was found in the "detailed end-use category part 1" table CE5.3a.

Stage II L_D^{CD}=516kWh.

Following the standard DC savings equation and values (Table 5.3), the expected DC load was calculated:

$$L_D^{CD} = L_A^{CD} \times (1 - \eta_{int}) \times (1 - \eta_{dir}) = 1055kwh \times (1 - 0.45) \times (1 - 0.11) = 516kWh \quad \text{(B42)}$$

Stage III Fitting annual DC load to monthly-hourly profile for clothes drying.

The basic eQuest model (Appendix 5.2) provided only hourly use profiles. As a simplification, and considering the low overall value of the load, the annual clothes drying load was considered to be spread evenly across the year, so the average daily load could be calculated by the trivial calculation:

$$D_m^{CD} = \frac{L_D^{CD}}{365} = \frac{516k}{365} = 1.41kWh/day \quad \text{(B43)}$$

The basic eQuest models hourly-use profiles separately for weekdays, Saturdays, and Sundays (Table B20), so the appropriately weighted calculation for hourly demands was thus:

$$H_{m,h}^{CD} = D_m^{CD} \times \left\{ \left(\frac{5}{7}\right)\left(\frac{\varepsilon_{h,w}}{\varepsilon_{T,w}}\right)^{CD} + \left(\frac{1}{7}\right)\left(\frac{\varepsilon_{h,Sat}}{\varepsilon_{T,Sat}}\right)^{CD} + \left(\frac{1}{7}\right)\left(\frac{\varepsilon_{h,Sun}}{\varepsilon_{T,Sun}}\right)^{CD} \right\} \quad \text{(B44)}$$

Table B20 – eQuest hourly profiles for Clothes Drying			
Hourly profile (weekday)	Weekday	Saturday	Sunday
	ε^{w}_{h}	ε^{Sat}_{h}	ε^{Sun}_{h}
0:00	0.00	0.00	0.00
1:00	0.00	0.00	0.00
2:00	0.00	0.00	0.00
3:00	0.00	0.00	0.00
4:00	0.00	0.00	0.00
5:00	0.00	0.00	0.00
6:00	0.00	0.00	0.00
7:00	0.00	0.00	0.00
8:00	0.40	0.00	0.00
9:00	0.40	0.00	0.00
10:00	0.40	0.52	0.45
11:00	0.40	0.48	0.40
12:00	0.40	0.48	0.40
13:00	0.40	0.48	0.40
14:00	0.40	0.55	0.45
15:00	0.50	0.84	0.82
16:00	0.40	0.89	0.88
17:00	0.90	0.78	0.75
18:00	0.90	0.65	0.62
19:00	0.70	0.58	0.52
20:00	0.50	0.58	0.50
21:00	0.50	0.57	0.50
22:00	0.20	0.20	0.35
23:00	0.20	0.20	0.25
ε_T:	7.60	7.80	7.29

Clothes drying DSM output.

As there is no seasonal variation in clothes drying load, only the hourly variation within a day for clothes drying (Figure B19) is evaluated.

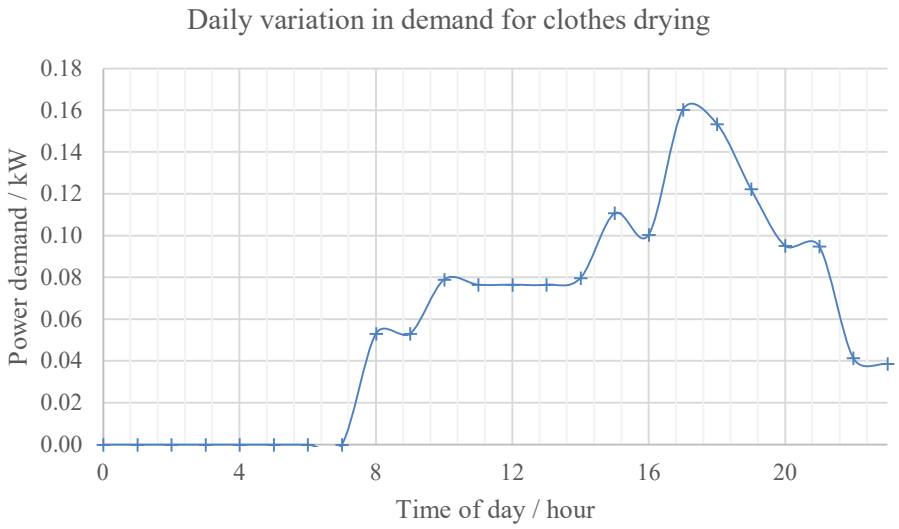

Figure B19 - As modeled demand for the clothes drying category is only in terms of hourly rather than monthly variation, this graph is presented to display the weighted average (for weekdays, Saturdays, and Sundays) for the average day in any given month.

The result is unremarkable and broadly intuitive: zero loads overnight, with a pick-up early in the morning, and peak loads in the evening. The morning pick-up could be explained by the need to dry an overnight washing load or to quicky dry damp clothing for work or school, the middle of the day loads by adults staying at home conducting household chores, and the evening peak by all adults at home maximizing the use of laundry appliances. The demand continuing until 23:00 seems a high amount until quite late, but not unreasonable given the low overall amount (0.04kWh). Weekend loads contribute more to the afternoon and evening loads, roughly equally with weekdays, all peaking in the evening when, on weekdays at least, highest occupancy would occur. In summary, this profile appears reasonable and trustworthy, although the magnitudes will have only a low impact on overall loading.

7 Miscellaneous (C=M)

This final end-use category covers the remaining significant electrical residential loads that would be relevant for a CSG house (Table 5.2). For example, while ceiling fans and microwaves would be installed and expected to be used, the CSG community would not be built with a pool or hot tub in every backyard. It should be noted at this point that electric vehicle (EV) charging has not been included in this study, but rather is considered as an option for further work (Section 9.2).

Due to the need to calculate DC loads of multiple appliance types, Stages I and II have been combined.

Stages I and II L^{Misc}_{A}=1950kWh L^{Misc}_{D}=1322kWh.

The appliance types / end-use loads (Table B21) were taken from the detailed end-use tables in RECS-15, all from the four-household member data, on the basis that household size would be the primary driver of all these demands. DC savings were calculated from the expected AC loads, the relevant DC savings according to the standard Equation 5.2, and these were summed to provide the final expected DC load for miscellaneous end-uses. Cooking has a lower DC-internal savings than other end-uses as this is represented by a device change from electric resistance heating to an induction cooktop: a worthwhile saving, but less than some of the other changes covered in this study through heat pumps, VSDs or BDCPM motors. As modern TVs, personal electronic devices (phones, laptops, tablets, computers, smart speakers, entertainment systems) already run of DC-internal systems, there are no further internal electric savings; however, all end-uses have the benefit of direct-DC savings.

Table B21 - Appliance types within the Miscellaneous end-use category, along with the relevant RECS tables, AC loads, DC-internal and direct-DC savings and the expected DC loads after savings.					
Relevant RECS table	Appliance types	Expected AC loads / kWh	DC efficiency savings		Expected DC Load / kWh
			DC-internal	Direct-DC	
CE5.3a	Ceiling fans	323	0.30	0.13	197
	Clothes washers	77	0.30	0.13	47
CE5.3b	Cooking	300	0.12	0.12	232
	Microwaves	141	0.87	0.13	16
	Dishwashers	153	0.51	0.12	66
	TVs, personal electronic devices, and related	956	0.00	0.20	765
			Total:		1323

Stages III Fitting annual DC load to monthly-hourly profile for miscellaneous loads

The basic eQuest model produces monthly and hourly use profile for miscellaneous loads that include all categories not already modeled in this study and so broadly includes the appliance types in Table B21. The cumulative DC load for a given month, *m*, is derived from the annual expected DC load:

$$M_m^{Misc} = L_D^{Misc} \times s_m^{Misc} = L_D^{Misc} \times \left(\frac{q_m}{q_T}\right)^{Misc} \quad \text{(B45)}$$

The average daily load for each month of the year was then calculated from Equation 5.21. All necessary computations are summarized in Table B22.

Table B22 - Values and intermediate results in computation of average daily demand for a given month, m, in the miscellaneous end-use category												
	Jan	Feb	Mar	Apr	May	Jun	Jul	Aug	Sep	Oct	Nov	Dec
$L^{Misc}{}_D$:	1323kWh											
$q^{Misc}{}_m$	1.46	1.31	1.44	1.4	1.46	1.4	1.45	1.45	1.4	1.46	1.4	1.44
$s^{Misc}{}_m$	0.086	0.077	0.084	0.082	0.086	0.082	0.085	0.085	0.082	0.086	0.082	0.084
$M^{Misc}{}_m$ / kWh	113	102	112	108	113	108	112	112	108	113	108	112
$D^{Misc}{}_m$ / kWh	3.65	3.63	3.60	3.62	3.65	3.62	3.62	3.62	3.62	3.65	3.62	3.60

The hourly end-use profiles in eQuest for miscellaneous loads (Table B23) are, as with clothes drying, split between weekdays, Saturdays, and Sundays, and so the hourly demands are calculated by a weighted average using an equation in the same form as for clothes drying:

$$H_{m,h}^{Misc} = D_m^{Misc} \times \left\{ \left(\frac{5}{7}\right)\left(\frac{\varepsilon_{h,w}}{\varepsilon_{T,w}}\right)^{Misc} + \left(\frac{1}{7}\right)\left(\frac{\varepsilon_{h,Sat}}{\varepsilon_{T,Sat}}\right)^{Misc} + \left(\frac{1}{7}\right)\left(\frac{\varepsilon_{h,Sun}}{\varepsilon_{T,Sun}}\right)^{Misc} \right\} \qquad \text{(B46)}$$

Table B23 – Hourly eQuest user profiles for miscellaneous use category			
	Weekday	Saturday	Sunday
	ε_h		
Hour	z=w	z=Sat	z=Sun
0:00	0.00	0.00	0.00
1:00	0.00	0.00	0.00
2:00	0.00	0.00	0.00
3:00	0.00	0.00	0.00
4:00	0.00	0.00	0.00
5:00	0.00	0.00	0.00
6:00	0.00	0.00	0.00
7:00	0.00	0.00	0.00
8:00	0.40	0.00	0.00
9:00	0.40	0.00	0.00
10:00	0.40	0.52	0.45
11:00	0.40	0.48	0.40
12:00	0.40	0.48	0.40
13:00	0.40	0.48	0.40
14:00	0.40	0.55	0.45
15:00	0.50	0.84	0.82
16:00	0.40	0.89	0.88
17:00	0.90	0.78	0.75
18:00	0.90	0.65	0.62
19:00	0.70	0.58	0.52
20:00	0.50	0.58	0.50
21:00	0.50	0.57	0.50
22:00	0.20	0.20	0.35
23:00	0.20	0.20	0.25
ε_T:	7.60	7.80	7.29

Miscellaneous load DSM output.

Whilst there is monthly variation in the miscellaneous loads both absolute and proportional changes are, as expected, very small. This seems a reasonable estimation given that use of cooking equipment, clothes washers, and electronic devices would be broadly consistent across the year. As with the lighting category, this may be inaccurate for a real house, but given the small scale of demand in this category (around 1.4 kWh/day) any difference between this approximation and reality will have little impact on the effectiveness of the model.

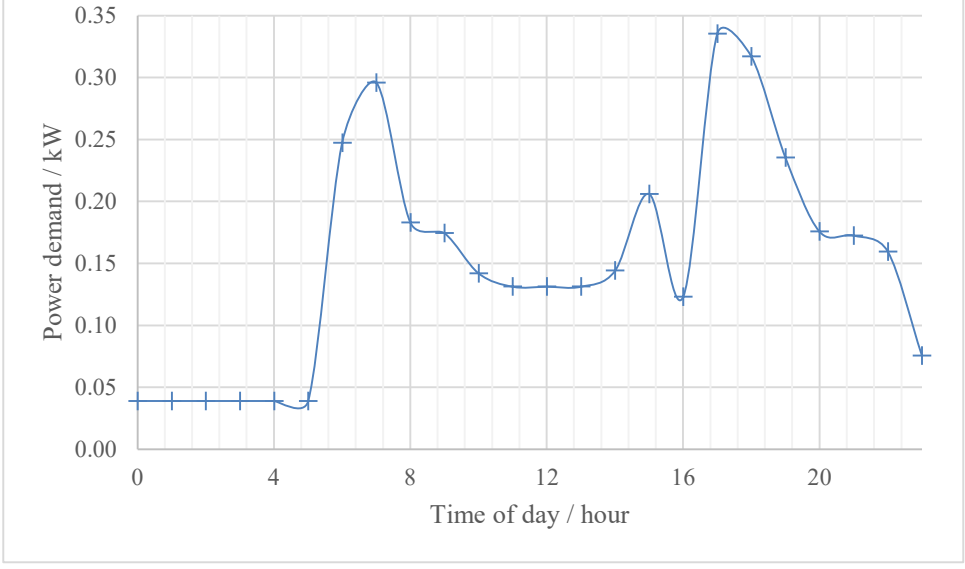

Figure B20 – Hourly variation in miscellaneous loads

Hourly variation through the day is shown here in Figure B20. As expected, there are some very low loads overnight (for example, the charging of personal electric devices) followed by a sudden peak in the morning when all household members are awake and are at home, likely using appliances such as cooking equipment and possibly TVs. During the middle of the day, the miscellaneous load decreases with occupancy, but there is a significant background demand that would include loads such as clothes washers, ceiling fans (in summer months), and electronic devices. The evening peak that starts at 5p.m. is expected as this coincides with high occupancy, maximum cooking loads, and some dishwasher, clothes washer and electronic device use.

Appendix C1: SAM parameters.

Six of the specifically selected SAM parameters (Table 6.1) are self-selecting:

- Solar resource library weather file: Athens_GA TMY file.
- Desired DC to AC Ratio is set to 1 as the CSG concept is fundamentally predicated on DC-only distribution and no AC inversion is required.
- Tracking: 1-axis, as detailed in Section 6.2.
- Orientation: azimuth = 180^{o} (South-facing) for a Northern-hemisphere location
- Backtracking enabled: this allows the simulation to include the tilt angle tracking back, away from low Sun angles, in cases where it would increase PV output when self-shading is high.
- Snow loss estimation not enabled: this is an unnecessary aspect of simulation for the Athens, GA, location in the CSG initial context; however if this work is repeated in other locations it may be necessary to include this feature.

Some other choices, while not as obviously self-selecting, were relatively straightforward to select. The choice of the *CEC Performance Model with Module Database* within the *Module* tab was selected as the simplest model available that also allowed for self-shading calculations. The *Estimate Subarray 1 configuration* was selected to simplify choices as it allows SAM to configure the number of modules per string, and the number of strings in parallel, in each subarray, as the specificity of these choices are beyond the scope of this study.

The *Desired Array Size* was selected to be the lowest value that would achieve both an array area of 1.0 acres in the *System Design* tab and an integer number of rows in the *Shading and Layout* tab. Unlike the *Module model* and *Subarray Estimation* choices, the Desired Array Size value was contingent upon other parameters (Appendix C2).

Appendix C2: Determining detailed SAM parameters.

1. Number of module rows: 10

The central PV array at the Reynold's Landing development has a footprint of approximately 1.0 acres in the shape of a parallelogram of sides around 57m (Northern and Southern sides) and 71m (slanted Eastern and Western sides), with 11 rows of arrays stretching East to West (Appendix 6.1). These are either fixed arrays or seasonal tilting arrays, with GCR suggesting the former. The CSG PV array is arranged in a square footprint, 63.6m x 63.6m, producing a 4,046m^2 array, within 2m^2 of 1.0 acre. The square shape allows simplicity of design and aims for the widest applicability of the model to broader contexts. As the length of the side along which rows will be arranged in the CSG array is reduced from 71m (at Reynold's Landing) by 7.4m to 63.6m (10.4%), the default CSG array design was to have 10 rows of PV modules, albeit in a North-South single-axis orientation (Section 6.2).

Increasing the number of rows within a fixed area may increase the output simply by increasing the number of modules and thus the area of PV material that can generate electricity from the available sunlight. However, this is not guaranteed for tilted or tracker-mounted modules as the resulting increased GCR can cause greater self-shading that outweighs the benefit of increased PV area. Even if that is not the case and increased output is achieved with increased row numbers, doing so beyond 10 rows has not been considered for the CSG as would push the CSG to 66%, beyond the recommended range of GCR:

$$GCR = \frac{row\ length}{PV\ field\ lengt} = \frac{n \times w}{63.6m} = \frac{11 \times 3.83}{63.6m} = 66.2\%$$

(6.1)

Annual energy was simulated for lower numbers of rows to test that output was not increased with fewer rows and fewer self-shading; the results demonstrated that the greater row number (n=10) delivered the greater annual energy.

2. Module choice: Sunpower SPR-X22-480-COM

The Sunpower SPR-X22-480-COM module was selected simply as it had the highest power density (222.2W/m^2) of the available mono-crystalline silicon (Mono-C-Si) modules within the CEC Performance Model with Module Database. Restricting the choice to Mono-C-Si was important as SAM was able to perform self-shading analysis for Mono-C-Si (non-linear) and Thin-Film (linear) cells only, and Mono-C-Si was preferred for its better conversion efficiency – the selected module has a nominal efficiency of 22.24% which is in-line with high-performance non-experimental modules currently available (https://www.nrel.gov/pv/cell-efficiency.html). The expense of a high-performance module is likely to be high, but the CSG concept allows for maximum utilization and performance through centralized use and high levels of maintenance. Thus, while economic assessment is beyond the scope of this work, the principle of high investment for high-end infrastructure is appropriate for this model.

When designing a real solar power system for a specific location, a designer would need to consider the temperature profile of the cell's performance, the relative proportions of direct and diffuse radiation, and other factors; the choice here does not consider these factors to great depth as this requires specific expertise beyond that of the author and the scope of this work. While the module choice is broadly appropriate, a more detailed analysis and design may yield greater performance and should be considered either for further theoretical work with this model on in the case of practical design.

3. Array dimension: portrait orientation, 2x56 module rows

The arrangement of modules within each row (portrait or landscape, how many modules along the width and along the length of the row) has a significant impact on the generated electrical output as these arrangement options affect the dimensions of the row and thus the degree of self-shading when solar tracking modules are employed. Using the selected modules, three options appeared feasible given the individual module dimensions (1.1272m x 1.91625m = 2.16m^2):

- Portrait module orientation, 2 modules along the side of each row and 56 along length
- Landscape module orientation, 2 modules along the side of each row, 33 along the length
- Landscape module orientation, 3 modules along the side of each row, 33 along the length

The effectiveness of each arrangement was tested via iterations with SAM simulations of varying numbers of rows resulting in the clear indication that the first configuration – Portrait orientation – produced the optimum output. The landscape orientations had lower height profiles and thus produced less self-shading effects; however, this does not appear to have overcome their disadvantage of simply not holding enough modules per row (66 and 99) compared to the portrait orientation (112 modules per row). Therefore, the portrait orientation was selected (1120 modules in total).

4. Array tilt

The tilt angle for a solar array is measured from the plane of the ground to the plane of the module; therefore, a tilt angle of 0 represents a horizontal module, with 90^{o} representing a vertical one. When applied to a single-axis North-South oriented array, the tilt angle is the fixed angle between the module and the ground, measuring the degree to which it is generally tilted towards the Sun (i.e., towards the South, in the Northern hemisphere), not the changing angle as the array rotates from East to West to track the Sun's apparent position over the course of a day. Tilting the array so its angle is the same as the latitude of the location has the advantage of decreasing the angle between the incident radiation and the normal to the module, that is increasing the intensity of the radiation. This effect is maximized around the equinoxes when the elevation of the Sun at noon is closest to the latitude angle; however, it can decrease the output in Summer months, compared to a flat array, when the Sun's zenith angle is higher. Also, with increased tilt there are increased self-shading effects. Comparing a tilted array (divided into four sub-arrays to a flat array in 10 North-South single-axis tracking rows over the 1.0 acre footprint demonstrates some significant differences (Table C1):

- A tilted array produces 7.2% more energy, annually (905 compared to 844 MWh)
- A tilted array produces more energy in Winter months and less in Summer months, as expected (a December:May (the greatest and lowest output months) ratio of just 0.68 for the tilted array compared to 0.39 for flat array.

Table C1 – comparison of annual and seasonal PV output from flat and tilted single axis rotational arrays with north-south orientation

Array format	Annual energy	December output	May output	Dec:May ratio
Zero tilt; single array	844 MWh	38 MWh	97 MWh	0.39
Tilt = latitude; divided into four sub-arrays	905 MWh	58 MWh	85 MWh	0.68

As the average house CSG energy demand (Section 5) has both a sharp peak in July (given the TMY data and thermostat settings) but also a sustained higher demand in the Winter months, there may seem, initially, an argument for either system or a preference for a flat system. However, further inspection suggests that a tilted system would be better suited for the CSG model:

- Even if the CSG would be as large as 85 houses, this would result in 1Mwh of electrical energy per house in July with the tilted array. This is only marginally less than the July demand (per household) with energy surpluses in the previous months, therefore even with the tilted array, meeting the July peak demand should not prove difficult.
- The increased, prolonged demand in Winter months (an average of 789.5 kWh per household from December to February inclusive, indicates the benefit of maximizing output in Winter if the Summer peak can be met. Being able to meet demand directly from PV generation when it is required, rather than first storing it in a battery, reduces the initial material infrastructure demand, the ongoing battery maintenance demand, and the energy losses through charging/discharging inefficiencies.

However, while tilting the array may be advantageous in principle, it is impractical for very long North-South arrays (at most latitudes) is it would require large elevations at the Northern end; indeed, for the CSG model, the height would be $63.6m \times \sin(33.97^o) = 35.4m$, an infeasibly

large structure, both in terms of the engineering challenge and that of residential planning. Dividing each long row into smaller segments, e.g. 2x4 modules in a portrait orientation, provides an opportunity to realize some of the benefits from tilting the array: with a module width of 1.1272m, the row length would be 4.51m long and the Northern elevation just 2.52m, a feasible height. Reducing this by one module to just three modules brings the elevated height to only 1.89m, little over six foot. Unfortunately, SAM only allows the array to be subdivided into four smaller subarrays, which each would be much longer (approx. 15.9m long) than is practical. Thus, three modeling options presented themselves:

i. Modeling the array as flat (tilt = 0). This is the most cautious or conservative option, ignoring the benefits of the tilting option but also removing the risk of over-estimating the supply.

ii. Modeling the array as tilted (at an angle equal to latitude) and split into four large sub-arrays, each of which reaching 15.9m high at the Northern end. This is the least favorable option as it is both practically infeasible and would result in very large self-shading effects.

iii. Modeling the array on a smaller scale that the CSG, as 10 much shorter rows, each split into four feasibly sized sub-arrays, and then scale the results up to represent the output if this was built over the entire 1.0 acre of the CSG array. The sub-arrays would be 1.89 or 2.51m high each, depending on which provided a better PV generation result once the trade-off between maximized module number (nameplate capacity) and shelf-shading is considered. This would be the optimum approach but would require detailed modeling to determine optimum spacing between sub-arrays and very careful scaling to ensure that self-shading effects were correctly included.

While the third option may produce the greatest simulated output, it was not considered a reliable modeling options due to its complexity and the resultant opportunity for error,

particularly through under-estimation of self-shading. Thus, option (i), tilt=0, was pursued, with the opportunity for seasonal- or dual-axis simulation discussed in Section 9.3.

5. Ground Coverage Ratio (GCR) = 0.602

In this design methodology, GCR is not a direct feature, but an indirect characteristic of row number (10). It is thus calculated as:

$$GCR = \frac{n \times w}{63.6m} = \frac{10x3.83}{63.6m} = 60.2\%$$

(6.2)

Where n and w have the same meanings as in Section X. The accuracy of this calculation was verified by the fact that the SAM calculates the total land area of the array as exactly 1.0 acres with the GCR set at this value, but not at others.

6. Desired array size = 539kW$_{dc}$

Counter-intuitively, given its place near the start of the SAM input variables, the desired array size was one of the final parameters to be determined. As area constraints and row numbers took priority in the design, desired array size was subjugated to an indirect variable. Simply, the highest value (in kWdc) was entered that resulted in SAM calculating the correct number of rows (10) as an integer (the SAM functionality calculates the number rows, in part, from the desired array size).

Table C2 – annual anergy by range of motion

ROM /º	AE / MWh
38	850.0
40	850.1
42	850.1
44	850.0
46	849.9
48	849.7
50	849.6
52	849.5

7. Inverter selection: Schneider Electric Solar Inverters – Inc: Conext Core XC540-NA

The inverter most closely matched the maximum DC power of the array size, 558kWdc and 539kWdc, respectively.

8. Tracker rotation limit (Range of Motion, ROM) = 40º

Industry research (Ref-white paper) indicates that single-axis tracker ROM should be at least 45º, with some energy advantage in most locations, of around 1%, achieved by increasing the ROM to

52°. Further increases in ROM result in negligible energy advantages and are not considered worth the additional rotational mechanics required. The ROM value was iterated from values ±7° of 45° at 2° intervals producing minimal changes in annual energy, only 0.62% from the maximum, which was achieved with the ROM equal to 40° (Table C2). Self-shading effects and energy costs in rotating the arrays would likely account for reduced output with larger ROM; increased angle between solar radiation and the normal to the arrays at when the solar angle is above 40° would account for the reduced output when the ROM is below that value.

Appendix D1: Example of energy surplus and deficit values for N=60.

Hourly surplus or deficit values, $E_{m,h}$ for a given month, m and hour, h is calculated by:

$$E_{m,h} = S_{m,h} - 60\ H_{m,h}^{T} \quad \text{(D1)}$$

where $S_{m,h}$ are monthly-hourly values of the PV supply calculated for the CSG (Section 6) and $H_{m,h}^{T}$ are the monthly-hourly values for the total electric demand for a single CSG house (Section 5).

Table D1 – Hourly values of energy difference, between PV supply and total load, for CSG community size N=60. Negative values represent deficits, positive values, surpluses. The color scale indicates the degree of deficit and surplus, with deeper blues representing greater deficits and deeper reds, greater surpluses.

Month:	**Jan**	**Feb**	**Mar**	**Apr**	**May**	**Jun**	**Jul**	**Aug**	**Sep**	**Oct**	**Nov**	**Dec**
Hour	Hourly energy differences in kWh											
00:00	-46	-36	-34	-7	-7	-7	-7	-7	-7	-13	-33	-46
01:00	-45	-36	-35	-7	-7	-7	-7	-6	-6	-12	-32	-45
02:00	-45	-36	-36	-7	-7	-7	-7	-6	-6	-12	-35	-45
03:00	-45	-38	-37	-7	-7	-7	-7	-6	-6	-12	-35	-45
04:00	-48	-38	-38	-7	-7	-7	-7	-6	-6	-15	-35	-45
05:00	-59	-51	-49	-14	-12	-12	-12	-11	-11	-24	-44	-56
06:00	-95	-87	-83	-48	25	40	17	-22	-32	-54	-76	-90
07:00	-97	-91	-43	-21	165	82	34	48	78	-47	-65	-95
08:00	-43	-16	128	-31	311	259	8	198	236	33	15	15
09:00	36	-3	177	45	344	205	223	182	287	299	238	163
10:00	-17	168	195	110	295	262	227	241	289	310	99	228
11:00	37	178	240	127	236	136	212	253	121	304	197	217
12:00	50	179	211	257	324	325	191	227	231	300	241	208
13:00	14	234	170	364	321	274	189	204	211	303	248	217
14:00	39	289	148	362	313	168	162	204	93	310	253	228
15:00	-16	52	124	351	298	-25	169	143	222	281	180	151
16:00	-39	166	130	293	276	184	161	-19	150	140	42	4
17:00	-91	-27	20	117	157	115	51	73	47	-29	-64	-94
18:00	-101	-110	-79	-53	9	22	-61	-20	-53	-70	-79	-104
19:00	-97	-104	-82	-86	-51	-47	-90	-48	-49	-66	-72	-100
20:00	-87	-94	-74	-79	-41	-40	-48	-39	-40	-61	-64	-93
21:00	-86	-91	-73	-79	-39	-37	-37	-37	-37	-58	-61	-90
22:00	-64	-71	-53	-60	-28	-28	-27	-27	-28	-39	-40	-68
23:00	-50	-60	-44	-52	-18	-17	-17	-17	-17	-28	-31	-57
D'_m/ kWh	-996	276	788	1470	2850	1833	1317	1500	1667	1737	748	356
E_m / MWh	-30.9	7.7	24.4	44.1	88.3	55.0	40.8	46.5	50.0	53.9	22.4	11.0
E_{annual}	414.3 MWh											

Appendix D2: Battery charge values for N=60.

Applying the battery charging algorithm (Equations 7.6) to the surplus/deficit values (Appendix D1) for a community of N=60 houses and maximum battery capacity of B^{max} = 3000kWh, produced the following battery charge values (Table D2). Note that the start-point for annual assessment of energy independence has been set at 9a.m. on the average solar day in April.

Table D2 – CSG battery charge model for N=60 and battery capacity of 3000 kWh

Month:	Apr	May	Jun	Jul	Aug	Sep	Oct	Nov	Dec	Jan	Feb	Mar	Apr
Hour	Hourly battery charge for N=60												
00:00		1347	2794	2803	2679	2781	2736	2569	2489	2270	1127	1155	1719
01:00		1340	2786	2795	2671	2774	2722	2533	2438	2219	1087	1116	1711
02:00		1332	2779	2788	2664	2768	2708	2495	2387	2168	1048	1076	1703
03:00		1325	2772	2781	2657	2761	2694	2456	2337	2117	1005	1034	1696
04:00		1317	2764	2773	2651	2754	2678	2417	2286	2064	962	992	1688
05:00		1303	2751	2760	2638	2741	2651	2368	2224	1998	905	938	1672
06:00		1325	2786	2776	2614	2706	2590	2283	2123	1892	807	845	1618
07:00		1473	2860	2806	2657	2775	2537	2211	2016	1784	706	797	1595
08:00	↓	1751	3000	2813	2834	2987	2567	2224	2030	1736	688	911	1560
09:00	41	2058	3000	3000	2997	3000	2835	2437	2175	1768	684	1070	
10:00	139	2322	3000	3000	3000	3000	3000	2525	2379	1748	834	1244	
11:00	253	2533	3000	3000	3000	3000	3000	2702	2573	1781	993	1459	
12:00	483	2823	3000	3000	3000	3000	3000	2918	2759	1826	1152	1647	
13:00	808	3000	3000	3000	3000	3000	3000	3000	2953	1838	1362	1799	
14:00	1132	3000	3000	3000	3000	3000	3000	3000	3000	1873	1620	1932	
15:00	1446	3000	2972	3000	3000	3000	3000	3000	3000	1855	1667	2043	
16:00	1708	3000	3000	3000	2979	3000	3000	3000	3000	1812	1815	2159	
17:00	1812	3000	3000	3000	3000	3000	2967	2928	2895	1710	1785	2177	
18:00	1753	3000	3000	2932	2977	2941	2888	2840	2779	1597	1661	2090	
19:00	1656	2943	2947	2831	2924	2886	2814	2759	2666	1489	1545	1998	
20:00	1568	2897	2903	2777	2879	2842	2746	2688	2562	1392	1440	1916	
21:00	1480	2853	2861	2736	2838	2800	2682	2619	2461	1295	1339	1835	
22:00	1413	2822	2830	2705	2808	2769	2638	2575	2385	1224	1259	1776	
23:00	1355	2802	2811	2686	2789	2750	2606	2540	2321	1168	1193	1727	

Appendix D3: Year-round off-grid assessment with battery charge for N= 95.

Table D3– First 15 and last 14 iterations of energy-independence feasibility assessment for N=114 size community. Other rows are removed for brevity. Maximum battery capacity was effectively removed from the model by setting $B^{max} = 10^6$kWh. At this size of community, energy independence is not achieved, with the failure point occurring at 18:00 in January – almost three months short of the endpoint at 09:00 in April.

Month	Hour	Hourly surplus / kWh	Charge or discharge of battery	Energy storage / kWh	Month	Hour	Hourly surplus / kWh	Charge or discharge of battery	Energy storage / kWh
Apr	9	7.9	Charge	7.0	Dec	16	-53.1	Discharge	1790.6
Apr	10	72.4	Charge	71.7	Dec	17	-166.2	Discharge	1604.6
Apr	11	89.8	Charge	152.0	Dec	18	-184.8	Discharge	1397.9
Apr	12	210.3	Charge	339.9	Dec	19	-177.9	Discharge	1198.8
Apr	13	308.2	Charge	615.5	Dec	20	-165.2	Discharge	1014.0
Apr	14	299.4	Charge	883.1	Dec	21	-159.9	Discharge	835.1
Apr	15	282.3	Charge	1135.5	Dec	22	-121.0	Discharge	699.8
Apr	16	226.0	Charge	1337.6	Dec	23	-101.0	Discharge	586.8
Apr	17	44.0	Charge	1376.9	Jan	0	-81.7	Discharge	495.4
Apr	18	-123.5	Discharge	1238.8	Jan	1	-80.7	Discharge	405.2
Apr	19	-153.0	Discharge	1067.6	Jan	2	-80.6	Discharge	315.0
Apr	20	-140.2	Discharge	910.8	Jan	3	-80.6	Discharge	224.9
Apr	21	-139.7	Discharge	754.5	Jan	4	-84.9	Discharge	129.9
Apr	22	-106.0	Discharge	636.0	Jan	5	-103.8	Discharge	13.8
Apr	23	-91.3	Discharge	533.9	Failure point		↑ Stored energy in sufficient ↑ to meet hourly energy deficit		

Whether the battery is modeled as charging or discharging, it is a function of hourly surplus: positive energy difference (a surplus) results in charging (the battery energy storage then increases by an amount equal to the surplus less charging inefficiency losses, 10.6%); the reverse is the case if there is a negative surplus (i.e., a net deficit), the battery charge decreasing by the size of the deficit plus 10.6% to overcome discharging inefficiencies.

System failure occurs in the final row, 18:00 on the average solar day in January, as the PV supply is in deficit, and the stored energy in the battery is insufficient to meet the shortfall.

Appendix D4 Off-grid assessment failure when B^{max} is 1 kWh below required value.

Table D4 – First 15 and last 14 iterations of a year-round assessment for N=83 and B_{max} = 5735kWh, i.e. 1kWh below the minimum energy required for independence. Energy storage, B, is insufficient to meet hourly demand at 7a.m. on the average solar day in March, demonstrating the sensitivity of the system to maximum battery capacity, 26-hour intervals short of completion, demonstrating the sensitivity of the system to battery capacity.

Month	Hour	Hourly surplus / kWh	Charge or discharge of battery bank	Energy storage / kWh	Month	Hour	Hourly surplus / kWh	Charge or discharge of battery	Energy storage / kWh
Apr	9	17.0	Charge	15.2	Feb	18	-170.8	Discharge	1468.8
Apr	10	80.4	Charge	87.0	Feb	19	-160.9	Discharge	1288.8
Apr	11	97.4	Charge	174.1	Feb	20	-145.2	Discharge	1126.4
Apr	12	218.0	Charge	369.0	Feb	21	-140.6	Discharge	969.1
Apr	13	316.2	Charge	651.6	Feb	22	-110.1	Discharge	846.0
Apr	14	309.3	Charge	928.1	Feb	23	-92.6	Discharge	742.4
Apr	15	294.1	Charge	1191.1	Mar	0	-52.6	Discharge	683.5
Apr	16	238.5	Charge	1404.3	Mar	1	-54.0	Discharge	623.1
Apr	17	61.1	Charge	1458.9	Mar	2	-55.5	Discharge	561.0
Apr	18	-103.8	Discharge	1342.8	Mar	3	-57.0	Discharge	497.3
Apr	19	-133.7	Discharge	1193.2	Mar	4	-58.2	Discharge	432.2
Apr	20	-122.5	Discharge	1056.2	Mar	5	-75.5	Discharge	347.8
Apr	21	-122.1	Discharge	919.7	Mar	6	-128.8	Discharge	203.7
Apr	22	-92.6	Discharge	816.1	Mar	7	-91.2	Discharge	101.7
Apr	23	-79.8	Discharge	726.9	Failure point		↑ Stored energy is insufficient ↑to meet hourly energy deficit once energy is lost in discharge		

It is notable that the surplus, charge/discharge state, and energy storage values for the first 15 time-intervals (from 9 a.m. to 11 p.m. (23:00) on the average solar day in April are identical to those in Table 7.5, as the limit of the battery capacity has not affected the system at that point. However, the effects further along the assessment are significant, bringing failure point to 25 hourly intervals before the completion of the year. Failure occurs at 7a.m. on the average solar day in March, where the 101.7kWh of battery charge is insufficient to meet the 91.2kWh of system energy deficit, given that 10.6% of the stored energy (10.8kWh) is modeled as lost through discharge inefficiencies.

A like-for-like comparison (in terms of time intervals) between success (with B^{max} = 5736kWh) and failure (with B^{max} = 5735kWh) is provided in Table 7.7.

Table D5 – Comparison of hourly surplus, charge/discharge state, and energy storage values between 18:00 in February and 07:00 in March for N=83 community, between a community with B^{max} = 5736kWh and another with B^{max} = 5735 kWh.

B^{max} = 5736kWh					B^{max} = 5735kWh				
Month	Hour	Hourly surplus / kWh	Charge or discharge of battery	Energy storage / kWh	Month	Hour	Hourly surplus / kWh	Charge or discharge of battery	Energy storage / kWh
Feb	18	-170.8	Discharge	1469.8	Feb	18	-170.8	Discharge	1468.8
Feb	19	-160.9	Discharge	1289.8	Feb	19	-160.9	Discharge	1288.8
Feb	20	-145.2	Discharge	1127.4	Feb	20	-145.2	Discharge	1126.4
Feb	21	-140.6	Discharge	970.1	Feb	21	-140.6	Discharge	969.1
Feb	22	-110.1	Discharge	847.0	Feb	22	-110.1	Discharge	846.0
Feb	23	-92.6	Discharge	743.4	Feb	23	-92.6	Discharge	742.4
Mar	0	-52.6	Discharge	684.5	Mar	0	-52.6	Discharge	683.5
Mar	1	-54.0	Discharge	624.1	Mar	1	-54.0	Discharge	623.1
Mar	2	-55.5	Discharge	562.0	Mar	2	-55.5	Discharge	561.0
Mar	3	-57.0	Discharge	498.3	Mar	3	-57.0	Discharge	497.3
Mar	4	-58.2	Discharge	433.2	Mar	4	-58.2	Discharge	432.2
Mar	5	-75.5	Discharge	348.8	Mar	5	-75.5	Discharge	347.8
Mar	6	-128.8	Discharge	204.7	Mar	6	-128.8	Discharge	203.7
Mar	7	-91.2	Discharge	102.7	Mar	7	-91.2	Discharge	101.7
System success		↑ Stored energy is sufficient to meet hourly ↑ energy deficit			Failure point		↑ Stored energy is insufficient to meet hourly ↑ energy deficit		

Comparing the two scenarios shows that the extra 1kWh of battery capacity in the energy independent community provides exactly 1kWh of extra stored energy in each hourly interval, which is enough to meet demand in the critical hour of 7a.m. on the average solar day in March. The next hour exhibits energy surplus therefore battery charging, which continues until 4p.m. (16:00), providing a battery charge of 1167.8kWh, sufficient to last till the year-end. Peak charge (not shown in the Table 7.6) occurs between 3p.m. and 5pm. (1500 and 1700) on the average solar day in October and is equal to B^{max}; the 1kWh difference in battery charge between the two battery bank models is manifest from that point to the year-end.

Appendix D5 Numerical result of required battery capacity, and B/N ratio, for variously sized CSG developments.

The results in Table D6 have the full error margins already applied.

Table D6 – Required battery capacity, and battery capacity per house, for CSG communities between 50 and 83 houses in size.

N	B^{max} / kWh	$B^{max} \cdot N^{-1}$ / kWh·house^{-1}	N	B^{max} / kWh	$B^{max} \cdot N^{-1}$ / kWh·house^{-1}
50	3357	67.1	67	5640	84.2
51	3438	67.4	68	5811	85.5
52	3521	67.7	69	5981	86.7
53	3602	68.0	70	6150	87.9
54	3686	68.3	71	6321	89.0
55	3815	69.4	72	6491	90.1
56	3945	70.4	73	6660	91.2
57	4077	71.5	74	6831	92.3
58	4208	72.5	75	7001	93.3
59	4338	73.5	76	7193	94.6
60	4470	74.5	77	7395	96.0
61	4622	75.8	78	7596	97.4
62	4791	77.3	79	7797	98.7
63	4961	78.7	80	8000	100.0
64	5132	80.2	81	8201	101.2
65	5301	81.6	82	8402	102.5
66	5471	82.9	83	8604	103.7

END